Stony Brook University

Investigating the roles of p53 stability and its interactions with chaperone proteins during mitochondrial permeability transition

A Dissertation Presented

by

Ivan Lebedev

to

The Graduate School

in Partial Fulfillment of the

Requirements

for the Degree of

Doctor of Philosophy

in

Biochemistry and Structural Biology

Stony Brook University

August 2016

Stony Brook University
The Graduate School

Ivan Lebedev

We, the dissertation committee for the above candidate for the
Doctor of Philosophy degree, hereby recommend
acceptance of this dissertation.

Markus A. Seeliger, PhD – Dissertation Advisor
Assistant Professor, Department of Pharmacological Sciences

Ute Moll, MD, MS – Dissertation Advisor
Professor, Department of Pharmacology

Steven E. Glynn, PhD - Chairperson of Defense
Assistant Professor, Department of Biochemistry and Cell Biology

Mark E. Bowen, PhD - Committee Member
Associate Professor, Department of Physiology and Biophysics

Daniel Bogenhagen, MD - Outside Committee Member
Professor, Department of Pharmacological Sciences

This dissertation is accepted by the Graduate School

Charles Taber
Dean of the Graduate School

Abstract of the Dissertation

Investigating the roles of p53 stability and its interactions with chaperone proteins during mitochondrial permeability transition

by

Ivan Lebedev

Doctor of Philosophy

in

Biochemistry and Structural Biology

Stony Brook University

2016

Tissue necrosis as a consequence of ischemia-reperfusion injury and oxidative damage is a leading cause of permanent disability and death worldwide. The complete mechanism by which cells undergo necrosis upon oxidative stress is not understood. In response to an oxidative insult, wildtype p53 has been implicated as a central regulatory component of the mitochondrial permeability transition (mPT), triggering necrosis. This process is associated with cellular stabilization and translocation of p53 into the mitochondrial matrix. I explore the mechanism by which p53 activates the key mPT regulator cyclophilin D (CypD); how the stability of p53 affects its ability to interact with CypD; and how Trap1, an Hsp90-related mitochondrial matrix chaperone protein and member of the mitochondrial unfolded protein response (mtUPR), is able to suppress mPT in a p53-dependent manner. I find that p53 needs to be structurally destabilized in order to interact with CypD and that catalytically active CypD causes strong aggregation of wildtype p53 protein (both full length and isolated DNA binding domain) into amyloid-

type fibrils in vitro. NMR studies of CypD reveal slow exchange behavior, characteristic of a dynamic process such as isomerization. Moreover, I find that inhibition of Trap1 by the mitochondria-specific HSP90 ATPase antagonist gamitrinib strongly sensitizes primary mouse embryonic fibroblasts (MEFs) to mPT and permeability transition pore (mPTP) opening in a p53- and CypD-dependent manner. The result of my work proposes a model by which influx of unfolded p53 into the mitochondrial matrix in response to oxidative stress indirectly activates the normally inhibited CypD by displacing it from Trap1 complexes. This activates CypD's isomerase activity. Liberated CypD then isomerizes multiple proteins including p53 (causing p53 aggregation) and the structural components of the mPTP pore, inducing pore opening.

Dedication

This work is dedicated to my family and all of my friends who've helped me along the way. Without your help and support, none of this would have been possible.

Table of Contents

List of Figures

Chapter 1

Chapter 3

Chapter 4

List of Tables

List of abbreviations

ΔΨm – electrochemical proton gradient

5HT3R – type 3 serotonin receptor

AIF – apoptosis-inducing factor

ANT – adenine nucleotide translocase

APP – Amyloid Precursor Protein

ASGPR – asialoglycoprotein receptor

BBB – blood brain barrier

BMRB – Biological Magnetic Resonance Bank

CR – Congo Red

CsA – cyclosporine A

CypA – cyclophilin A

CypB – cyclophilin B

CypC – cyclophilin C

CypD – cyclophilin D

CypE – cyclophilin E

CypF – cyclophilin F

CypG – cyclophilin G

CypH – cyclophilin H

CypJ – cyclophilin J

DBD – DNA binding domain

DKO – double knockout

DSC – differential scanning calorimetry

ER – endoplasmic reticulum

ERK – extracellular signal-regulated kinase

ETC – electron transport chain

FBPase – fructose-1,6-bisphosphatase

FITC – fluorescein isothiocyanate

FKBP – FK-506 binding proteins

FL – full length

FPLC – fast protein liquid chromatography

GSK3ß – glycogen synthase kinase 3 beta

GST – glutathione s-transferase

HDGF – hepatoma-derived growth factor

HIV – human immunodeficiency virus

HMGB1 – high mobility group box 1

hnRNP A2 – nuclear translocation of heterogeneous nuclear ribonucleoprotein A2

HSP – heat shock protein

HSQC – heteronuclear single quantum coherence

I/R – ischemia/reperfusion

IL2 – interleukin 2

IMM – inner mitochondrial membrane

ITC – isothermal titration calorimetry

MALDI – matrix-assisted laser desorption/ionization

MEF – mouse embryonic fibroblast

MOMP – mitochondrial outer membrane permeabilization

mPT – mitochondrial permeability transition

mPTP – mitochondrial permeability transition pore

mtUPR – mitochondrial unfolded protein response

nAChR – homo-oligomeric a7 neuronal nicotinic receptor

NMR – nuclear magnetic resonance

OCSP – oligomycin sensitivity conferring protein

OMM – outer mitochondrial membrane

p53 – Tumor protein p53

PiC – mitochondrial phosphate carrier

PDB – protein databank

PPIase – peptidyl-prolyl *cis-trans* isomerases

PSI – pounds per square inch

PTM – post-translational modification

ROS – reactive oxygen species

SfA – Sanglifehrin A

SH3 – Src-homology 3

SIRT3 – sirtuin 3

sol. – soluble

SPG7 – Spastic Paraplegia 7

TAD – transactivation domain

TEV – tobacco etch virus

TEM – transmission electron microscopy

ThT – Thioflavin T

TIM – translocase of the inner membrane

TFE – trifuoroethanol

T_m – melting temperature

TOM – translocase of the outer membrane

Trap1 – Tumor necrosis factor receptor-associated protein-1

TSPO – peripheral benzodiazepine receptor

VDAC – voltage dependent anion channel

WT – wild type

Zpr1 – zinc-finger protein

Acknowledgements

Thank you first and foremost to my family. You have been the ones who have kept me motivated to push through all of the setbacks and difficult times to get things done. Lydia, you have been the most patient and supportive partner I could have ever asked for. Thank you for always being so positive and providing the encouragement I needed when I had doubts. You have always been my greatest motivation to be successful and I thank you for all of your sacrifices to achieve it. Thank you for staying up late with me, making me smile, always keeping me company and supporting my decisions (however poor they may have been). Thank you to my parents for keeping me levelheaded and keeping my expectations in check. Without sharing your own experiences with graduate school and life, I would not have been able to stay focused through the pressure and difficulties. I could not have asked for better role models. Pops, thanks for always making sure to stop to remind me that “I need to get my PhD first,” before thinking about anything else.

My fellow lab mates: we’ve been through a lot together, thank you for always being there to lend a helping hand or listen to a rant. Thank you George for starting me in the lab and always being eager to celebrate or brood with me. Thank you Zack for getting this project moving and being there to discuss the many twists and turns the work has taken. Thank you especially to Maya, I could not have asked for a better helper throughout these last few years and I much appreciate your always-pleasant personality. Grace, you’ve been a fantastic coworker, friend and housemate. Thanks for always commiserating with me and having my back. Matt, I consider you an honorary lab member since you’re always there to lend an ear and join me for lunch. Thanks for being a great friend and awesome workout buddy. Mike, thank you for your help with experiments and for keeping things mysterious. Agatha, you have been wonderful new addition to our lab and an excellent friend. Tyler, I appreciate your comradery especially when riding out a late night of experiments, good luck in your own graduate studies. An enormous thank you to Weibing for all of your help in the lab. I cannot imagine how much more difficult the last few years would have been without you. Alice, while this might not be serious, it will be perfect.

Thank you to my advisors Markus and Ute for all of the advice and guidance throughout my time here. I appreciate your helpfulness and patience with this whirlwind of a project that was full of ups, downs and surprises. Thank you for always challenging me and keeping me focused on what is important. You have helped me develop not just as a student, but as a person and I will be forever grateful to you. I will always fondly look back to BBQs at Markus' house and the lively Christmas gift exchanges.

Thank you to my committee members Dr. Steven Glynn, Dr. Mark Bowen and Dr. Daniel Bogenhagen. I appreciate all of the time you have invested and valuable advice you have given me to move this project along. I feel fortunate for having been able to work with such talented and creative individuals. I would like to additionally thank Dr. Bogenhagen for his personal time spent teaching me new experiments and kindly sharing his lab resources. I would like to thank Kim DeStefano and Joann Delucia-Conlon for helping me with the hurdles of graduate school.

I would like to thank Dr. Franz Schmidt and Dr. Philipp Schmidpeter for their help in establishing the CypD activity assays and sharing of resources. I am additionally thankful for their valuable contribution to the data interpretation and presentation.

Chapter 1: Introduction

Stroke is one of the leading causes of death and permanent disability worldwide [1]. Currently, no prophylaxis exists to prevent tissue damage and tissue loss from stroke and only limited treatment options exist for stroke victims. It is of great importance to better understand the underlying cellular processes which lead to cell death and permanent tissue damage in order to develop better preventive medicines and treatments. Recent work has implicated the protein p53 as an important component of the necrotic cell death process in response to ischemic stroke and reperfusion [2]–[7]. The purpose of my work was to better understand the mechanism by which p53 is able to trigger cell death by necrosis. Using the functional DNA binding domain of the p53 protein (p53DBD), I investigated how protein stability affects p53's interaction with mitochondrial prolyl-isomerase cyclophilin D (CypD), the key regulator of mitochondrial permeability transition (mPT) and subsequent necrotic cell death [8]–[10]. I uncovered a novel and unexpected mode of interaction between p53DBD and CypD that depends on the catalytic activity of CypD and ultimately leads to aggregation of p53DBD into amyloid-like fibrils. These discoveries led me to question the involvement of mitochondrial chaperone proteins Trap1, HSP90 and HSP60 in mediating p53- and CypD-dependent mPT. By using the mitochondrial HSP90 and Trap1 inhibitor Gamitrinib, which sensitizes cells to mPT [11]–[13], I was able to show that Trap1 inhibition-mediated mPTP depends on p53. This work has allowed me to develop a new model for the mechanism by which p53 could trigger mPT and subsequent necrosis. Taken together, my work provides a framework of experiments that proposes a novel mechanism involving p53 that is responsible for mediating necrotic cell death in

response to ischemia and reperfusion injury. This paves the way for additional investigations that will ultimately help with the greatly needed search for effective stroke prevention and treatment therapies.

1.1 Stroke and Necrosis

Two categories of stroke exist: hemorrhagic and ischemic. Hemorrhagic stroke is less common and is characterized by the leakage of a weakened blood vessel or bursting of a brain aneurysm which causes blood to spill into the brain [14]. Accumulation of blood within the brain damages the cells and tissues due to the buildup of excessive pressure. Ischemic stroke accounts for 87% of strokes and is characterized by the acute blockage of a blood vessel to or in the brain, often due to a blood clot [14]. This work focuses on the cellular mechanism of the necrotic cell death program that is initiated by ischemia and progresses upon restoration of blood flow to the affected tissue.

1.1.1 Ischemic Stroke and Reperfusion Injury

Each year, nearly 700,000 people in the United States suffer an ischemic stroke [14]. An ischemic stroke is caused by the blocking of a blood vessel to the brain most often due to a clot that either develops at the location of the clot (thrombosis) or forms elsewhere in the body and travels through the bloodstream until it reaches an impassible blood vessel where it restricts or completely blocks blood flow (embolism) [15]. Ischemia is defined as the period of time that the blood flow is restricted. During this time, cellular dysfunction occurs due to lack of oxygen, a decrease in pH, depletion of ATP and ion pump dysfunction which leads to an overload of calcium in the cell [16]. Restoration of blood flow to the affected region is known as reperfusion. Upon

reperfusion, oxygen delivery to the cell is restored, pH levels are normalized and aerobic ATP production through the electron transport chain (ETC) can resume once again. However, reperfusion does not come without consequences. It has been known since the 1960s that reperfusion of the ischemic heart leads to myocardial tissue damage and cell death through necrosis. This process is commonly known as reperfusion injury [17]. Reperfusion injury is brought on by a complicated cascade of events including oxidative stress from the generation of reactive oxygen species (ROS), calcium overload, rapid pH change, inflammation and mitochondrial permeability transition [18]. The effects of reperfusion injury events span from several minutes [19] to days. However, early intervention - through mild hypothermia or administration of glucose-insulin-potassium or 2-deoxyglucose - in a variety of animal models has been shown to reduce the extent of damaged tissues [20]–[24]. In some cases myocardial infarct size post ischemia/reperfusion (I/R) injury was reduced by as much as 50% [25]–[28]. Despite these encouraging findings in animal models, clinical outcomes have been less favorable [29]–[37] and no globally accepted general treatments for I/R injury exist to date.

1.1.2 Apoptosis, Necrosis and Necroptosis

Historically, the apoptotic cell death program has always been considered a regulated or programmed form of cell death, while necrosis was thought of as the unregulated or non-programmed mechanism for cell death [38], [39]. The primary morphological differences in cells undergoing necrosis versus apoptosis are characterized by the leaking of cellular contents into the extracellular environment [39], [40] in the case of necrosis, while cells undergoing apoptosis are phagocytized and

fragments are membrane-wrapped in an organized fashion before they are able to leak their contents [41].

Upon initiation of apoptosis by the caspase family of proteases, cells begin to shrink and condense, the nucleus and nuclear DNA are broken up and the cytoskeleton collapses [42]. Once initiated, apoptosis cannot be terminated or reversed. In the final stages of apoptosis, the cell undergoes budding into apoptotic bodies which contain the intact organelles and these apoptotic bodies are phagocytosed and degraded [43].

The mechanisms that trigger cells to undergo death by necrosis differ from those of apoptosis. Generally, apoptosis is confined to single or small clusters of cells while necrosis affects larger groups/masses of contiguous cells [43], [44]. Necrosis has historically been considered an unregulated, energy-independent death program that is initiated when the cell is a victim of a larger toxic insult. Whether a cell dies through the apoptotic or necrotic program largely depends on the type of insult, the type and age of the tissue, and the physiological environment [43], [45], [46]. Generally, necrosis is favored when the death-stimulus involves either direct damage to cell membranes, disruption of ATP production in the mitochondria or depletion of caspases [47]–[49]. Unlike apoptosis where cells shrink and compartmentalize, cells undergoing necrosis swell and spill their cytoplasmic contents into the surrounding extracellular environment which invokes a strong inflammatory response [43], [50], [51]. Though necrosis has generally been considered an unregulated process, there is an emerging body of research indicating that there may indeed be a set of signaling networks, with both unique and apoptosis-common regulatory components, within the cell which ultimately

determines whether cells follow the necrotic or apoptotic cell death programs [46], [48], [52], [53].

In light of the discovery of common regulatory components between apoptotic and necrotic cell death mechanisms, the newly coined term ‘necroptosis’ has been gaining significant attention in the literature [40], [44], [54]–[57]. Generally, the concept of necroptosis is not meant to serve as a new or separate cell death mechanism from the already characterized apoptotic and necrotic pathways, but rather aims to highlight key regulatory and signaling cascades that are involved throughout the progression of cellular dysfunction and ultimate death by necrosis. Some existing studies on regulated necrosis pathways have already taken on original names of their own, such as the necrosome signaling complex, ferroptosis, oxytosis, NETosis, ETosis, parthanatos, pyroptosis, pyronecrosis and CypD-mediated necrosis [55], [56]. Ultimately, the term necroptosis serves to unite these differently named pathways to highlight the various mechanisms that may be responsible for regulating necrosis.

1.2 Mitochondrial permeability transition

One major catalyst of cell death by necrosis is the disruption of ATP production due to some type of mitochondrial dysfunction [47], [49]. One highly studied phenomenon that ultimately leads to disruption of ATP production and cell death by necrosis is known as mitochondrial permeability transition (mPT), which is characterized by the prolonged opening of a non-selective low conductance protein pore spanning both the inner and outer mitochondrial membranes known as the mitochondrial permeability transition pore (mPTP) [58]–[61].

1.2.1 Function of the mitochondrial permeability transition pore

The mitochondrial permeability transition pore is a small non-selective pore that spans both the inner and outer mitochondrial membranes and allows for the free passing of molecules of up to 1.5 kDa in size [61]–[64]. The mechanism of mPTP assembly and opening has been debated for many years. However, it is generally accepted that in healthy, unstressed, cells the mPTP remains closed or unassembled and its opening is brought on by prolonged cellular stress. mPT has been extensively studied in the context of reperfusion injury following ischemic stroke or myocardial infarction [2], [65]–[70]. The increase in intracellular Ca^{2+}, formation of excess ROS and pH changes caused by reperfusion are postulated to trigger opening of the mPTP [18]. The physiological role of the mPTP has also been debated extensively where conventional thinking that mPTP opening serves only to mediate cell death has been challenged by evidence indicating that the mPTP can open and close very transiently to allow for mitochondrial regulation of Ca^{2+} [71]–[74]. Nonetheless, it is generally agreed that prolonged opening of the mPTP ultimately leads to cell death by apoptosis or necrosis, depending on the stressor [58], [60], [61], [75], [76].

1.2.2 Components of the mitochondrial permeability transition pore

Another major point of contention for many years has surrounded the specific protein components that make up the physical mPTP. The only essential and indisputable protein component of the mPTP that has prevailed throughout the many years of scrutiny is cyclophilin D (CypD), the sole mitochondrial member of the cyclophilin prolyl-isomerase family which serves as the key regulator of the mPTP [8], [9], [61], [77]–[80]. Various other proteins have been proposed to associate with the

mPTP including but not limited to the voltage dependent anion channel (VDAC), adenine nucleotide translocase (ANT), mitochondrial phosphate carrier (PiC) and peripheral benzodiazepine receptor (TSPO) [60], [61]. However, subsequent experimentation has shown that many of these proteins are in fact non-essential mPTP components. For example, genetic co-deletion of VDAC1 and VDAC2 in mice did not prevent VDAC null mitochondria from undergoing mPT [81], mouse liver mitochondria devoid of ANT also undergo normal mPT [82], knockout of mitochondrial phosphate carrier (PiC) in mice does nothing to prevent normal mPT [83], and mouse hearts devoid of TSPO continue to be sensitive to mPT in response to I/R injury [84]. Recent work has implicated the F1Fo ATP synthase as the physical pore component through which small (<1.5 kDa) molecules can pass [58], [77], [85]–[88]. However, the debate continues over what the oligomeric state of the F1Fo ATP synthase must be to function as a pore, -as well as which additional proteins are necessary for full, functional, assembly of the mPTP [77], [89]–[91].

1.3 Cyclophilins and the mitochondrial matrix-specific member cyclophilin D

The physiological roles of peptidyl-prolyl *cis-trans* isomerases (PPIases) in the cell have historically been to serve as protein folding chaperones through the catalysis of *cis-trans* interconversion of proline bonds which, if uncatalyzed, is a slow process [92]. Cyclophilin D is the key regulator of the mPTP, and is the sole mitochondrial member of the PPIase cyclophilin family which consists of 10 known cyclophilins A-J and CypNK. It should be noted that the cyclophilin nomenclature does not currently associate any genes or proteins with CypI [93]–[98].

1.3.1 The cyclophilin family of prolyl-isomerases

Cyclophilins are one of three families of peptidyl-prolyl *cis-trans* isomerases that together with FK-506 binding proteins (FKBPs) and parvulins make up the larger protein family of immunophilins [99], [100]. FKBPs are characterized by their ability to bind the inhibitors FK506 (tacrolimus) and rapamycin (sirolimus), while cyclophilins are unique in their ability to bind cyclosporins [93]. The cyclosporins and FKBP inhibitors are structurally different but both types are fungal peptides with immunosuppressive properties which are currently being investigated for a variety of treatments ranging from hepatitis C to reperfusion injury, viral infections, inflammation, and cancers [101], [102].

It is important to point out that the naming of individual cyclophilins has become somewhat convoluted and in some cases the use of one name can apply to more than one protein without additional clarification. In general, the protein name corresponds to the gene name: for example, the gene PPIA in humans codes for CypA, PPIB codes for CypB and so on. The primary confusion surrounds the naming of CypD. The gene PPID encodes for the protein CypD which is 40 kDa and primarily located in the cell nucleus and cytoplasm; its most commonly used name is Cyp40 (UniProtKB - Q08752). However, conventional use of the name CypD refers to the sole mitochondrial cyclophilin which is in fact encoded by the gene PPIF and therefore technically should be named CypF (UniProtKB - P30405). Use of CypD in this thesis will follow conventional use and will refer to the mitochondrial cyclophilin encoded by the PPIF gene. Table 1.1 summarizes the respective genes, protein names and alternative names that are commonly used to refer to each respective gene product.

Table 1.1: Relation of cyclophilin gene names to names of conventional and alternate protein products

Gene	Protein Name	**Conventional Protein Name**	Alternate Protein Names	Uniprot Accession Number
PPIA	CypA	CypA	PPIase A, Rotamase A	P62937
PPIB	CypB	CypB	PPIase B, Rotamase B, CYP-S1, S-cyclophilin	P23284
PPIC	CypC	CypC	PPIase C, Rotamase C	P45877
PPID	CypD	Cyp40	PPIase D, Rotamase D, Cyclophilin-40, Cyp40	Q08752
PPIE	CypE	CypE	PPIase E, Rotamase E, Cyclophilin-33	Q9UNP9
PPIF	**CypF**	**CypD** **(used in this thesis)**	**PPIase F, Rotamase F, Mitochondrial cyclophilin, CyP-M, mtCypD**	**P30405**
PPIG	CypG	CypG	PPIase G, Rotamase G, CASP10, Clk-associating RS-cyclophilin, CARS-Cyp, SR-cyclophilin, SRcyp	Q13427
PPIH	CypH	CypH	PPIase H, Rotamase H, USA-CYP	O43447
PPIL3	CypJ	PPIL3	Rotamase PPIL3	Q9H2H8
NKTR	CypNK	NKTR	Natural-killer cells cyclophilin-related protein	P30414

Cyclophilin A is the most widely distributed member of the cyclophilin family with functions both inside and outside of the cell [103]. CypA has important roles in mediating protein folding and stability with targets including HIV-1 Gag [104], [105], Homo-oligomeric a7 neuronal nicotinic receptor (nAChR) [106], [107], type 3 serotonin receptor (5HT3R) [106], [107], collagen [108], transferrin [109], and rhodopsin in

Drosophila [110], [111]. CypA also facilitates a myriad of cellular trafficking systems including translocation of apoptosis-inducing factor (AIF) to induce cell death after cerebral hypoxia-ischemia [112], [113], nuclear translocation of heterogeneous nuclear ribonucleoprotein A2 (hnRNP A2) [114], transport of CD147 to the plasma membrane [115], trafficking asialoglycoprotein receptor (ASGPR) between the plasma membrane and endosomes [116], import of fructose-1,6-bisphosphatase (FBPase) to vesicles [117], and nuclear export of zinc-finger protein 1 (Zpr1) [118]. CypA can be secreted to the extra cellular matrix where it can serve as a signaling molecule to promote apoptosis and inflammation [119]. One of the most significant roles of CypA is its immunosuppressive response upon inhibition with the pan-cyclophilin inhibitor cyclosporine A (CsA). CsA is commonly used during organ transplantation to suppress rejection [103], [120], [121]. Inhibition of CypA by CsA inhibits the calcineurin phosphatase which in turn suppresses inflammatory proteins TNF alpha and interleukin 2 (IL2) via NFAT signaling [103], [120], [121].

Cyclophilins B and C are primarily localized to the endoplasmic reticulum (ER) where they have less studied roles in regulation of the redox homeostasis and modulation of protein secretion and transport to the plasma membrane [122], [123]. Cyp40 is localized in the cytoplasm where it functions as a co-chaperone with HSP90 for the regulation of steroid-receptors complexes [124], [125] and regulation of the transcription factor c-Myb which regulates hematopoiesis in mammals [126], [127]. Cyclophilins E, G, H and J (PPIL3) have unique sequences but each contain an RNA-binding domain and are primarily located in the nucleus where they have been associated with the spliceosome for pre-mRNA processing [94], [128]–[132]. Finally,

CypNK (NKTR) serves as a protein folding chaperone and is the largest of the cyclophilins at ~150 kDa [97], [133], [134]. It was one of the earliest discovered cyclophilins, sometimes referred to as only a cyclophilin-like protein due to its size and sequence differences, and is the only cell-membrane associated cyclophilin.

1.3.2 Cyclophilin D: the sole mitochondrial member of the cyclophilin family

Cyclophilin D is the only cyclophilin family member that resides in the mitochondria. It is synthesized as a ~22 kDa protein in the cytoplasm containing a 29-residue, N-terminal, mitochondrial localization signal which is cleaved upon entry into the mitochondrial matrix for a final, functional, ~18 kDa protein [135]–[137]. In addition to being a key regulator of the mPTP, CypD has also been implicated in the suppression of apoptosis through interaction with Bcl2 [138]–[140], promotion of autophagy [141], as well as controlling cell cycle progression and cell motility from outside the mitochondria by interaction with the transcription factor STAT3 [142]. Interestingly, STAT3 has also recently been characterized within the mitochondria and has been proposed to stimulate mitochondrial respiration and inhibit mPT [143].

CypD is the only component that has been shown to be genetically indispensable for mPT and subsequent necrotic cell death [8], [9], [61], [77]–[80]. CypD requires its PPIase activity in order to trigger opening of the mPTP, because inhibitors known to prevent mPT have also been shown to inhibit PPIase of CypD [144]–[146]. Several recent models intended to explain the formation and opening of the mPTP have proposed that CypD isomerizes a component of the assembled mPTP which then leads to a conformational change and subsequent opening of the pore [58]–[60]. CypD targets implicated in these models have included both the lateral stalk of the ATP synthase, or

the oligomycin sensitivity conferring protein (OCSP) subunit of the ATP synthase, which also assembles along the lateral stalk of ATP synthase [59], [85], [147], [148]. These models propose that conformational change in the dimers of the ATP synthase are responsible for forming and opening the mPT pore component itself [59], [85], [147], [148]. Similarly, ANT and the mitochondrial phosphate carrier (PiC) have been suggested as CypD targets which in turn bind to the c-subunit rings of the F1Fo-ATP synthase; ANT and PiC have also been implicated as the mPT pore component itself [59], [88], [149]. Yet another proposed model hypothesizes that the oligomycin sensitivity-conferring protein (OSCP) serves as a negative regulator of the mPTP and the removal of the OSCP or binding of CypD and PiC to the OSCP induce a conformational change in the F1Fo-ATP synthase that would in turn uncover a Ca^{2+} binding site and further sensitize the mPTP to opening at lower Ca^{2+} concentrations [58]. This model supports the notion that the mPTP can function as a transient Ca^{2+} release channel since it has been shown that cells can still undergo mPT in the absence of CypD but at elevated Ca^{2+} concentrations [79], [150]–[152]. In such a model, CypD could serve as a signaling molecule to initiate opening of the mPTP and subsequent necrosis in response to ROS and Ca^{2+} stress, such as is encountered in I/R injury, thereby supporting the concept of regulated necrosis or necroptosis. While the specific components of the mPTP still cannot be agreed upon to date, these models serve as an encouraging starting point for additional research to hammer down the exact composition of the elusive mitochondrial permeability transition pore.

In addition to the identification of new CypD binding partners and substrates, the involvement of posttranslational modifications (PTMs) on CypD have recently come into

question. For example, CypD is acetylated at Lys166, presumably by the enzyme acetyl coenzyme A [153], and subsequent deacetylation of CypD at Lys166 by sirtuin 3 (SIRT3) has been shown to inhibit mPT [154], [155]. Moreover, SIRT3 is known to deacetylate the OSCP in response to nutrient- and exercise- induced stress [156], which raises an interesting question regarding the involvement of PTMs, and specifically acetylation, in the regulation of mPT and subsequent necrosis. CypD can be phosphorylated on Ser/Thr residues, which to date have not been specifically mapped, by glycogen synthase kinase 3 beta (GSK3ß); CypD phosphorylation then activates mitochondrial extracellular signal-regulated kinase (ERK) and subsequently leads to mPT [157], [158]. Conversely, ROS-induced mPT can be inhibited by S-nitrosylation of Cys 203 of CypD [159]. These examples highlight the level of complexity in the mechanisms by which CypD could facilitate opening of the mPTP and reinforced the notion that a complex signaling network could exist to regulate the necrotic cell death process.

1.4 Cyclosporins and Other Cyclophilin Inhibitors

Cyclosporins are a family of fungal-derived cyclic peptides with potent immunosuppressive properties. They are known for their ability to broadly bind to the cyclophilin family of PPIases and there is growing interest in achieving increased selectivity for individual cyclophilins, namely CypA, CypD and Cyp40 for a variety of treatments.

1.4.1 Cyclosporine A

Cyclosporine A (CsA) is a cyclic undecapeptide of fungal origin and distinguishes the cyclophilin family of immunophilins from FKBPs and parvulins as all cyclophilins

bind-to and are inhibited by CsA. It was discovered in 1972 during a screen for non-cytotoxic immunosuppressants at the company Sandoz [101], [160]. It has since been explored for use in a myriad of treatments including: psoriasis, rheumatoid arthritis, uveitis, antiviral therapies, hepatitis C, inflammation, reperfusion injury and even certain cancers [101], [161]. CsA is a potent immunosuppressant that primarily functions through inhibition of CypA which, in turn, further inhibits the calcineurin phosphatase which in turn suppresses inflammatory proteins TNF alpha and interleukin 2, this prevents T-cell activation and immune response [103], [120], [121], [162]. CsA is most commonly known for it use during organ transplantation in order to prevent rejection. CsA binds all cyclophilins including CypD and has been shown to protect mouse hearts and brains from mPT in response to I/R injury and subsequent necrosis [2], [101], [161]–[164]. Despite these encouraging findings, CsA remains an unattractive target for the treatment or prevention of I/R injury because of its unfavorable side effects in humans including induction of blood-brain barrier (BBB) permeability and dysfunction [165]–[167] as well as a dose-dependent neuro-, hepato-, and nephro- toxicity [162], [168]–[171]. Importantly, high dose administration of CsA can negatively impact infarct size by increasing the damaged area and can have a neurotoxic effect [172]. Furthermore, a recent clinical trial investigating the effectiveness of CsA in acute ischemic stroke showed that only a marginal subdivision of patients had a significantly reduced infarct size 30 days after treatment compared to patients who only received standard thrombolytic therapy only [173]. Taken together, there is a clear need for an improved CypD-selective inhibitor that can potentially protect patients from I/R-injury.

1.4.2 Cyclosporine Analogs

In an effort to reduce many of the side effects of CsA, including its immunosuppressive properties, many researchers have been looking to identify CsA-like compounds that can preferentially inhibit CypD over the additional cyclophilin family members. One promising CsA analog was the development of alisporivir which still binds to all of the cyclophilin family members but does not lead to inhibition of calcineurin when bound to CypA and in turn does not evoke an immunosuppressive effect [174], [175]. Alisporivir is currently being studied as an hepatitis treatment through its inhibition of Cyp40 [175]–[177]. Another group of drugs known as Sanglifehrins are non CsA-derived large macrocyclic peptides. Sanglifehrins bind to all members of the cyclophilin family more potently than CsA (PDB:1YND) [146], [178]. Sanglifehrin A (SfA) does still have immunosuppressive properties however not through the inhibition of CypA-calcineurin binding [146], [178]. While the immunosuppressive mechanisms and relative toxicity is still being investigated, SfA and SfA-analogues are being developed and investigated for use as treatments in response to I/R injury in light of their high affinity for CypD over CsA [101], [146], [179], [180]. Despite these research advances, there is still no ideal inhibitor that can selectively bind to CypD instead of the other cyclophilin family members to specifically target the regulation of mPT and subsequent necrosis.

1.5 p53 and its mitochondrial function

p53 is a transcription factor commonly known as the ‘guardian of the genome’ or ‘cellular gatekeeper’ for its critical role as a tumor suppressor [181]–[184]. It is the most commonly mutated gene in human cancer and the most commonly mutated tumor

suppressor gene, and is arguably one of the most intensely studied gene and protein [185], [186]. The canonical function of p53 serves to protect cells from a variety of stressors including, but not limited to, DNA damage, hyperproliferative signals, oxidative stress, hypoxia and nutrient deprivation [182], [183], [187]. The canonical consequence of p53 activation by these stressors is that it leads to the stabilization of p53 and transcriptional activation of its target response genes, ultimately leading to repair of the damaged DNA, cell cycle inhibition, senescence or cell death through apoptosis or autophagy [182], [183], [187]. Recent work has expanded the function of p53 to a non-canonical role which include transcription-independent initiation of apoptosis [188]–[193] and necrosis at the mitochondria via protein-protein interaction in response to various stressors [2], [5], [194]–[196].

In response to cellular stress, p53 can be translocated to the mitochondria where it triggers mitochondrial outer membrane permeabilization (MOMP) by interacting with members of the Bcl-2 family which are responsible for either inhibiting or activating apoptosis [191], [197]–[201]. Activation of pro-apoptotic BH1-3 proteins monomeric Bax and Bak lead to their insertion (in the case of Bax) and oligomerization in the mitochondrial outer membrane. These oligomers form a dynamic lipid pore and spill the enzymatic contents of the intermembranous space, notably cytochrome c, iAPP inhibitors Smac/Diablo [202]–[204] and serine protease Omi/HtrA2 [205]–[207], to trigger apoptosis by activating the caspase cascade in the cytoplasm. Direct activators of Bax/Bak are the proteins tBid and Bim, while the proteins Puma, Noxa and Bad initiate apoptosis indirectly by inhibiting the antiapoptotic Bcl-2 family members including Bcl-2, Bcl-xL and Mcl1 [191], [208]. p53 interacts with both direct and indirect activators

of apoptosis. It can free Bax, Bak, and tBid from their inhibitory counterparts Bcl-xL and Bcl-2 to indirectly activate apoptosis, while on the other hand it can also directly activate apoptosis by interacting with Bak and Bax. Finally, in the absence of stress, cytosolic p53 is sequestered and inactivated by binding of Bcl-xL [191], [209]. In response to stress, nuclear p53 transactivates its target gene *Puma*, which in turn displaces cytosolic p53 from the inactive complex with Bcl-xL. This liberates p53 which can then activate cytosolic Bax.

In addition to its role in apoptosis initiation, p53 has recently been implicated in driving cell death by necrosis, also by way of the mitochondria but independent of any pro/anti-apoptotic Bcl2 family members [2]. As discussed, the key regulator of I/R-induced necrosis is cyclophilin D. Myocardial infarction and stroke models of CypD $^{-/-}$ mice have shown that CypD $^{-/-}$ mice are resistant to I/R-induced necrosis but remain sensitive to apoptosis driven by the Bcl-2 family members [8], [9], [210], [211]. While this highlights that the signaling pathways regulating apoptosis and necrosis are functionally distinct from each other, they seem to overlap when it comes to the involvement of p53. The hallmark of cells undergoing death by necrosis is the release of the proteins high mobility group box 1 (HMGB1) and hepatoma-derived growth factor (HDGF) into the surrounding environment [212]. As characterized by electron microscopy and the release of HMGB1 into the surrounding medium, targeting p53 to the mitochondrial matrix by fusing it to a mitochondrial localization signal in Bax/Bak double knockout (DKO) mouse embryonic fibroblasts (MEFs) reveals that H_2O_2 stress causes the cells to undergo death by necrosis [2]. Moreover, this cell death shows a lack of caspase-3 cleavage, the classical marker of cells undergoing apoptosis. Furthermore, knockdown

of p53 in p53 heterozygous mice [2], [213] or prevention of p53 translocation into the mitochondria using the cytosolic HSP70 inhibitor pifithrin-μ protects cells from undergoing mPT [195], [214]. Taken together, these results indicate that indeed, stress-induced influx of p53 into the mitochondrial matrix can drive the necrotic cell death pathway.

1.6 Heat-shock proteins and stability of p53

p53 is one of the most commonly mutated transcription factors in human cancers and many of the associated mutations have been shown to affect the structural stability of p53 protein to various degrees ranging from hyperstabilization to total unfolding [215]–[217]. Many cancer types overexpress a variety of chaperone proteins which are known to associate with both mutant and WT forms of p53 in order to override the conventional tumor suppressive functions of p53 [218]–[224]. Combining what we know about how the structure and function of p53 is affected by the multitude of well-studied chaperone proteins in the cell, perhaps we can infer and draw new parallels to understand how p53 might function within the mitochondria.

p53 is composed of five distinct regions, two N-terminal transactivation domains (TAD1, residues 1-43, and TAD2, residues 44-63), followed by a proline-rich region (residues 64-92), the DNA-binding domain (DBD, residues 93-292), a nuclear localization signal (residues 293-319), the tetramerization domain (residues 320-355) and finally a C-terminal regulatory domain (residues 356-393) [225]. The N-terminal transactivation domains, central DNA-binding domain and C-terminal tetramerization domain form individual, stable, globular, folded structures that are connected by unstructured, flexible chains. The full, functional, quaternary structure of p53 exists as a

tetramer where the tetramerization domains tie four individual p53 proteins together and coordinate the DNA-binding domains around their DNA target as modeled in (Figure 1.1).

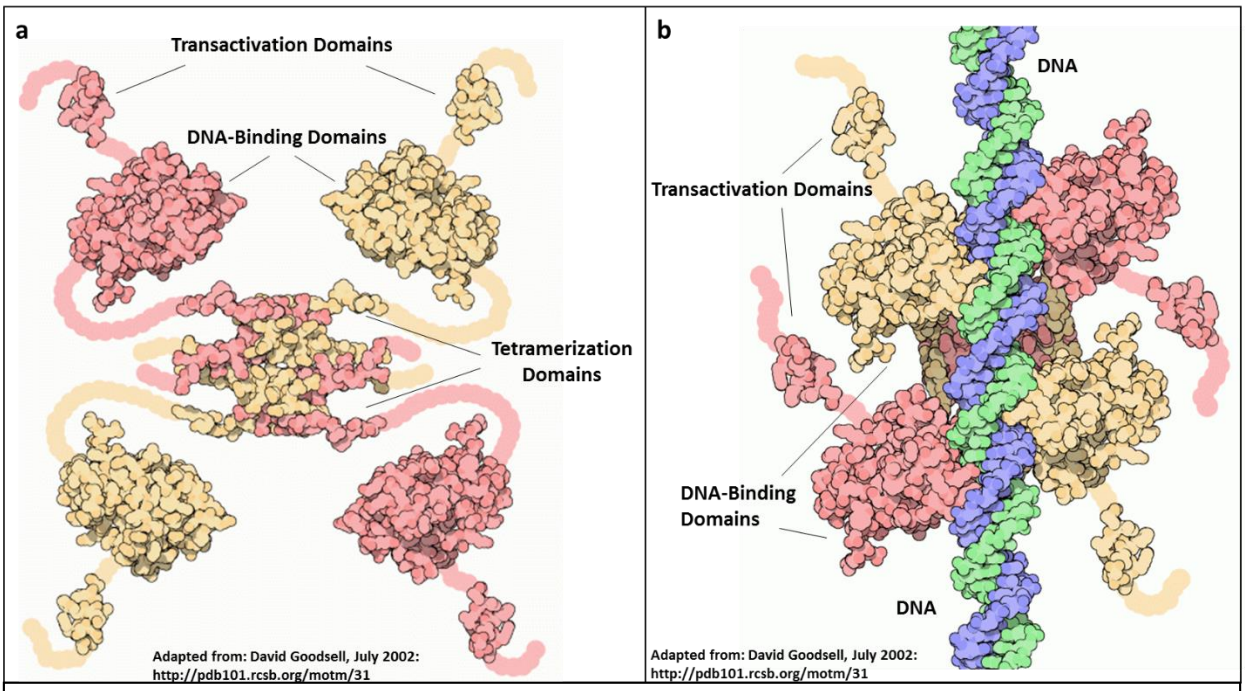

Figure 1.1: Quaternary structure of p53. a) Model of the relative arrangement of p53 domains in the fully assembled tetrameric state. b) Model of p53 tetramer bound to DNA.

The DNA-binding domain of p53 (p53DBD), also referred to as the core-domain (p53core), is the minimal functional domain that is required for interaction with CypD [2]. Though further minimal truncation mapping of p53 has shown that CypD interacts somewhere along the N-terminal region of p53DBD between residues 80-220 [2], this construct is likely unstructured because three out of seven important β-strands are missing from the core β-sandwich structure of p53DBD as highlighted in Figure 1.2. The DBD of WT p53 is inherently an unstable molecule with an apparent melting temperature (T_m) of 42°C that loses its ability to bind DNA and begins to form insoluble aggregates *in vitro* at 37°C [215], [226], [227].

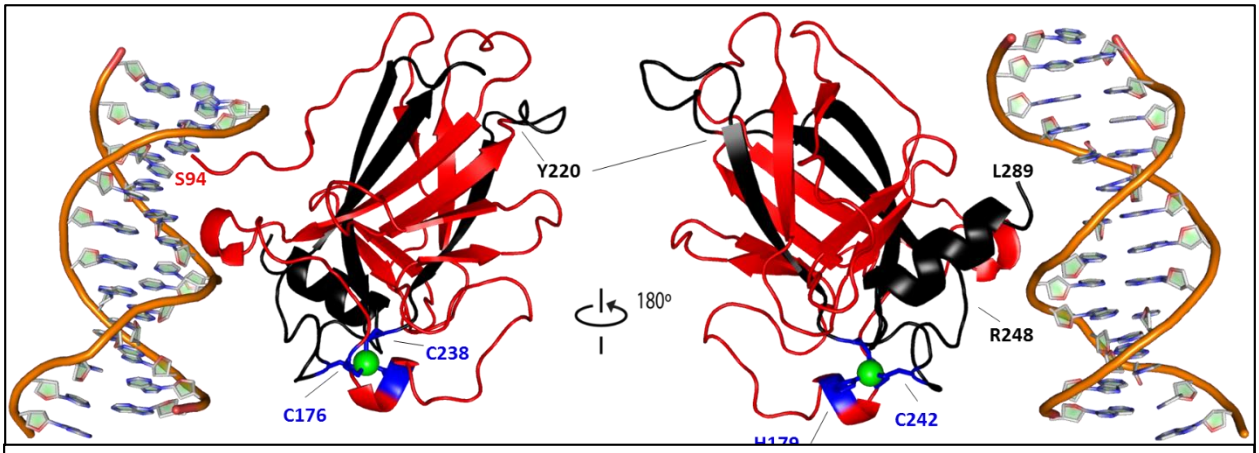

Figure 1.2: Crystal structure of p53DBD bound to DNA (PDB: 1TUP) with red highlighted region indicating the minimal construct (residues 80-200) of p53 that has been shown to interact with CypD by pulldown. It should be noted that beyond containing mostly unstructured regions, three β-strands of the p53DBD are absent from the minimal construct indicating that the minimal construct would not be able to properly fold. Zinc is colored green and the zinc-coordinating residues (C176, H179, C238 and C242) are highlighted in blue.

Over 50% of p53-related cancer mutations are associated with point mutations in p53DBD [215], [228]. These point mutations generally fall into three categories, DNA-contact mutations, DNA-binding region mutations and structural mutations [215], [229]. Contact mutants account for 20% of p53 missense mutations and are residues that actively participate in binding to DNA. These mutations typically do not have a significant impact on the folding or stability of p53; for example, mutations R273H and R248Q cannot bind DNA but more than 85% of molecules are folded at 37°C and they adopt native or slightly distorted folds [229]. DNA-binding region mutations tend to have less of an effect on DNA binding but influence the structure of p53DBD more. For example, DNA-binding region mutant R282W is globally denatured with less than 50% of the protein folded at 37°C but it can still bind DNA [229]. Finally there are structural mutations which are often associated with large global distortions in the protein such as V143A in the β-sandwich region or R175H and C242S in the Zinc-binding region which

are globally denatured and less than 50% folded at 37°C (near blue-colored residues in Figure 1.2) [229]. The relative stabilities of these mutant p53 proteins can alter the signaling mechanism and outcome of p53-driven cell cycle arrest or apoptosis. Additionally, these mutations can lead to changes in the interaction of p53 with other signaling molecules. Of specific importance is the interaction between p53 and the diverse chaperone family of heat shock proteins (HSPs) [230]–[234].

1.6.1 p53-associated Heat-Shock Proteins

WT p53 is short-lived in the cell and its half-life ranges from roughly 5 to 30 minutes starting from synthesis to ubiquitination and proteasomal degradation. p53 is ubiquitinated by the E3 ligase MDM2 primarily on C-terminal lysine residues 370, 371, 372, 381, 382 and 386 [235]–[239]. MDM2-targeted degradation of p53 under non-stress conditions is an efficient process that keeps the relative cellular levels of p53 low [235]. Inhibition of MDM2 leads to cellular stabilization and accumulation of p53 which ultimately causes cell cycle arrest and cell death by apoptosis. Stabilization of p53 through inhibition of MDM2 is currently being investigated as a potential cancer treatment to restore the tumor suppressive functions of p53 [240]. Conversely, some cancer types overexpress MDM2 which depletes p53 levels and inhibit p53's function as a tumor-suppressor [235], [241], [242]. While the mechanisms in different cancers vary, there is a growing body of evidence that cellular stability of p53 is influenced by multiple chaperone proteins. For example, heat shock protein gp96 promotes cancer cell survival by interacting with both p53 and MDM2 to decrease the levels of p53 [243]. Conversely, knockdown of gp96 inhibited tumor growth *in vivo* and promoted apoptosis. Similarly, heat-shock protein 90 (HSP90) has been shown to both directly interact with

WT and structurally destabilized mutant p53 to restore its cellular function as well as protect WT p53DBD from aggregation during prolonged incubation at 37°C *in vivo* [230], [244], [245]. HSP90 can also inactivate MDM2 and thereby maintain the tumor suppressor functions of p53 [246], [247]. Finally, both WT and misfolded p53 mutants have been associated with stabilization by HSP70. Overexpression of HSP70 has been proposed to sequester pools of misfolded p53 to allow natively folded p53 to regain its tumor suppressive functions [222], [233], [248].

p53 protein is an inherently unstable and stress-sensitive protein that can be easily destabilized by single point mutations which commonly occur across many cancers. Furthermore, additional stressors such as changes in pH [215], [249]–[251], the presence of unfolded proteins such as during ER stress [252], [253], and numerous PTMs [254]–[257] can also drastically reduce the stability of p53 protein. In instances where p53 is destabilized, HSP chaperone proteins are required for the rescue of p53 function.

1.6.2 Mitochondrial Heat-Shock Proteins

Human mitochondria contain almost 1000 distinct proteins; however only 13 protein coding genes exist in the mitochondrial genome indicating that the majority of mitochondrial proteins are imported from the cytosol [258], [259]. The majority of proteins imported into the mitochondria enter through the translocase of the inner membrane / translocase of the outer membrane (TIM/TOM) complex [136], [260], [261]. The TIM/TOM complex pore diameter is estimated to be 1.9-2.9 nm, depending on the assembly, which suggests that proteins must be unfolded in order to pass through [261]–[263]. Once inside or concomitant with import into the mitochondria, the unfolded

proteins need to be refolded to regain functionality. As such, the mitochondria have an extensive network of chaperone proteins to assist with protein refolding. One of the most prominent and most studied family of mitochondrial chaperone proteins is the HSP70 family which has been associated with the TIM/TOM complex on both the cytosolic and mitochondrial matrix sides [259], [264]. On the cytosolic side, HSP70 partially unfold proteins targeted to the mitochondria and on the receiving end, HSP70 associated with TIM serves as a motor protein to drive import of the target protein. The cytosolic interaction of p53 and HSP70 has already been discussed in *1.6.1* however it is important to add that mitochondrial HSP70 overexpression protects cells against mPT following I/R injury [265], [266] implying that it could be possible for p53 and mitochondrial HSP70 to have a joint role in ROS-induced mPT and necrosis.

An additional set of chaperones exists in the mitochondrial matrix to facilitate refolding of the entering proteins. The HSP60 family of chaperones are known to form large homo-oligomeric complexes that facilitate folding of proteins within a large inner cavity [267], [268] . Moreover, both cyclophilin D [269] and p53 [2], [270], [271] have been shown to be associated with mitochondrial HSP60 with roles relating to both mPT and apoptosis [16], [269]–[271].

In addition to HSP60, both CypD and p53 interact individually with HSP90. In the context of unfolded, mutant, p53 in cancer cells, cytoplasmic HSP90 can bind to and stabilize misfolded p53 [12], [218]. Furthermore, HSP90 prevents aggregation of WT p53 under elevated temperatures *in vitro* indicating that HSP90 has a critical role in maintaining the homeostasis of proper p53 folding [230], [244], [272]. Human mitochondria contain both a pool of cytosolic HSP90 that has been translocated into the

matrix as well as a more prominent mitochondrial-specific HSP90 homolog known as the Tumor Necrosis Factor Receptor-Associated Protein-1 (Trap1) which does not have any known cytoplasmic function; both of these mitochondrial HSP90-family chaperones are significantly overexpressed under stress conditions and in multiple cancers [12], [273], [274]. Inhibition of Trap1 and HSP90 using the mitochondria-targeted HSP90 inhibitor Gamitrinib (a 17-AAG analogue), sensitizes cells to mPT in a CypD-dependent manner [11], [275]. It is also known that overexpression of Trap1 protects cells from undergoing mPT in response to I/R injury while knockout, similar to inhibition, of Trap1 sensitizes cells to mPT in response to I/R injury [266], [274]–[276].

1.7 General overview of chapters

The following section summarizes the individual chapters of this thesis and gives an overview how they are connected in an effort to ease the reader's understanding of the motivation, specific content and global implications of this thesis work.

1.7.1. Chapter 1

Chapter 1 introduces the specific biological concepts and molecules that are the focus of this thesis. It is structured to first broadly introduce the globally motivating concept of irreversible tissue damage caused by necrotic cell death in response to reperfusion injury following a period of ischemia as is observed in victims of ischemic stroke. Since necrosis is triggered by opening of the mitochondrial permeability transition pore, the mPTP's function and known components are then discussed with a focus on its key regulator, cyclophilin D. A brief discussion about cyclophilin inhibitors follows before transitioning into the recent, groundbreaking work, which for the first time, implicates the tumor suppressor p53 in regulating necrotic cell death in response to I/R

injury. The introduction ends with a discussion of protein-folding chaperones, specifically the heat-shock proteins, and their currently known interactions with CypD and p53. The focus of this thesis is to better understand how CypD, p53 and certain members of the mitochondrial heat-shock proteins collaborate to regulate mPT and subsequent necrosis.

1.7.2. Chapter 2

This chapter describes common methods that are used across multiple chapters in an effort to minimize redundancy. More specific methods are described in the relevant chapters.

1.7.3. Chapter 3

As discussed in the introduction, p53 is an inherently unstable protein and its relative folding state has a major influence in its ability interact with other proteins. This chapter discusses how the expression of recombinant p53, either in *E.coli* or SF9 cells, affects the protein's stability and how this in turn influences the interaction between p53 and CypD. The general findings indicate that p53 expressed in SF9 cells is thermodynamically destabilized when compared to protein expressed in *E.coli.* We find that CypD will only interact with the less stable protein from SF9 cells.

1.7.4. Chapter 4

Having established that there is an interaction between CypD and p53 expressed in SF9 cells, this chapter aims to further characterize the nature of the CypD interaction with p53. I find that p53 readily aggregates in the presence of active CypD. When considering the mechanism by which CypD and p53 regulate opening of the mPTP, the observation that p53 aggregates *in vitro* after interacting with CypD questions the

potential involvement of additional proteins, such as mitochondrial chaperone proteins, for functional regulation of the mPTP. Indeed, when probing the involvement of the mitochondrial chaperone Trap1 on mPT sensitization, I found that, as expected, inhibition of Trap1 sensitizes cells to mPT. Importantly, this sensitization depends on p53 as $p53^{-/-}$ cells are significantly less sensitive to mPT by Trap1 inhibition. The result of these findings is the proposition of a new model where influx of unfolded p53 into the mitochondrial matrix releases CypD from a constitutively inactive complex with HSP60/HSP90/Trap1 that then allows for CypD to participate in isomerization of its substrates including p53 and members of the mPTP to trigger its opening and subsequent cell death by necrosis.

1.7.5. Chapter 5

A general discussion and future directions.

Chapter 2: General Methods

This chapter will introduce common methods that are used across multiple chapters in an effort to minimize redundancy and potential errors. Additional, chapter-specific, methods will be described in the subsequently relevant chapters.

2.1 Protein Expression and Purification

Purified WT full-length human p53 was purchased from OriGene (Cat # TP300003). The protein was expressed in HEK293 cells as a C-terminal MYC/DDK fusion protein and affinity purified. Protein purity is > 80% as determined by SDS-PAGE and Coomassie staining.

2.1.1 Expression and purification of recombinant human CypD and p53DBD

N-terminally His6 tagged human CypD (residues 45-206) was cloned into expression vector 2BT (Addgene, Plasmid #29666) transformed into *E.coli* BL21 DE3 cells, lysed by sonication and purified by FPLC (GE AKTA purifier) using an ion exchange column (GE HiTrapS) followed by a Ni-NTA affinity purification (GE HisTrap). 6xHIS tag was cleaved using tobacco etch virus (TEV) protease during overnight dialysis into 20 mM KHPO4 pH 7.7, 1 mM DTT for gel-filtration (GE HiLoad 16/60 Superdex 200) by FPLC.

WT GST-CypD and the GST-CypD mutants R55A, F60A, F113A, and W121A were cloned into expression vector 2GT (Addgene, Plasmid #29707), transformed into *E.coli* BL21DE3 cells and lysed using a high-pressure homogenizer (Avestin Emulsiflex C3). Proteins were purified by FPLC using a Ni-column (GE HisTrap) followed by an ion exchange column (GE HiTrapS). 6xHIS was cleaved using TEV during overnight dialysis into 20 mM TRIS pH 8.0, 50 mM NaCl, 1 mM DTT, 5% glycerol followed by gel filtration (GE HiLoad 16/60 Superdex 200) by FPLC.

^{15}N CypD (residues 45-206) was expressed in BL21DE3 cells grown in M9 minimal media containing $^{15}NH_4Cl$ [277] then lysed by sonication. Protein was purified by FPLC with ion exchange column (GE HiTrapS) followed by Ni-column (GE HisTrap). 6xHIS tag was cleaved using TEV during overnight dialysis into 20 mM $KHPO_4$ pH 7.7, 1 mM DTT for gel filtration (GE HiLoad 16/60 Superdex 200) by FPLC.

N-terminally tagged 6xHIS-p53DBD (residues 94-312) was expressed using the Bac-to-Bac Baculovirus Expression System (LifeTechnologies) and vector pFastBac HTb and purified with standard protocol. In brief, cells were lysed (50 mM Tris-HCl pH 8.5, 500 mM NaCl, 20 mM Imidazole, 5 mM 2-mercaptoethanol, 10% glycerol) and p53 was purified from cleared lysates by batch Ni-NTA purification. Protein 6xHIS tag was cleaved using TEV during overnight dialysis into 50 mM NaH_2PO_4 pH 7.4, 5 mM DTT. Protein purity is > 90% as determined by SDS-PAGE and Coomassie staining.

2.2 Tissue Culture and Lysate Generation

Mouse embryonic fibroblasts (MEFs) and human HCT116 cells were grown in DMEM+10%FBS. WT and $p53^{-/-}$ MEF cell lines were established from E13.5 embryos [2] and $CypD^{-/-}$ MEFs were purchased from ArtisOptimus [2]. HCT116 WT and isogenic HCT116 $p53^{-/-}$ cells were provided by Dr. Bert Vogelstein, Howard Hughes Medical Institute, Baltimore, MD. Lysates were generated by scraping cells into PBS with 1%TritonX100 and complete EDTA-free protease inhibitors (Sigma), lysed by 3x freeze-thaw and cleared of cell debris by centrifugation at 4000 g for 5 min. Cyclosporine A was purchased from Sigma (Cat #30024). Calcein and Ionomycin were purchased from LifeTechnologies (Cat #C3100MP and #I24222). Gamitrinib was kindly provided by Dr. Dario Altieri, Wistar Institute, Philadelphia, PA.

2.3 Biochemical Assays

2.3.1 Pulldown Assay

GST pulldown experiments were conducted in PBS/1%TritonX100. GST, GST-CypD or GST-CypD mutants were bound to glutathione beads for 1 hr at 4 °C (ThermoScientific, Cat #15160), then blocked in PBS/1%TritonX100/1%BSA for 1 hr at 4 °C. Blocked beads were incubated with lysates for 16 hours at 4 °C in the presence of CsA where indicated. Beads were pelleted, thoroughly washed in PBS/1%TritonX100 and analyzed by immunoblot.

2.3.2 NMR Experiments

The ^{1}H, ^{15}N HSQC spectra were obtained on 50 μM ^{15}N CypD in the presence or absence of 100 μM p53DBD using a Bruker Avance3 700 MHz magnet. The spectra were obtained at 25 °C with 64 scans, TD2=2048, TD1=128 with spectral widths of 13,586.95 Hz (^{1}H) and 3101.73 Hz (^{15}N). Topspin 3.2 (Bruker) was used for processing the spectrum and CCPNMR analysis 2.1 was used to generate the figure. CypD crosspeak assignments were taken from Biological Magnetic Resonance Bank (BMRB) accession number 7310 [278]. We obtained NMR data in two different buffers: 50 mM NaH_2PO_4, 5 mM DTT, 10% D_2O, pH 7.4 and 20 mM Tris pH 8.0, 0.25 M KCl, 5 mM β-ME, 0.1 M Imidazole, 5% glycerol, 1% Triton X-100, 10% D_2O.

2.3.3 CypD Activity Assay

Prolyl cis/trans isomerization of the fluorescent aminobenzoyl-Ala-Phe-Pro-Phe-4-nitroanilide (Abz-AFPF-pNA) peptide was monitored by changes in fluorescence emission at 416 nm upon excitation at 316 nm (FM4 Horriba-Jobin Yvon) in 50 mM NaH_2PO_4 + 5 mM DTT at 15 °C. Abz-AFPF-pNA maintains the fluorescence-quenched

cis conformation in anhydrous trifuoroethanol (TFE) + 50 mM LiCl, but adopts the fluorescent trans conformation in aqueous buffer 50 mM NaH_2PO_4 + 5 mM DTT. CypD (0-15 nM) was pre-equilibrated and the isomerization reaction was started by addition 3 nM Abz-AFPF-pNA. The reaction was monitored for 400 sec and data points were recorded every second with an integration time of one second.

2.4 Protein Denaturation Assays

2.4.1 Urea Denaturation Assay

Denaturation of *E.coli* and SF9 p53DBD as well as WT CypD was monitored by changes in protein fluorescence using a Jobin Yvon Fluoromax-4 (Horiba) spectrofluorimeter exciting at 280 nm (bandpass 2.5 nm) and scanning emission 300-400 nm (bandpass 7 nm), integration time 0.1 sec. Each protein was individually added to a final concentration of 2 µM in 900 µl of buffer containing 50 mM NaH_2PO_4 + 5 mM DTT and increasing amounts of urea from 0-8 M in 48 increments of 166.7 mM. The sample was incubated for 30 minutes at 25 °C before the fluorescence was recorded.

2.4.2 Thermal Denaturation Assay

Denaturation of *E.coli* and SF9 p53DBD as well as WT CypD and CypD mutants was monitored by changes in protein fluorescence using a Jobin Yvon Fluoromax-4 (Horiba) spectrofluorimeter exciting at 280 nm (bandpass 2.5 nm) and scanning emission 300-400 nm (bandpass 7 nm), integration time 0.1 sec. Each protein was individually added to a final concentration of 2 µM in 200 µl of buffer containing 50 mM NaH_2PO_4 + 5 mM DTT. The sample was incubated for 1 minute at each 1 °C from 20-80 °C before the fluorescence at each temperature was recorded.

Chapter 3: Investigating the role of p53 stability on its interaction with CypD

Work in this chapter is credited to several people:

Ivan Lebedev designed, performed and analyzed all the SF9 p53DBD-related biochemical and DSC-related experiments.

Zachariah Foda designed, performed and analyzed the initial *E.coli* p53DBD-related experiments prior to SF9 expression.

Dr. Franz Schmidt and Dr. Philipp Schmidpeter designed the CypD activity assay.

Dr. Markus Seeliger and Dr. Ute Moll advised the design, techniques and analysis of the biochemical experiments.

3.1 Introduction

Recent work has uncovered a novel function of p53 in the mitochondria relating to the regulation of mitochondrial permeability transition and subsequent necrotic cell death [2]. In this study, it was shown that in response to cellular stress, a cytoplasmic pool of p53 translocates into the mitochondrial matrix where it interacts with the key regulator of mPT, CypD, and triggers opening of the mPTP. Knockdown of p53 or inhibition of CypD prevents mPT and this phenomenon is verified in a mouse stroke model. This is the first time that p53 has been associated with cell death by necrosis and opens numerous opportunities for pharmacological intervention to prevent necrotic cell death which is the ultimate result of I/R injury such as observed in victims of ischemic stroke and myocardial infarction.

The overarching aim of this work is to better understand the nature of the interaction between p53 and CypD and how it regulates opening of the mPTP. The initial model used to motivate the original approach at characterizing the CypD interaction with p53 postulated that the p53 protein, through its DNA binding domain, binds to and forms a stable complex with CypD which activates CypD and allows for it to facilitate opening of the mPTP. This model was supported by the ability of CypD to pulldown and co-immunoprecipitate p53 from purified mitochondria [2]. With this first model in mind, the original approach was to characterize the binding interface of CypD and p53DBD using biophysical methods such as X-ray crystallography and NMR in order to identify the key CypD and p53DBD residues involved in binding. However, all attempts to capture and quantify a binding event of *E.coli* expressed CypD with *E.coli* expressed p53DBD failed. All quality control experiments indicated that both proteins

were folded, had the correct mass and behaved *in vitro* as expected, however no *in vitro* binding data could be successfully obtained. Moreover, the mammalian cell work maintained that CypD and p53DBD bind to each other and the animal data was clear that some kind of interaction between CypD and p53 did exist [2].

Several explanations for why *E.coli* p53DBD was incompatible with CypD binding arose including, the potential need for post translational modifications on either protein, differential folding of *E.coli* expressed p53DBD compared to mammalian or some unknown bridging protein to facilitate the interaction of p53 with CypD. Producing sufficient quantities of p53 protein expressed in mammalian cells for biophysical experiments such as X-ray crystallography and NMR is prohibitively costly. However, a baculoviral expression system from SF9 cells had already been established. Expressing protein in SF9 cells could also partially address some of the limitations of *E.coli* expression including some post translational modifications as well as more complex protein folding machinery that *E.coli* lack [279]. Indeed, p53DBD that was expressed in SF9 cells was able to interact with CypD however the nature of the interaction did not fit the originally proposed model. Specifically, p53 and CypD did not form a stable complex but the activity of CypD caused formation of insoluble p53 aggregates which is discussed in greater detail in Chapter 4. This chapter explores the effect of the protein expression source on p53DBD, with emphasis on the intrinsic protein stability and how it affects its ability to interact with CypD *in vitro*. The general findings are that SF9 expressed p53DBD is thermodynamically destabilized when compared to *E.coli* p53DBD, and only the destabilized SF9 p53DBD interacts with CypD *in vitro*.

3.2 Methods

The work in this chapter employs some of the general methods described in chapter 2 including expression and purification of CypD and p53DBD from both *E.coli* and SF9 sources, urea denaturation assays, thermal denaturation assays, pulldown assays, and NMR.

3.2.1 FITC Labeling of CypD and p53

CypD and *E.coli* p53DBD proteins were fluorescein isothiocyanate (FITC) labeled (Thermo 46424) on lysine residues by buffer exchanging each protein into 50 mM NaH_2PO_4 + 5 mM DTT pH 7.4 using a PD-10 desalting column (GE). A ratio of 20 mM protein to 100 mM FITC in 3.5 ml 50 mM NaH_2PO_4 + 5 mM DTT pH 7.4 was incubated overnight at 25 °C protected from light. Unbound label was removed by buffer exchanging the labeled protein into fresh 50 mM NaH_2PO_4 + 5 mM DTT pH 7.4 or 20 mM Tris pH 8.0, 0.25 M KCl, 5 mM β-ME, 0.1 M Imidazole, 5% glycerol, 1% Triton X-100 using a PD-10 desalting column (GE) as specified. The degree of labeling was determined by comparing the ratio of protein absorbance at 280 nm to FITC absorbance at 495 nm.

3.2.2 Fluorescence Anisotropy

Fluorescence anisotropy was measured with a Jobin Yvon Fluoromax-4 (Horiba) spectrofluorimeter by monitoring the anisotropy at 25 °C of 500 nM FITC-labeled CypD in at 520 nm upon excitation at 492 nm to which 50 μM of p53DBD was titrated. Measurements were taken in a 1 cm quartz cuvette (Starna Cells 16.160F-Q-10/Z15) containing a starting volume of 200 μl. Each anisotropy value at every concentration point was the average of three individual anisotropy measurements. Anisotropy buffers

used were 50 mM NaH_2PO_4 + 5 mM DTT pH 7.4 or 20 mM Tris pH 8.0, 0.25 M KCl, 5 mM β-ME, 0.1 M Imidazole, 5% glycerol, 1% Triton X-100.

3.2.3 Analytical Gel Filtration

E.coli p53DBD, CypD, or *E.coli* p53DBD with CypD samples were loaded on a Superdex 200 10/300 analytical gel filtration column (GE) connected to an Åkta Explorer FPLC system (GE). The column was equilibrated and run in the same buffer as that of the sample (100 mM NaH_2PO_4 pH 7.4) at 4 °C. The proportions of the different species were determined by integration of the areas of the elution peaks using the GE UNICORN Evaluation package.

3.2.4 Isothermal Calorimetry

The heat of p53DBD binding to CypD was measured in a VP-ITC instrument (Micro-cal) at 25 °C in 100 mM NaH_2PO_4 pH 7.4. 5 μM p53DBD was titrated to 500 nM CypD in 25 injections spaced across 130 seconds.

3.2.5 Differential Scanning Calorimetry

The melting temperature of 80 μM E.coli p53DBD was determined using a Microcal VP-DSC (MicroCal) in a cell volume of 0.52 ml. For each measurement, the samples were degassed for 30 minutes and the instrument recorded heat buffer blanks from 10-80 °C at the rate of 60 °C/hour followed immediately by cooling from 80-10 °C at the rate of 60 °C/hour in order to establish a thermal history as suggested by the manufacturer. Upon cooling to 10 °C, the buffer blanks were once again heated from 10-80 °C, the buffer blank was aspirated at approximately 15 °C and the protein-containing sample was injected while the instrument remained in-cycle as recommended by the manufacturer. The following heating cycle was continued followed

by one cooling cycle. This was repeated for each buffer and the pressure was always set to 2 pounds per square inch (PSI). Data analysis was performed with MicroCal Origin software [280].

3.3 Results

3.3.1 The expression source of p53 affects its ability to interact with CypD

Until this point, the standard biochemical assay to show an interaction between CypD and p53 was the pulldown assay where CypD was expressed as a GST fusion protein and immobilized on glutathione beads. These beads were then exposed to mammalian cell lysates from HCT116 cells or mouse embryonic fibroblasts (MEFs) to pulldown CypD-binding proteins. The pulldown, being the hallmark experiment to test for p53 binding to CypD, was among the first experiments attempted upon successful expression and purification of *E.coli* p53DBD. Surprisingly, no pulldown of *E.coli* p53DBD by CypD could be detected (Figure 3.1).

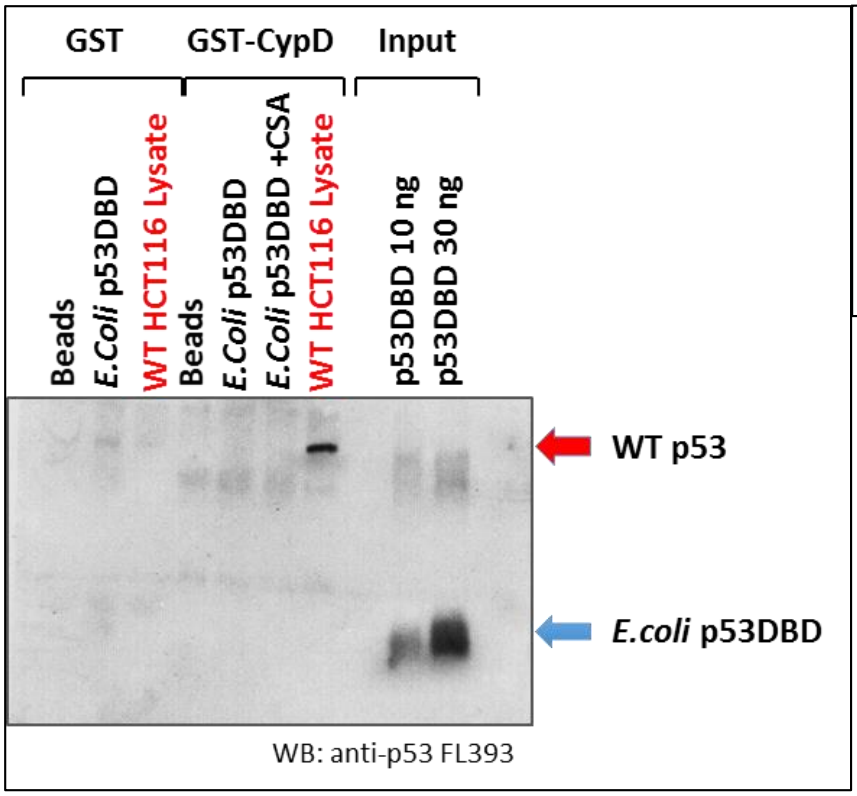

Figure 3.1 *E.coli* p53DBD is not pulled down by GST-CypD. While full-length, endogenous p53 from WT HCT116 cells, labeled in red, can be pulled down by GST-CypD, in a CsA dependent manner, as expected and previously shown [2].

In parallel to the standard pulldown assays, an established CypD activity assay was available which tracks the CypD-driven catalysis of *cis-trans* isomerization of a CypD substrate peptide 2-aminobenzoyl-Ala-Phe-Pro-Phe-4-nitroanilide (Abz-AFPF-pNA), as described in the general methods [281]. The peptide is stored in an anhydrous solution (50 mM LiCl in 2,2,2-trifuloroethanol) where it maintains the *cis* conformation about the proline bond bringing the fluorophore 2-aminobenzoyl into close proximity of the 4-nitroanilide quencher. When the peptide is diluted into an aqueous buffer (50 mM NaH_2PO_4 pH 7.4 + 5 mM DTT) it isomerizes to form the *trans* conformation which moves the 2-aminobenzoyl away from the 4-nitroanilide quencher and an increase in fluorescence at 412 nm (excitation 312 nm) can be monitored. CypD, catalyzes the *cis-trans* isomerization rate. This assay was initially developed by collaborators Franz Schmidt and Philipp Schmidpeter at the University of Bayreuth, Germany. We expected

that p53DBD could be an inhibitor or substrate of CypD and therefore compete with the Abz-AFPF-pNA peptide. CypD and p53DBD had both been successfully expressed and purified by both the Schmidt and Seeliger labs. To ensure one particular expression or purification wasn't to blame for lack of binding by pulldown, CypD activity assays were performed using each protein from each expression source; that is CypD and *E.coli* p53DBD purified by Philipp Schmidpeter (PS) and by Zachariah Foda (ZF) individually as can be seen in Figure 3.2 where the initials indicate purification source of each protein. It is clear that both purifications of CypD catalyze the isomerization of Abz-AFPF-pNA peptide and that addition of *E.coli* p53DBD from either source inhibit isomerization of Abz-AFPF-pNA by CypD indicating an interaction between CypD and p53DBD.

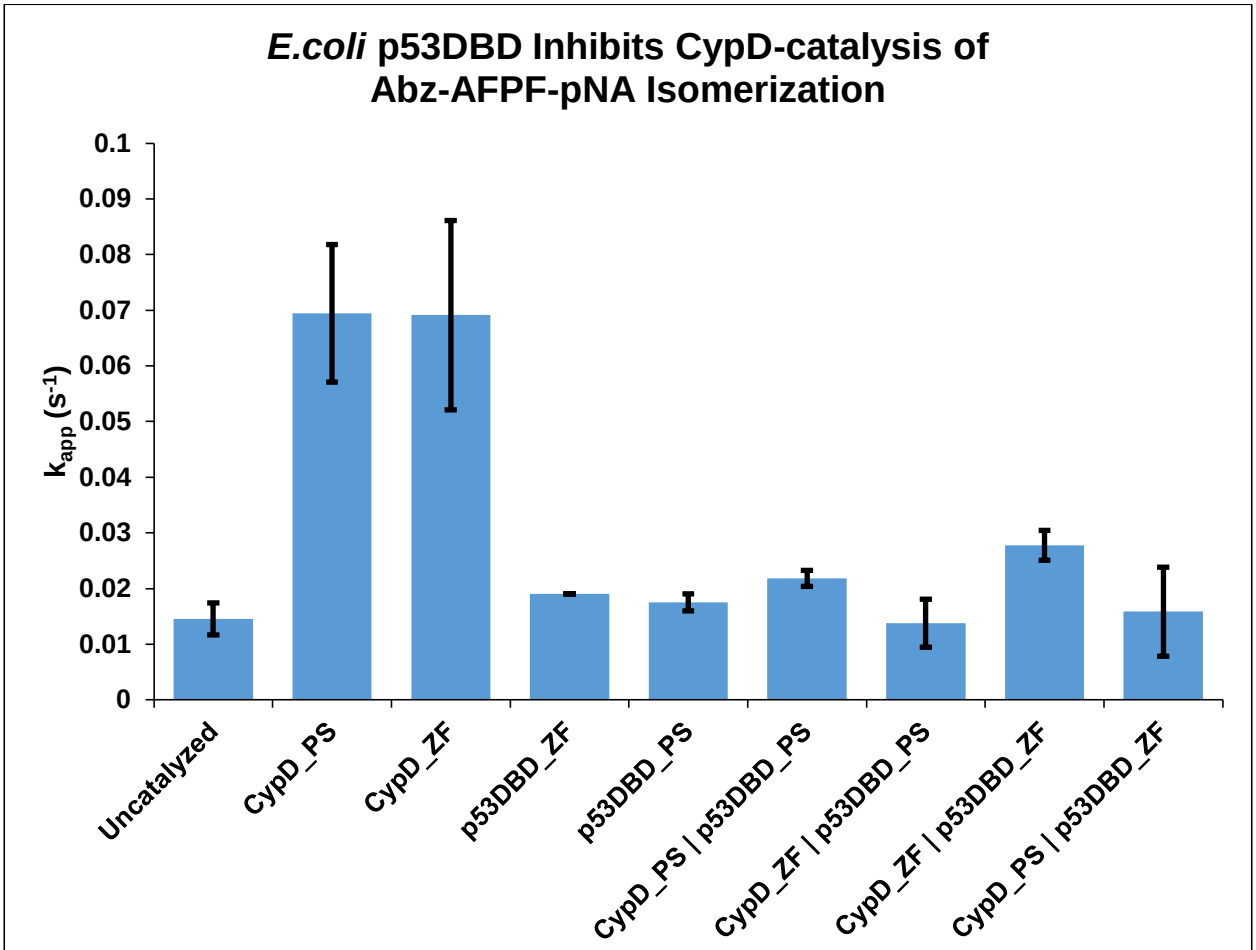

Figure 3.2: E.coli p53DBD Inhibits CypD-catalysis of Abz-AFPF-pNA Isomerization. CypD purified by both PS and ZF have the expected catalytic activity toward Abz-AFPF-pNA peptide. Addition of *E.coli* p53DBD to CypD purified by either PS or ZF inhibits CypD catalysis of Abz-AFPF-pNA peptide indicating an interaction between CypD and p53DBD. *E.coli* p53DBD alone does not affect the isomerization rate of Abz-AFPF-pNA peptide as expected. Data from 3 independent replicas, mean +/- SD are shown

Having what appeared to be an indication of an interaction between CypD and *E.coli* p53DBD, and while troubleshooting the pulldown assays, additional attempts at biophysical characterization of the CypD and *E.coli* p53DBD interaction were made at this point. The hypothesized model was still one where p53 forms a stable interaction with CypD. One simple experiment attempted was to use analytical gel filtration to compare chromatograms of CypD alone, p53DBD alone and CypD incubated with *E.coli* p53DBD. It would be expected that if a stable complex between CypD and *E.coli*

p53DBD was forming, the physically larger complex would elute at an earlier fraction than each of the other proteins on their own [282]. However, after incubating CypD with *E.coli* p53DBD and sending the expected complex through the analytical size exclusion column (buffer: 100 mM NaH_2PO_4 pH 7.4), the chromatogram failed to show any higher molecular weight species indicative of a CypD *E.coli* p53DBD complex; rather the proteins eluted at the respective individual fractions (Figure 3.3).

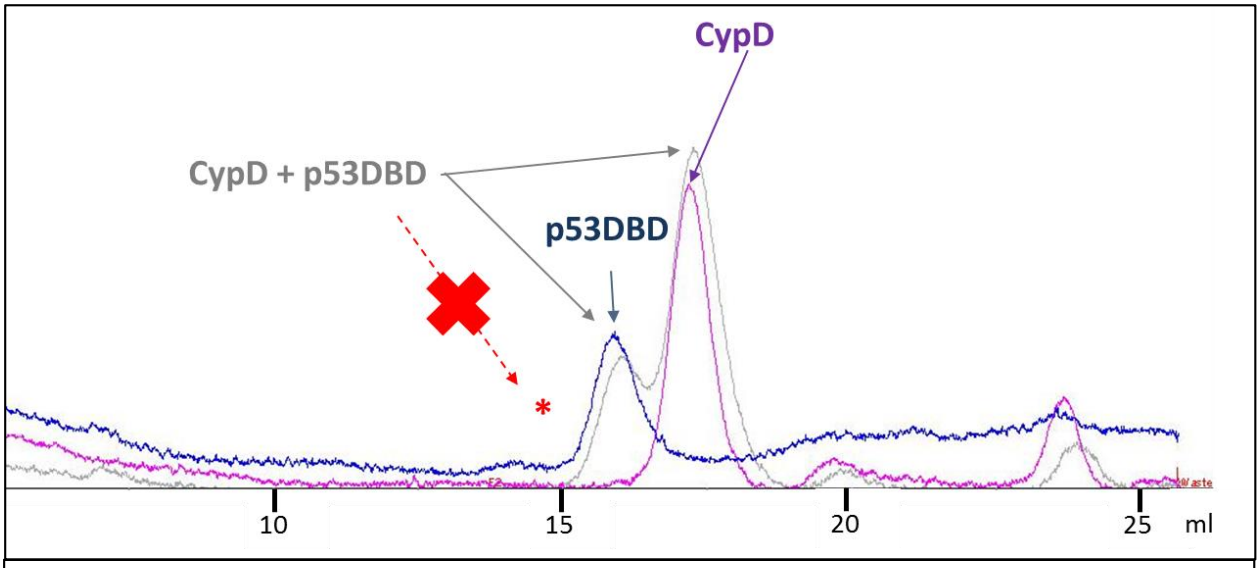

Figure 3.3 Chromatogram of analytical gel filtration of *E.coli* p53DBD alone in blue, CypD alone in purple and CypD incubated with *E.coli* p53DBD in grey. It is clear that no distinct, higher molecular weight, peak appears which would indicate a stable CypD-p53DBD complex as would have been expected and indicated in red. Instead, incubation of CypD with *E.coli* p53DBD leads only to each protein eluting at its own respective molecular weight and not in a complex as indicated in grey.

To ensure that the proteins were properly folded, thermal denaturation of *E.coli* p53DBD, and CypD, was performed while monitoring intrinsic protein fluorescence, with excitation at 280 nm and collection of the emission spectrum between 300-400 nm (buffer: 50 mM Tris pH 7.5, 100 mM NaCl, 5 mM DTT) [283]. Both CypD and *E.coli* p53DBD were found to be folded and the melting temperature (T_m) of *E.coli* p53DBD (42 °C) was similar to that previously reported in the literature [215] (Figure 3.4).

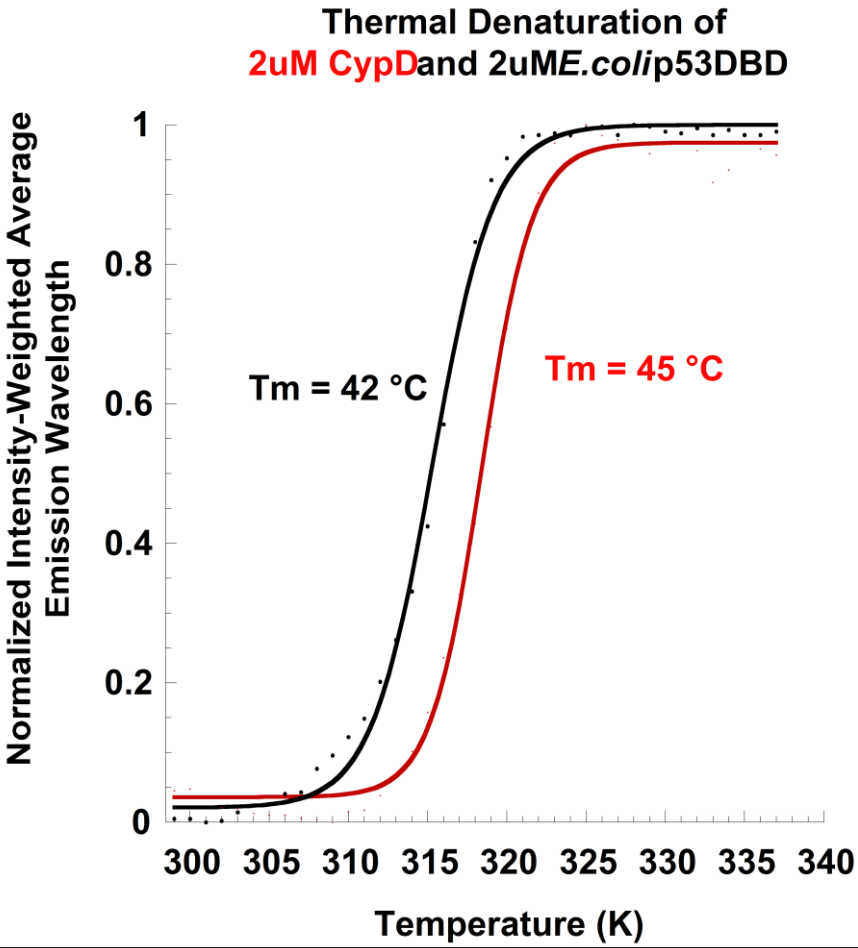

Figure 3.4 Thermal denaturation of CypD and *E.coli* p53DBD in 50 mM Tris pH 7.5, 100 mM NaCl, 5 mM DTT. The normalized intensity-weighted average emission spectrum upon thermal denaturation of 2 μM CypD is shown in red and 2 μM *E.coli* p53DBD is shown in black. These curves indicate that both proteins are folded at room temperature (approximately 25 °C or 298 K) and the T_m of *E.coli* p53DBD at 42 °C is consistent with previously published data also reporting a T_m of *E.coli* p53DBD at 42 °C [215].

Furthermore, to fully ensure that the correct protein had been expressed and purified, matrix-assisted laser desorption/ionization (MALDI) mass spectrometry [284] was employed to validate the masses of CypD and *E.coli* p53DBD proteins. The experimentally determined masses closely matched the calculated mass for each protein confirming that the correct proteins had been purified (Figure 3.5). Having established that both *E.coli* p53DBD and CypD were purified at the expected mass and that both proteins were folded, a more sensitive and exhaustive set of biophysical

experiments were employed in attempt to identify any indication of *E.coli* p53DBD binding to CypD or conversely CypD binding to *E.coli* p53DBD.

Firstly, isothermal titration calorimetry (ITC) was attempted by measuring the heat of binding upon titration of 300 μL *E.coli* p53DBD at 5 μM to 2.2 mL of 500 nM CypD (buffer: 100 mM NaH_2PO_4 pH 7.4). In brief, ITC measures the amount of energy it takes to maintain the temperature of a sample cell containing your protein sample to a reference cell [285]. Titration of a binding partner to the sample cell will cause either a small exothermic or endothermic reaction upon binding. If the reaction is exothermic, the ITC instrument will need to input less energy to maintain the sample cell temperature. If the reaction is endothermic, the ITC instrument will need to input more energy to maintain the sample cell temperature. By monitoring the energy required to maintain the sample cell temperature throughout the titration of a binding partner, the free energy of binding and dissociation constants can be calculated. However, in the case of titrating *E.coli* p53DBD to CypD, no changes in the heat of binding could be detected indicating that *E.coli* p53DBD did not bind to CypD (Figure 3.6).

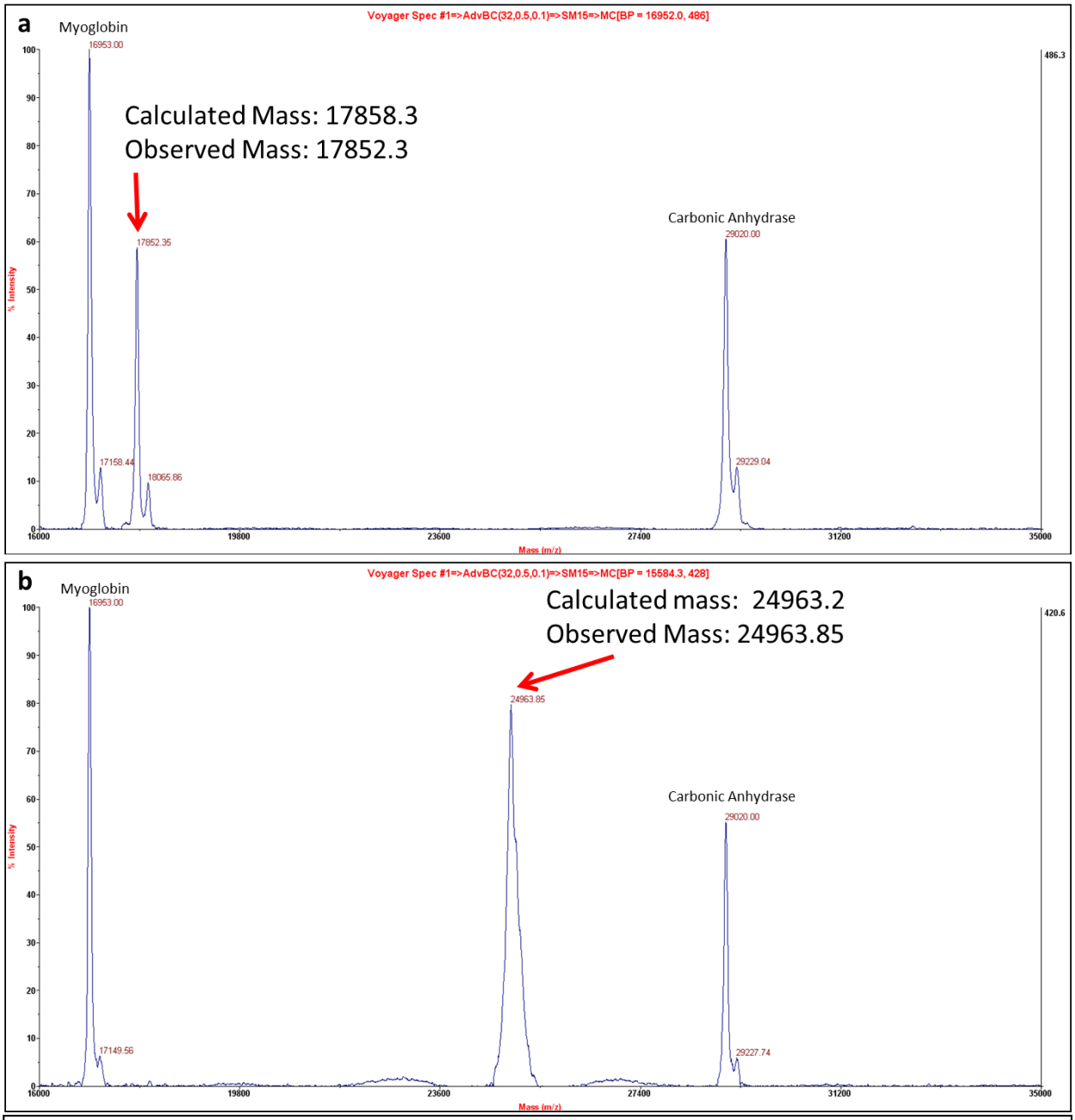

Figure 3.5 MALDI mass spectrum of CypD and *E.coli* p53DBD a) CypD with a calculated mass of 17,858.3 Da and observed mass of 17,852.3 Da and **b)** *E.coli* p53DBD with a calculated mass of 24,963.2 Da and observed mass of 24,963.85 Da indicating that both proteins were correctly purified with the expected masses.

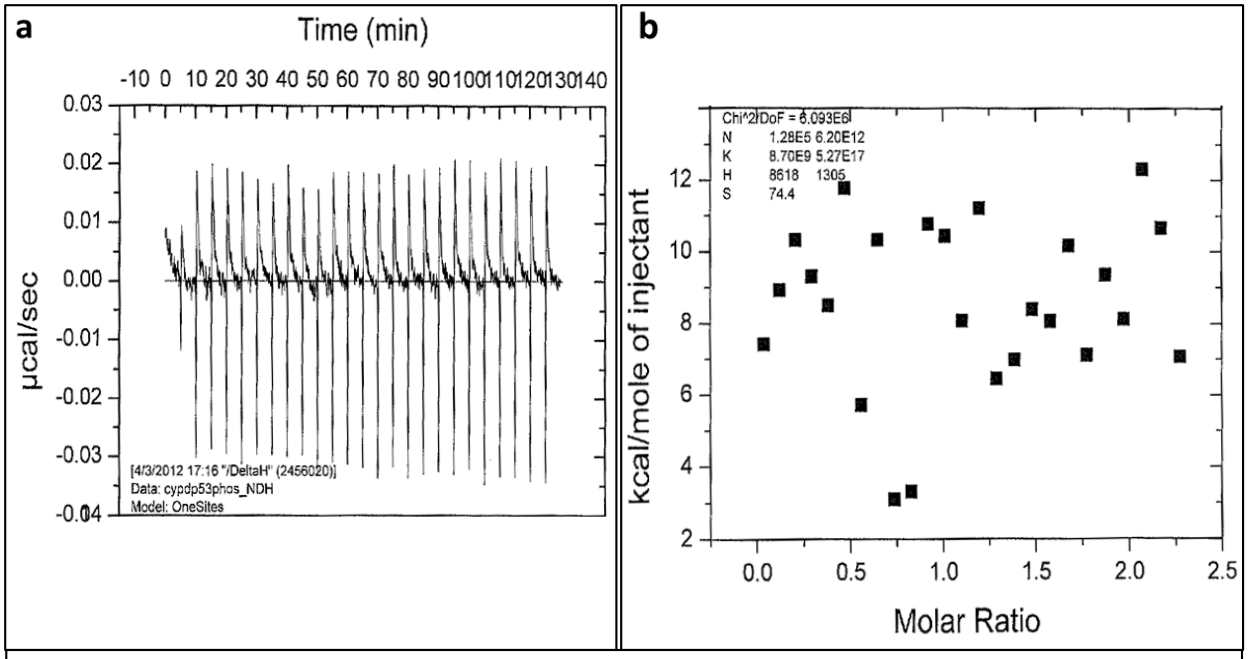

Figure 3.6 Isothermal titration calorimetry of 5 µM *E.coli* p53DBD to 500 nM CypD. a) Monitoring the change in heat input upon 25 injections of *E.coli* p53DBD to CypD over 120 minutes. It can clearly be seen that no systematic change occurs over the course of the titration indicating no ligand saturation and no binding of *E.coli* p53DBD to CypD. **b)** The energy of binding of *E.coli* p53DBD titrated to CypD does not change as the molar ratio of *E.coli* p53DBD to CypD increases indicating that no binding event occurs.

Another robust assay commonly used in the Seeliger lab to detect protein-protein or protein-ligand binding is titration fluorescence anisotropy [286]. In general, anisotropy monitors the tumbling of a fluorescently labeled ligand in solution which by itself tumbles at a certain rate that slows upon binding of a target protein due to the increased size of the complex upon binding [287]. Here, CypD was titrated to 1 µM FITC-labeled (as described in Chapter 3 methods, section 3.2.1) *E.coli* p53DBD and the anisotropy of FITC-*E.coli* p53DBD was monitored. Consistent with previous observations, no change in fluorescence anisotropy of *E.coli* p53DBD could be detected indicating once more that no binding event was occurring Figure 3.7.

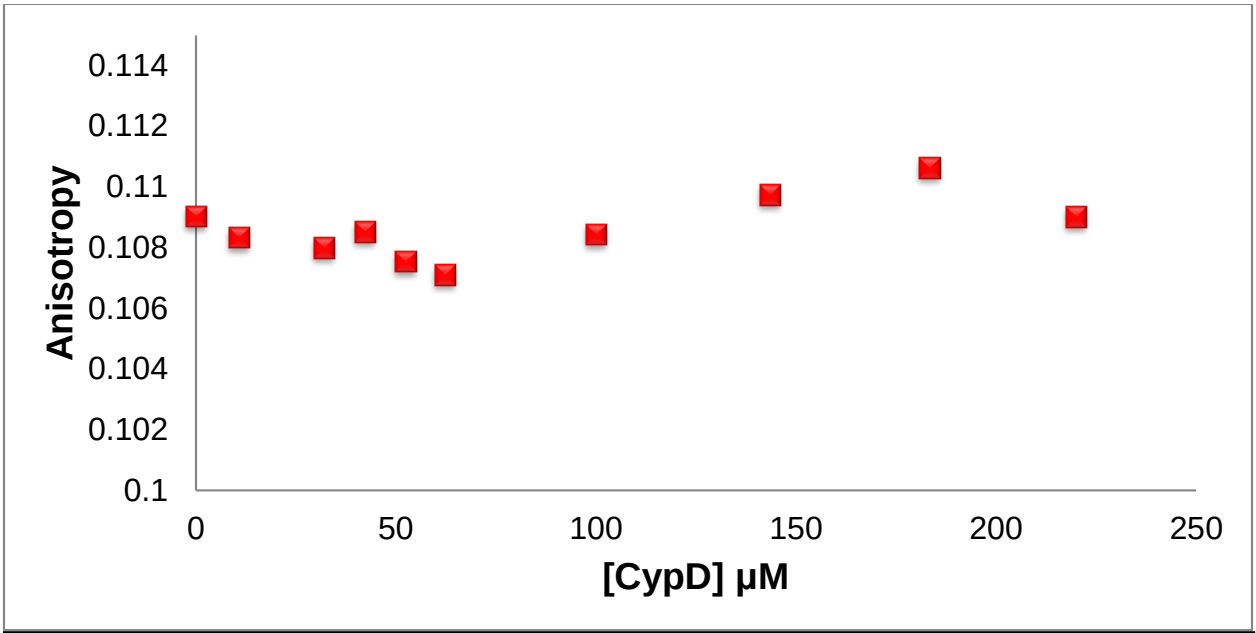

Figure 3.7 Fluorescence anisotropy of 1 μM FITC-*E.coli* p53DBD upon titration of CypD. There is no observable change in anisotropy of the FITC-labeled target *E.coli* p53DBD upon addition of CypD indicating that there is no binding of CypD to *E.coli* p53DBD.

In a final attempt to detect any indication of CypD binding to *E.coli* p53DBD, NMR was employed by recording the ^{1}H, ^{15}N heteronuclear single quantum coherence (HSQC) spectrum of ^{15}N isotopically labeled CypD upon titration of molar excess *E.coli* p53DBD. The ^{1}H, ^{15}N HSQC spectrum is commonly employed to primarily monitor the chemical shifts of backbone amides of individual residues, with the exception of proline, on a ^{15}N isotopically labeled protein. Upon binding of ligands or changes in the structure of the 15N-labeled protein, the chemical environment of the backbone nuclei change which results in a detectable change the chemical shift NMR signal [288]. Since the backbone peaks of substrate-free (apo) CypD have already been assigned (Biological Magnetic Resonance Bank [BMRB] accession number 7310 [278]), it is comparatively easy to transfer the peak assignments to the ^{1}H, ^{15}N HSQC spectrum of CypD acquired by us and monitor the relative changes in chemical shifts upon titration of *E.coli* p53DBD. The NMR peak assignment allows us to attribute each NMR signal to the

originating amino acid. Changes in the NMR spectrum (for example upon ligand binding) can then be rationalized on the protein sequence and structure. The ^{1}H, ^{15}N HSQC spectrum of apo 250 µM CypD was recorded followed by the addition of 0.6, 1.0 and 2.0 molar excesses of *E.coli* p53DBD (buffer: 50 mM NaH_2PO_4 pH 7.4, 1 mM DTT, 10 % D_2O). Unfortunately, no CypD chemical shifts could be observed once again indicating that there was no binding of *E.coli* p53DBD to CypD (Figure 3.8 a-d). As a positive control, 2 molar equivalents of CsA was added to the NMR sample already containing ^{15}N CypD and 2 molar equivalents of *E.coli* p53DBD. Upon addition of CsA, distinct chemical shifts on CypD could be detected; indicating that CsA successfully bound to CypD (Figure 3.8 e). Mapping the statistically significant chemical shift changes onto the structure of CypD bound to CsA (PDB: 2Z6W) highlights the CypD residues involved in binding CsA. Binding residues localize to the active site of CypD as would be expected from the crystal structure of CypD and CsA (Figure 3.8 f).

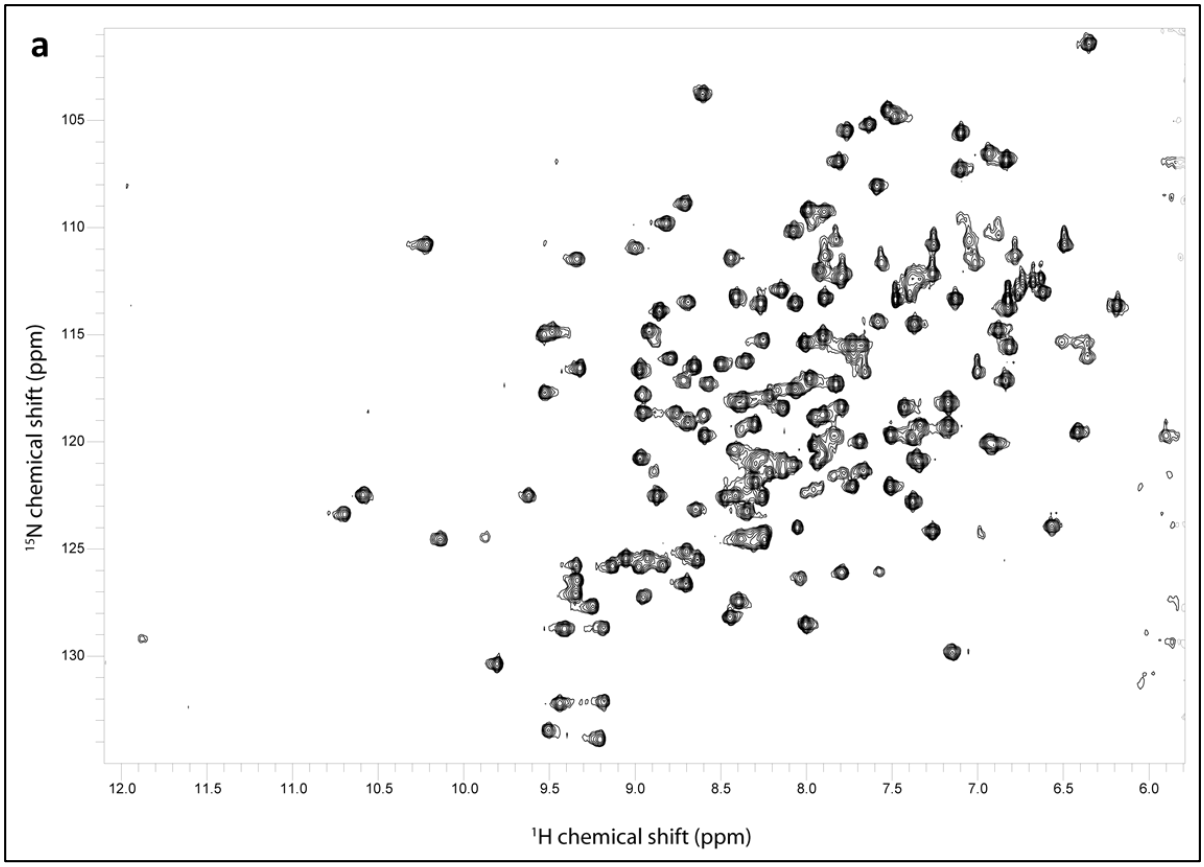
a
105
110
115
120
125
130
^{15}N chemical shift (ppm)
12.0
11.5
11.0
10.5
10.0
9.5
9.0
8.5
8.0
7.5
7.0
6.5
6.0
^{1}H chemical shift (ppm)

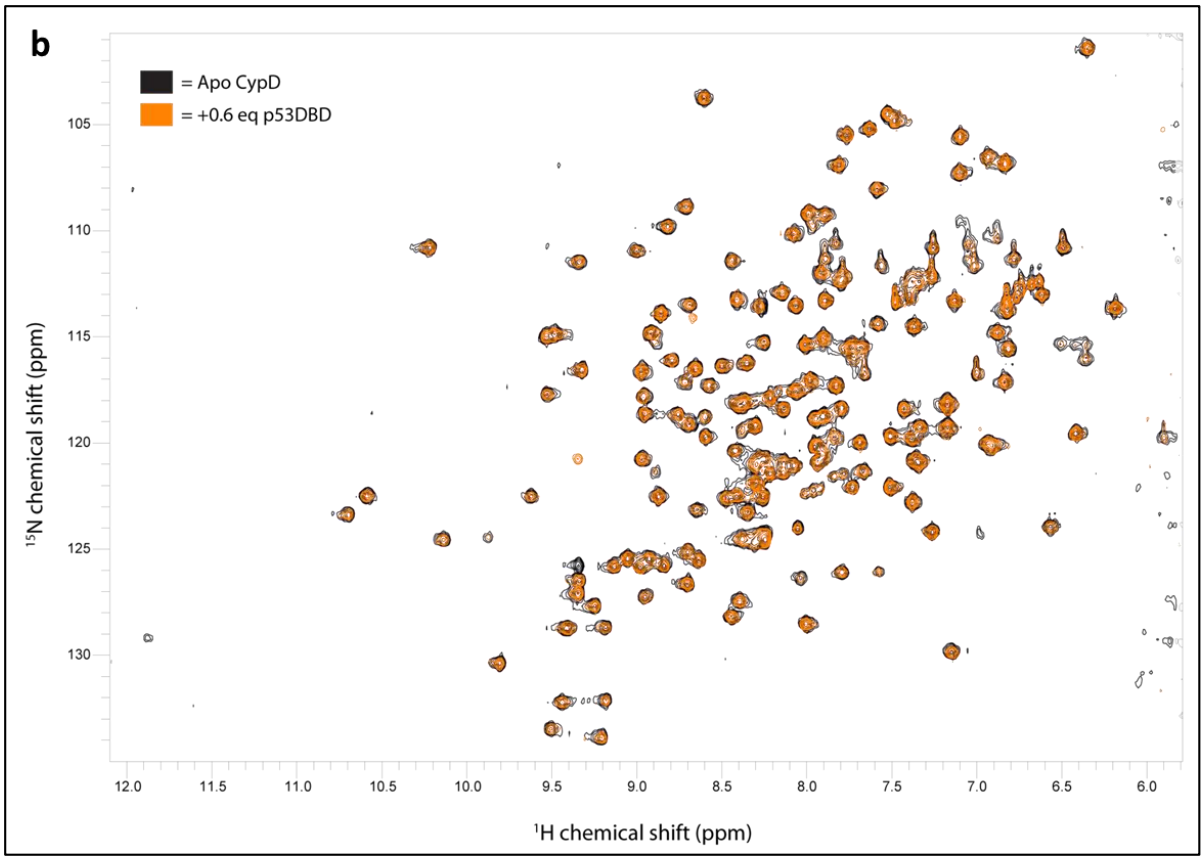
b
= Apo CypD
= +0.6 eq p53DBD
105
110
115
120
125
130
^{15}N chemical shift (ppm)
12.0
11.5
11.0
10.5
10.0
9.5
9.0
8.5
8.0
7.5
7.0
6.5
6.0
^{1}H chemical shift (ppm)

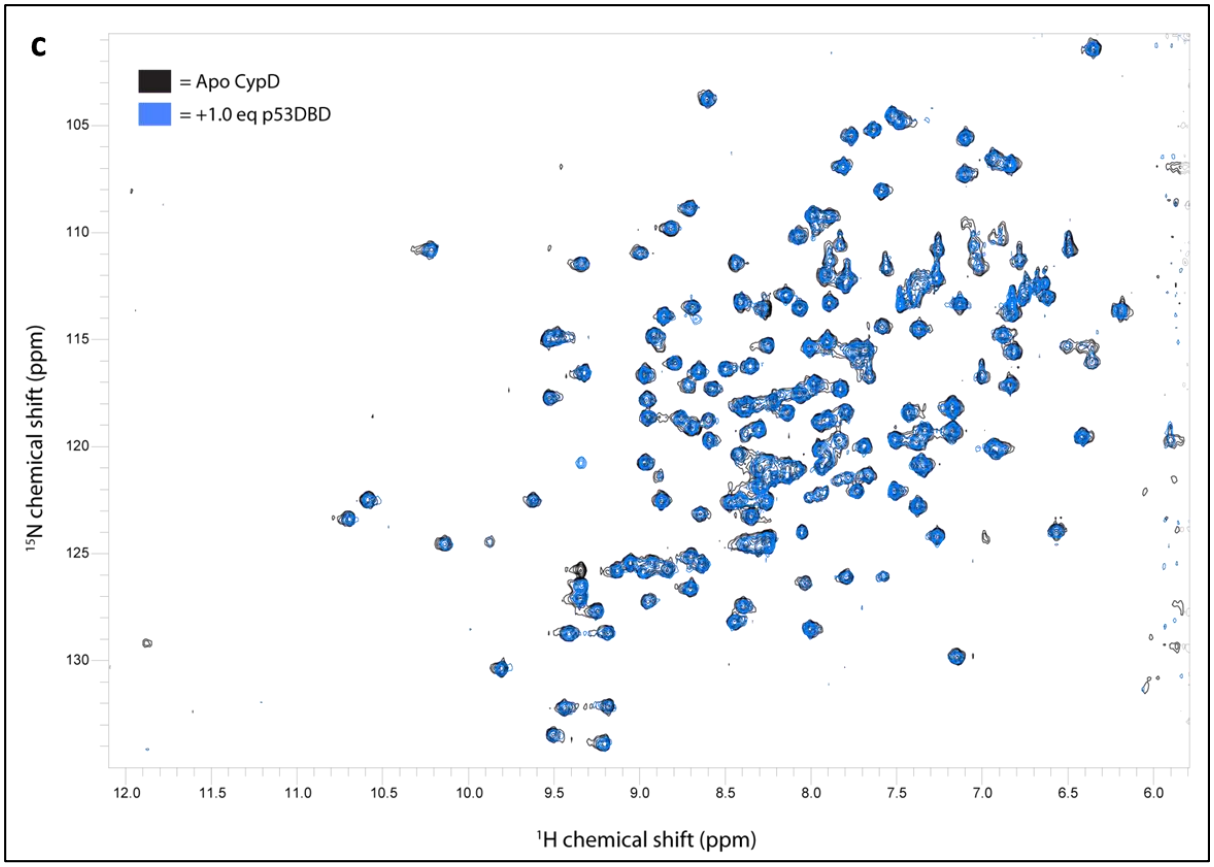
c
= Apo CypD
= +1.0 eq p53DBD
105
110
115
120
125
130
15N chemical shift (ppm)
12.0
11.5
11.0
10.5
10.0
9.5
9.0
8.5
8.0
7.5
7.0
6.5
6.0
1H chemical shift (ppm)

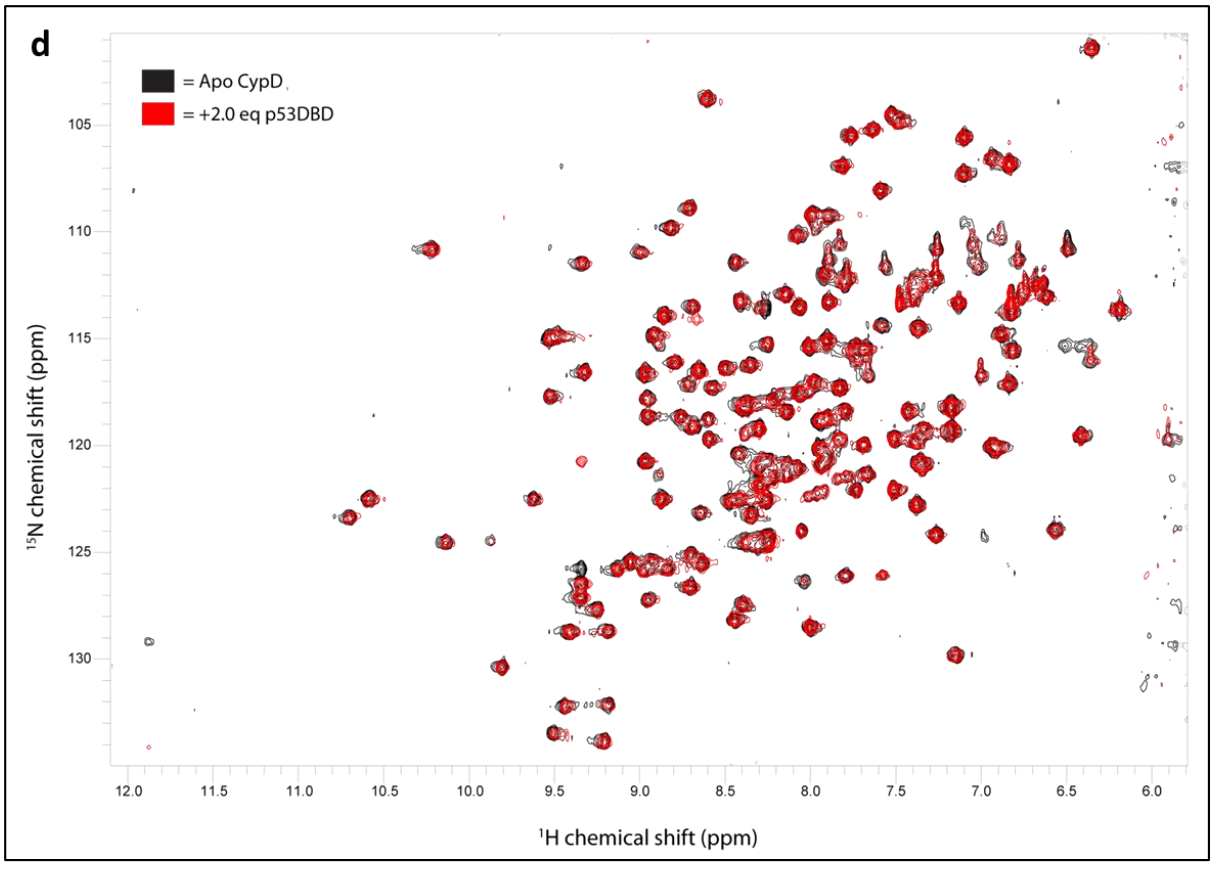
d
= Apo CypD
= +2.0 eq p53DBD
105
110
115
120
125
130
15N chemical shift (ppm)
12.0
11.5
11.0
10.5
10.0
9.5
9.0
8.5
8.0
7.5
7.0
6.5
6.0
1H chemical shift (ppm)

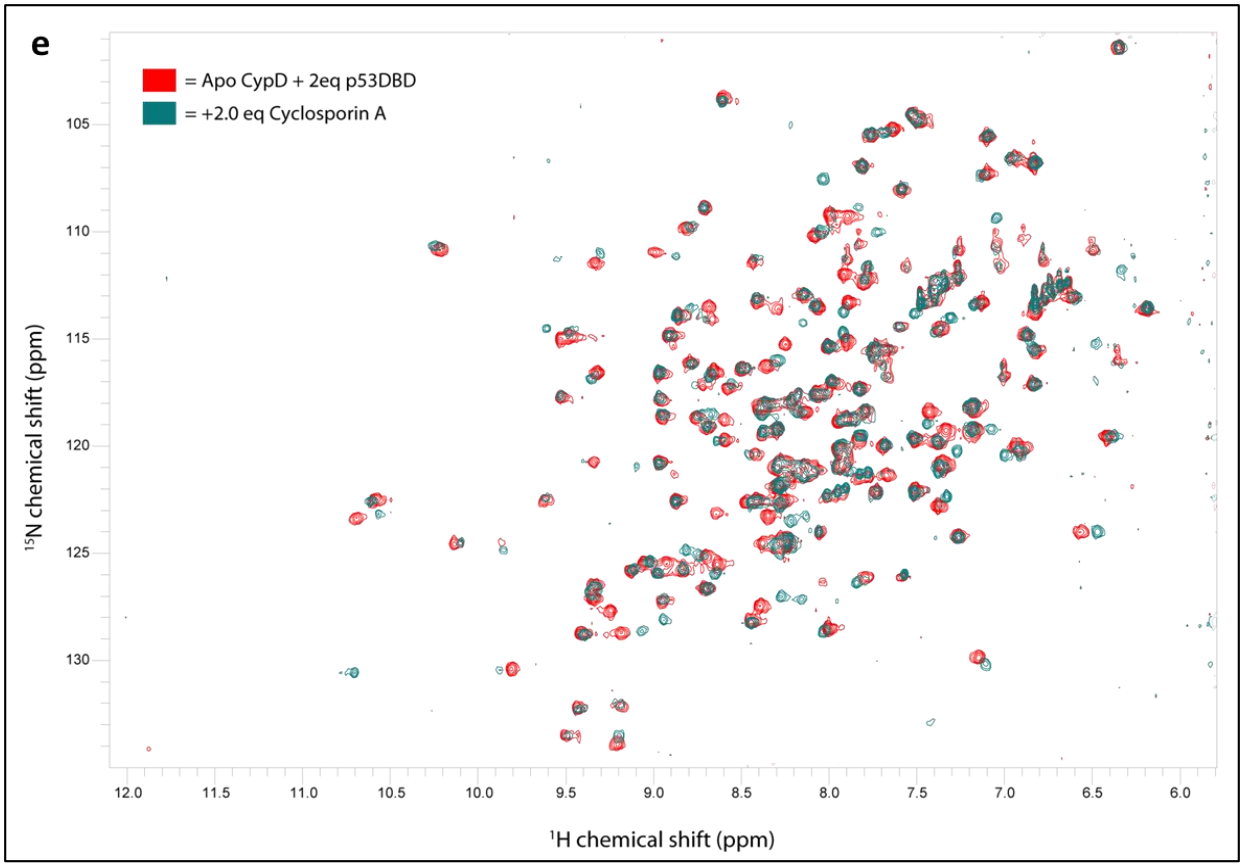

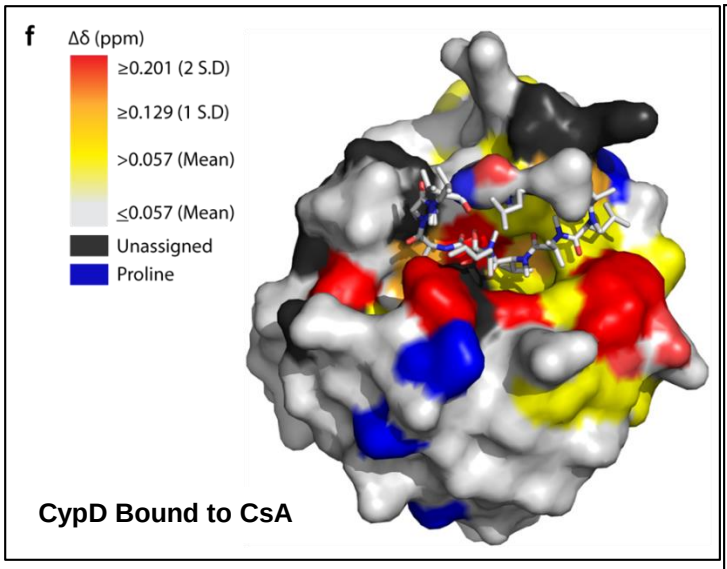

Figure 3.8 ^{1}H, ^{15}N HSQC spectrum of CypD and *E.coli* p53DBD a) apo CypD (black) and **b)** with the addition of 0.6 molar equivalents of *E.coli* p53DBD (yellow), **c)** equimolar amounts of *E.coli* p53DBD (blue) and **d)** 2.0 molar equivalent excess of *E.coli* p53DBD (red). It is clear that titration of *E.coli* p53DBD to ^{15}N CypD has no effect on the CypD chemical shift peaks indicating that no binding is occurring. **e)** ^{1}H, ^{15}N HSQC spectrum of CypD in the presence of 2 molar equivalent excess *E.coli* p53DBD (red) to which 2 molar equivalent of CsA is added (teal). Chemical shift perturbations can clearly be seen indicating successful binding of CsA to CypD as would be expected. **f)** Mapping of significant CypD chemical shift perturbations onto the crystal structure of CypD bound to CsA upon NMR titration of CsA to ^{15}N CypD. Active site residues that participate in binding to CypD according to the crystal structure are primarily perturbed as would be expected.

Having gathered no biophysical evidence that *E.coli* p53DBD binds to CypD, the original CypD peptide-isomerization activity assay was revisited where the original interpretation inferred that inhibition of CypD activity by *E.coli* p53DBD meant a direct interaction by binding of the two proteins. An additional set of proteins and peptides were included to see if inhibition of CypD activity was specific to p53DBD or if any proline-containing protein or peptide could have a similar effect. Indeed, I found that not only *E.coli* p53DBD inhibited CypD activity toward its fluorescent substrate peptide as would be expected of a CypD binding protein, but also unrelated, purified, proline-containing proteins and peptides available in lab that would not be expected to bind to CypD including; Src-kinase domain, and SH3 ligand peptide (sequence: KKAEEEIYGEFGGGGGGRPLPSPPKFG [289]) also inhibited CypD activity. However, the Src-optimal substrate peptide RS1 (sequence: AEEEIYGEFAKKK [290], [291]) which does not contain any prolines did not affect the activity of CypD (Figure 3.9) and does not bind to CypD by fluorescence anisotropy (data not shown). These results suggest that the fluorescence peptide isomerization assay, while a good measure of CypD catalytic activity, is not an appropriate indicator of specific p53 binding to CypD.

Table 3.1 Sequence of peptides used in CypD activity assays. Proline residues are highlighted in bold.

Peptide	Sequence
SH3-ligand peptide	KKAEEEIYGEFGGGGGGR**P**L**P**S**PP**KFG
RS1 peptide	AEEEIYGEFAKKK

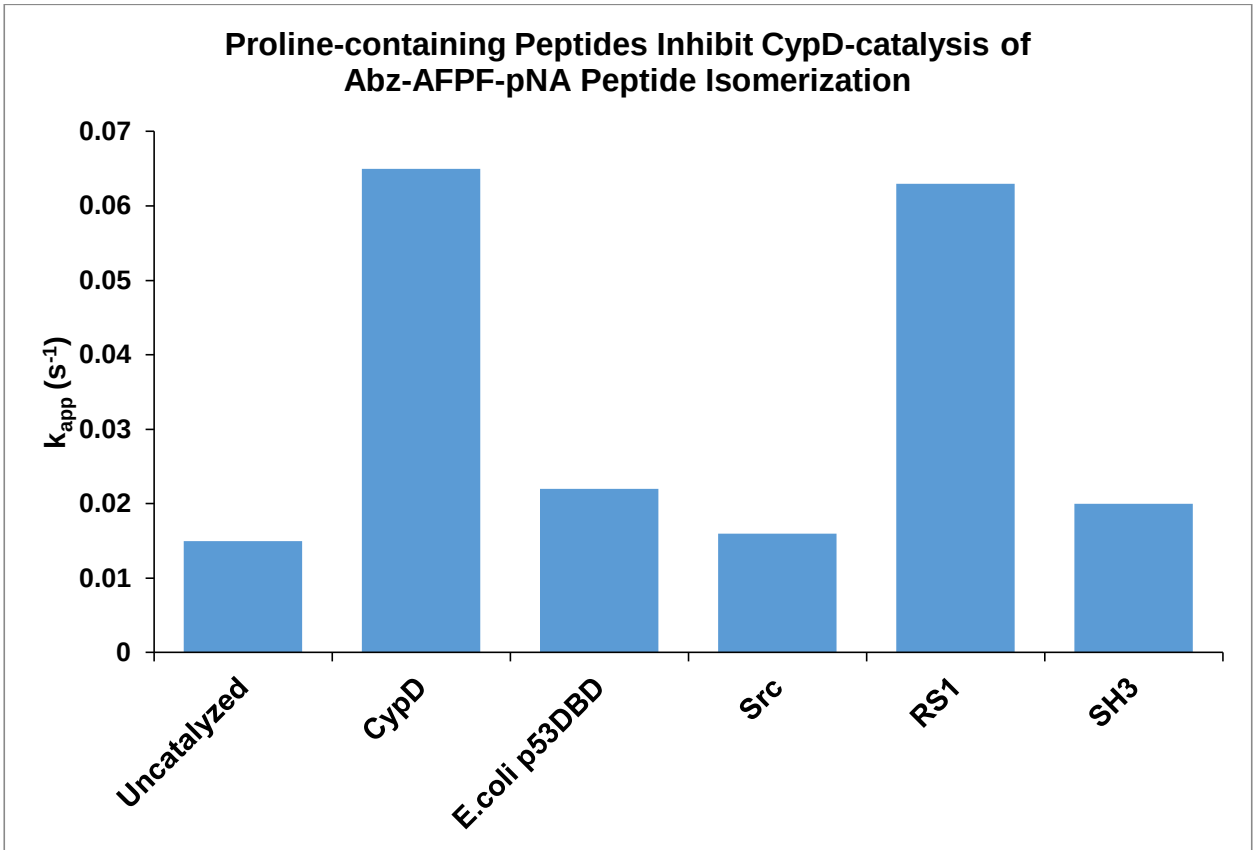

Figure 3.9 CypD peptide isomerization activity monitored in the presence of *E.coli* p53DBD as well as proteins and peptides not normally expected to bind to CypD. 1 μM of any proline-containing protein or peptide including *E.coli* p53DBD, Src and SH3-ligand peptide inhibit the activity of 500 nM CypD while RS1 peptide which does not contain any prolines has no effect on the activity of CypD.

Having gathered no biophysical evidence for CypD binding to *E.coli* p53DBD, the same construct of p53DBD (residues 94-312) was cloned into a baculoviral expression system for purification of p53DBD from insect (SF9) cells. The rationale for using an SF9 expression system was that large quantities of purified protein are required in order

to perform many of the employed biophysical experiments such as NMR and purifying p53 from mammalian cells would be too costly. Perhaps one reason no interaction between CypD and *E.coli* p53DBD could be detected is that *E.coli* bacteria might lack the appropriate post-translational modifications necessary for p53 to bind to CypD. SF9 cells have the ability to post-translationally modify proteins, whereas *E.coli* cannot. These PTMs may affect the folding of p53 or may be required for CypD binding. Furthermore, SF9 cells contain many protein-folding chaperones that *E.coli* do not which could in turn lead to differential folding of p53 protein when compared to *E.coli*. Since a robust expression and purification system had already been established in the lab, it was decided to see if p53DBD from SF9 cells would now be able to bind to CypD. After successful expression and purification of SF9 p53DBD, the classical pulldown experiment showed that indeed, SF9 p53DBD behaved like mammalian protein by CypD-pulldown, and therefore in contrast to *E.coli* p53DBD, which consistently was not observed among the CypD-pulldown fraction (Figure 3.10).

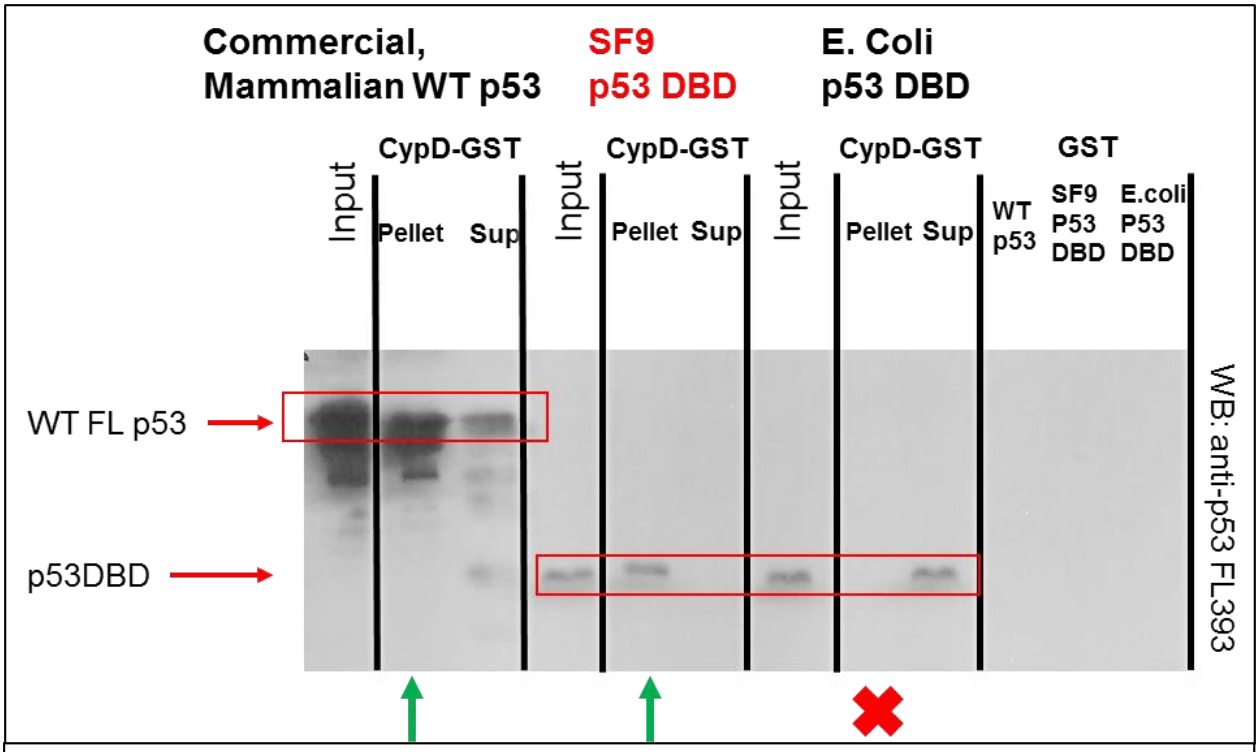

Figure 3.10 CypD pulldown of purified commercial WT full-length (FL) p53, SF9 p53DBD and *E.coli* p53DBD. CypD is able to pulldown both commercial WT FL p53 as well as SF9 p53DBD as indicated by green arrows but not *E.coli* p53DBD as indicated by red X which is consistent with previous observations.

Having established through the pulldown experiments that indeed an interaction between SF9 p53DBD and CypD existed, additional experiments then went on to show that the CypD interaction with SF9 p53DBD is not a classical protein-protein binding interaction where a stable protein-protein complex is formed, as would have been expected. Rather, the CypD interaction with SF9 p53DBD seems to be a transient substrate – enzyme interaction that ultimately leads to irreversible aggregation of SF9 p53DBD and is dependent on CypD activity. The details of these additional findings are discussed in Chapter 4. The remaining sections in Chapter 3 serve to detail some additional biophysical methods used to compare and contrast p53DBD protein from the two, expression sources, *E.coli* and SF9, which behave very differently *in vitro*.

3.3.2 The expression source of p53 affects the stability of the protein

One early observation while working with SF9 p53DBD was the relative ease at which the protein would precipitate during normal handling as compared to *E.coli* p53DBD protein. SF9 p53DBD was more sensitive to freeze-thaw, nearly each thawing cycle produced some aggregation. Similarly, it was observed that during side-by-side dialysis of SF9 and *E.coli* p53DBD into 50 mM NaH_2PO_4 pH 7.4 + 5 mM DTT that considerable white precipitate would form in the SF9 p53DBD dialysis tubing while little to none was seen for the *E.coli* p53DBD protein. The propensity for SF9 p53DBD to aggregate was observed in multiple protein purifications and led to the question of whether or not the SF9 p53DBD protein was intrinsically less thermodynamically stable than its *E.coli* counterpart. I determined the thermodynamic stability of p53 in equilibrium urea denaturation experiments monitored by protein fluorescence. The stability of *E.coli* p53DBD was -5.91 kcal/mol, the stability of SF9 p53DBD was -3.78 kcal/mol, corresponding to $\Delta\Delta G$ of 2.18 kcal/mol. Our determined thermodynamic stability of *E.coli* p53DBD is in close agreement with previously published data which determined the thermodynamic stability of *E.coli* p53DBD to be ΔG = -5.96 kcal/mol [215]. Most small proteins have a thermodynamic stability of approximately 5-15 kcal/mol at 25 °C which suggests *E.coli* p53DBD has only moderate thermodynamic stability at 25 °C that would be further decreased at 37 °C [215], [280]. By comparison, the decrease in thermodynamic stability ($\Delta\Delta G$) of -2.18 kcal/mol between SF9 and *E.coli* p53DBD proteins at 25 °C, is a decrease on the same order of magnitude of some known p53DBD cancer mutant proteins, which are known to be structurally distorted or globally unfolded [215]. For example, p53DBD cancer mutants R175H and C242S have

decreases in ΔΔG of -3.01 kcal/mol and -2.94 kcal/mol respectively, when compared to WT p53DBD, and both mutant proteins are known to be <50 % folded at 37 °C [215], [229]. Mutant p53DBD proteins R248Q and R249S have milder structural distortions (approximately 85 % folded at 37 °C) and their ΔΔG decreases are -1.94 kcal/mol and -1.95 kcal/mol, respectively, when compared to WT p53DBD [215], [229]. The ΔΔG decrease of SF9 p53DBD protein, compared to *E.coli* p53DBD, falls into this range of known structurally destabilized p53 cancer mutant proteins. This implies that despite being WT, the structure of SF9 p53DBD protein is likely to be intrinsically destabilized due to either differential folding of the protein in SF9 cells or the presence of a PTM. These findings support the hypothesis that mitochondrial p53 needs to be structurally destabilized or partially unfolded in order to become a CypD substrate and aggregate. As discussed in Chapter 1, proteins that enter the mitochondria require refolding and may employ a number of chaperone proteins in order to successfully do so. Paired with our evidence that CypD only interacts with SF9 p53DBD which is thermodynamically destabilized, it is possible that a similar requirement of p53 structural destabilization is also required in the mitochondria to facilitate interaction with CypD.

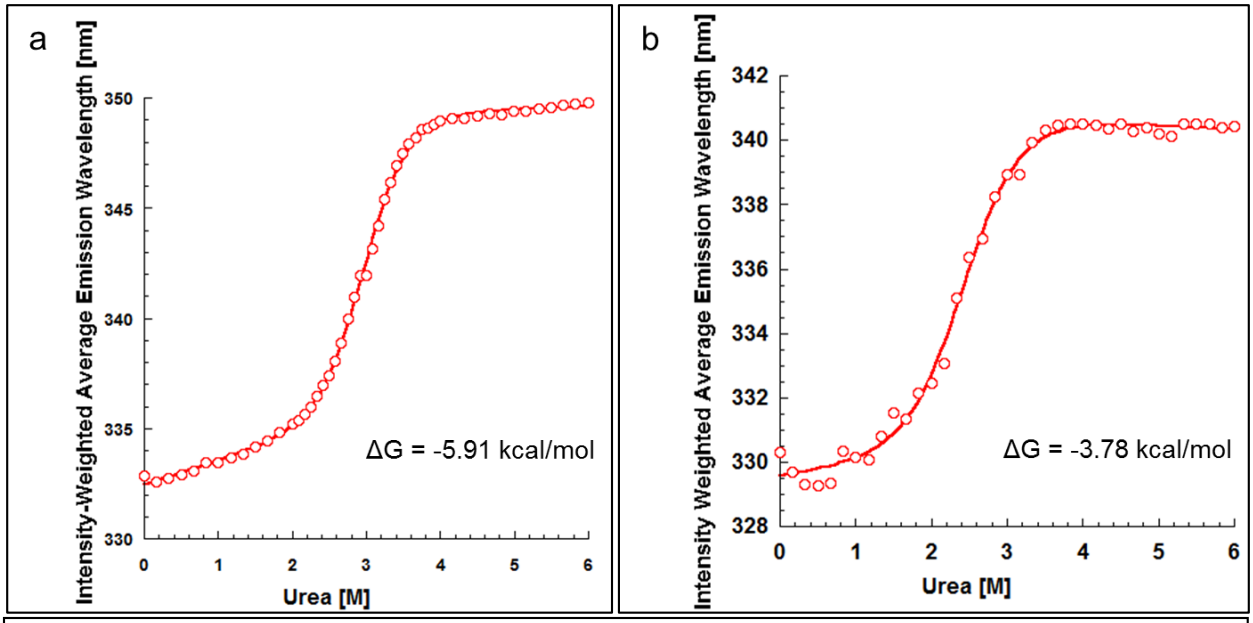

Figure 3.11 Urea denaturation of p53DBD purified from a) *E.coli* or b) SF9 cells. The thermodynamic stability of *E.coli* p53DBD is -2.12 kcal/mol higher than SF9 p53DBD at 25 ºC, the same 2 µM concentration and in the same buffer which indicates that SF9 p53DBD is intrinsically thermodynamically less stable than the *E.coli* expressed p53DBD which may influence the ability of p53DBD to interact with CypD.

One of the motivations behind expressing p53 in SF9 cells was to evaluate the role of potential post-translational modifications on the ability of p53 to interact with CypD. To probe for PTMs, a sample of ^{15}N-labeled *E.coli* p53DBD and SF9 6xHIS-p53DBD were submitted for MALDI mass spec analysis. ^{15}N labeled *E.coli* p53DBD and 6x-HIS affinity tagged SF9 p53DBD were used in order to more easily distinguish the masses of each protein and peptide fragments generated during the experiment. Analysis of the MALDI mass spectrum showed that *E.coli* p53DBD had one sharp, homogenous, peak of the expected size while the SF9 6xHIS-p53DBD protein had a much weaker and broader peak which would indicate a heterogeneous population of protein and potential PTMs though no obvious PTMs could be identified in this analysis (Figure 3.12).

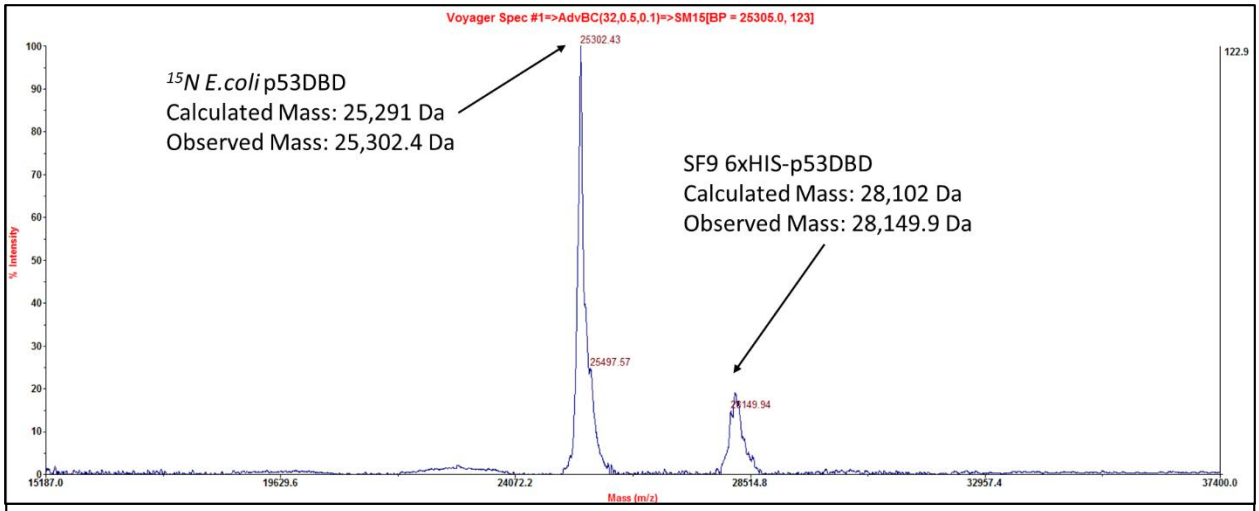

Figure 3.12 MALDI mass spectrum of *E.coli* p53DBD and SF9 6x-HIS p53DBD. *E.coli* p53DBD has one sharp, narrow, peak indicating a homogenous population of p53DBD protein at the expected mass. SF9 6x-HIS p53DBD has a lower and relatively broader peak indicating a heterogeneous population of p53DBD protein with potential PTM.

3.3.3 Detergents cause structural destabilization of p53DBD

The standard SF9 protein purification protocol involves the use of 1 % Triton X-100 for cell lysis and it was found during optimization of the protocol that protein yields could be increased by continuing to include 1 % Triton X-100 throughout the entire purification process as it reduced the amount of protein lost to precipitation. The use of 1 % Triton X-100 was also consistent with the method for generating mammalian cell lysates and standard pulldown experiments. Given what had been learned about the decreased thermodynamic stability of SF9 p53DBD protein, it was questioned whether the addition of detergent had an additional effect on the thermodynamic stability of p53DBD protein. Unfortunately, Triton X-100 absorbs strongly at 280 nm making standard fluorescence-based assays impossible to carry out [292]. Furthermore, the hydrophobic tail of Triton X-100 binds to and sequesters standard reporter dyes such as Sypro Orange, which is commonly used to track protein unfolding by binding to hydrophobic residues, which become exposed upon protein denaturation [293], [294].

Two approaches were taken to circumvent this limitation. The first was to substitute Triton X-100 for another detergent, Tween-20, which does not absorb strongly at 280 nm to get an indirect indication of the general effects of detergent of p53DBD stability using thermal and urea denaturation. The second approach was the use of differential scanning calorimetry (DSC) which does not depend on fluorescence and is compatible with Triton X-100 [295].

Substitution of 1 % Triton X100 with merely 0.1 % Tween 20 significantly impacted the thermodynamic stability of *E.coli* p53DBD which was diminished from -5.96 kcal/mol (buffer 50 mM NaH_2PO_4 + 5 mM DTT in the absence of 0.1% Tween 20) to -2.49 kcal/mol (Figure 3.13 a). Similarly, the melting temperature of *E.coli* p53DBD was decreased from 42 ºC to 39 ºC upon addition of 0.1 % Tween 20 to the same buffer (Figure 3.13 b).

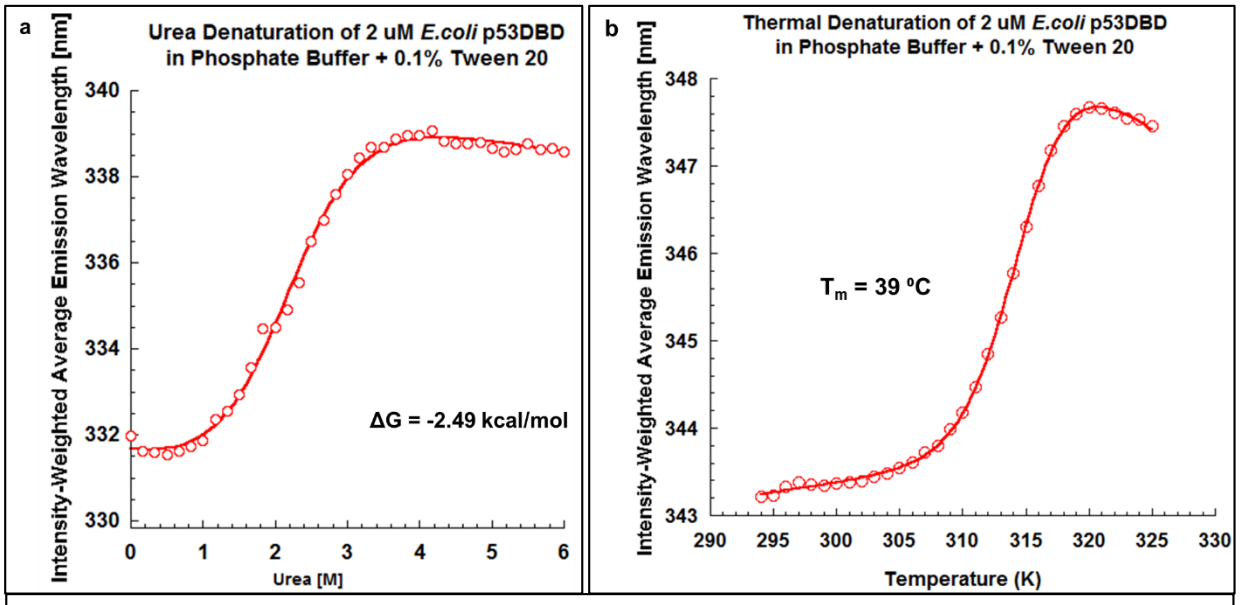

Figure 3.13 Denaturation of *E.coli* p53DBD in the presence of 0.1% Tween 20. a) Urea denaturation of 2 µM *E.coli* p53DBD in the presence of 0.1 % Tween 20 decreases the thermodynamic stability of p53DBD from -5.96 kcal/mol (previously reported) to -2.49 kcal/mol. b) Thermal denaturation of 2 µM *E.coli* p53DBD in the presence of 0.1 % Tween 20 decreases the melting temperature of p53DBD from 42 ºC (previously reported [215]) to 39 ºC.

Differential scanning calorimetry was used to determine the melting temperature of p53DBD in the presence of Triton X-100, due to the fact that the detergent absorbs strongly at 280 nm preventing fluorescence based methods, and sequesters reporter dye, which would otherwise bind hydrophobic residues of an unfolding protein. The general principal behind DSC is similar to ITC, as previously described before, but whereas with ITC the temperature remains constant while a substrate is titrated to its target, in DSC the cell contents remain constant while the temperature is varied. Similar to ITC, the instrument measures and compares the amount of energy it takes to maintain the temperature of a sample cell compared to a reference cell. But, whereas ITC remains at one temperature, DSC measures the energy required to heat a sample compared to its reference. For the purposes of determining the T_m of a protein sample, the reference is simply a buffer blank while the sample contains the same buffer and the protein of interest. Both cells are heated at a fixed rate and the amount of energy required to achieve the target temperature for each degree is monitored. Many phase transitions absorb heat: for example, heating 100 g of water from -5 °C to +5 °C requires more heat than heating the sample from 5 °C to 15 °C, because of the ice-liquid phase transition. Similarly, as a protein unfolds, a greater amount of energy will be required to heat the sample compared to its reference until it has fully unfolded, after which the amount of energy required to heat both samples will be the same. The T_m of the protein is determined by monitoring the specific heat capacity of the sample as a function of temperature. The specific heat needed for the phase transition (protein unfolding) increases near the transition and peaks at the melting temperature of the protein. It was found that indeed, the addition of Triton X-100 to 50 mM NaH_2PO_4 pH 7.4 + 5 mM DTT,

decreased the T_m of *E.coli* p53DBD from 45 ºC in the absence of detergent to 40 ºC in the presence of 1% Triton X-100 (Figure 3.14). Furthermore, the SF9 purification buffer, which also contains 1% Triton X-100 and is later used for NMR (Chapter 4), also brought down the T_m of *E.coli* p53DBD to 39 ºC. Addition of 0.1% Tween 20 to 50 mM NaH_2PO_4 pH 7.4 + 5 mM DTT had a marginal effect on the T_m of *E.coli* p53DBD as measured by DSC. The likely explanation for this inconsistency compared to the T_m determined using fluorescence based methods is the 40-fold increase in protein concentration, because 2 µM *E.coli* p53DBD was used for fluorescence assays compared to 80 µM *E.coli* p53DBD used for DSC. 2 µM and 10 µM *E.coli* p53DBD did not yield a detectable signal during thermal denaturation using DSC. In light of the higher concentrations needed to detect the phase transition of p53DBD unfolding, it is likely that the specific heat peak recorded reflects the temperature of aggregation rather than melting temperature of the protein, and this similar phenomenon has been described previously in the literature [215], [296]. This could also explain the 2 ºC increase in the T_m of *E.coli* p53DBD to 44 ºC from 42 ºC in the absence of detergents as measured by DSC compared to the fluorescence assays and would be consistent with the visually observed cloudiness of the sample upon completion of the experiment.

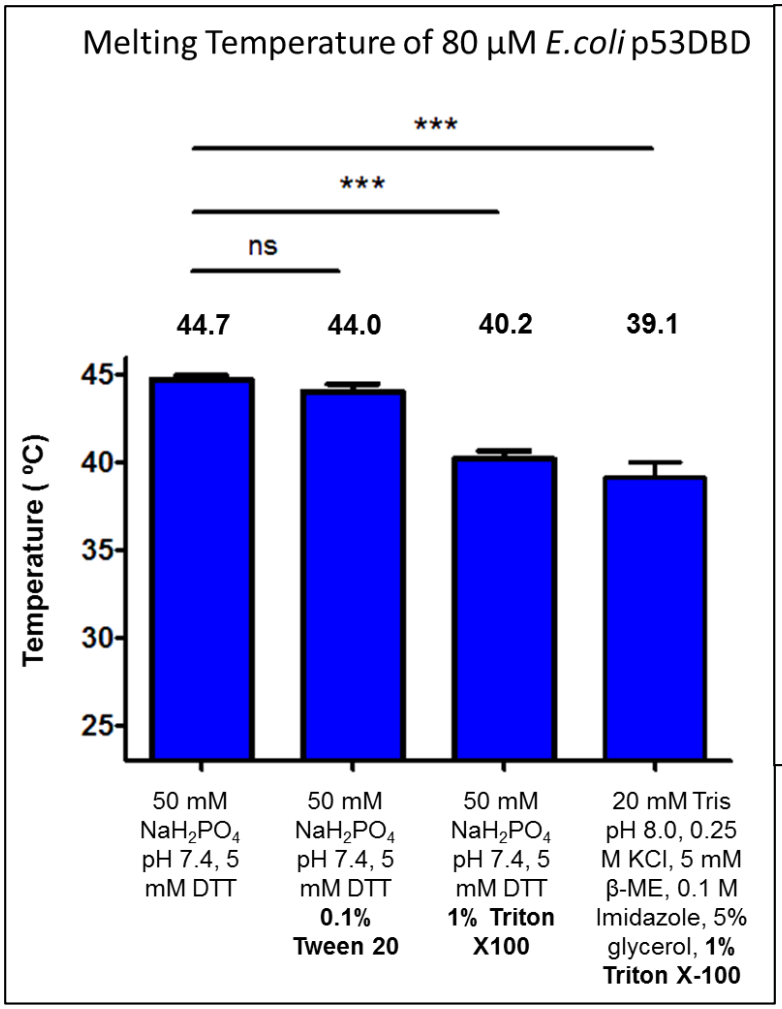

Figure 3.14 Melting temperatures of *E.coli* p53DBD measured by DSC and the effect of Triton X-100 or Tween 20 detergents. The addition of Triton X100 appears to decrease the melting temperature of *E.coli* p53DBD indicating that the detergent may have an effect on the structural stability of p53DBD protein. Addition of 0.1 % Tween 20 has an insignificant effect on the melting temperature of *E.coli* p53DBD as measured by DSC. This, along with the 2 ºC increase in T_m of *E.coli* p53DBD in the absence of detergents measured by DSC as compared to previously measured by fluorescence is likely due to the increased protein concentration necessary to detect a heat capacity signal. In turn, this suggests that the observed T_m is more reflective of the temperature of aggregation rather than melting temperature.

Taken together, both substitution of Triton X100 for Tween 20 and the DSC thermal denaturation of *E.coli* p53DBD in the presence of Triton X100, indicate that detergent decreases the thermodynamic stability of p53DBD. Considering that SF9 p53DBD protein is intrinsically less thermodynamically stable than *E.coli* p53DBD and that its thermodynamic stability is further decreased by the presence of Triton X100. I therefore hypothesized that CypD interacts with p53 only when the protein is unfolded or partially unfolded as would likely be the case early upon translocation into the mitochondrial matrix.

3.4 Discussion

As discussed previously, p53 is very commonly mutated in many different cancers. Many of these mutations have dramatic effects on the structure and function of p53. While some mutations only mildly perturb the structure of the protein, some hyperstabilize the structure and others completely abolish the ability of p53 to fold. The recently discovered roles for p53 mediating apoptosis and necrosis from within the mitochondria beg the question as to what the folded state of p53 in the mitochondria might be. Little is known about p53 folding or lack of folding in the mitochondria especially under stressed conditions which drive translocation of p53 into the mitochondria in the first place.

Previous work has shown that there is a distinct interaction between CypD and p53 in the mitochondria which ultimately leads to opening of the mPTP and cell death by necrosis [2]. The proposed mode of interaction between p53 and CypD was modeled after that of a classical protein-protein binding interaction where it was hypothesized that p53 bound-to and activated CypD, allowing for it to contribute to opening of the mPTP. However, extensive efforts to identify a stable complex between p53 and CypD, as presented in this chapter, were fruitless. My results support a different model where CypD transiently interacts with a structurally destabilized or partially unfolded p53 protein rather than forming a stable complex with folded p53. Such an interaction is plausible as p53 needs to be refolded upon translocation into the mitochondrial matrix, and conventional roles of prolyl isomerase proteins such as CypD include chaperone-like functions to help facilitate folding or activation of their target substrates through cis-trans prolyl isomerization [297]. Thus far, it can be hypothesized that CypD binds to an

unstructured region of p53 yet the events to follow are still unknown. As discussed in the introduction, the minimal construct of p53 that can be pulled down by CypD in classic pulldown assays has been mapped to p53 residues 80-220 located at the N-terminus of the p53DBD. The minimal construct (residues 80-220) lacks the central beta sheet (Figure 1.2, labeled in black) and it is therefore very unlikely that this minimal construct would be folded. Since p53 is already marginal stable and individual point mutations can effectively unfold the protein, it is unlikely, that removal of a central beta-sheet could be tolerated and yield folded protein.

As was shown by comparison of the minimal functional domain of p53, the DNA binding domain, expressed in either *E.coli* or SF9 insect cells, only the thermodynamically destabilized p53DBD protein from SF9 cells is able to interact with CypD, while the more structurally stable *E.coli* p53DBD protein does not interact with CypD in any attempted biophysical assay. Moreover the presence of detergents, specifically Triton X-100, is also shown to be thermodynamically destabilizing to p53DBD protein which is consistent with previous biochemical experiments, such as the CypD pulldown assays, that were conducted in the presence of Triton X-100 [2]. The conclusions of these experiments motivate additional biophysical characterization of the CypD interaction with SF9 p53DBD in order to better understand how p53 could be activating CypD to open the mPTP leading to subsequent necrosis. The outcomes of that biophysical characterization and resulting new model for p53 activation of CypD are detailed in Chapter 4.

Chapter 4: p53-mediated mitochondrial permeability transition is suppressed by the mitochondrial chaperone Trap1

Work in this chapter is credited to several people:

Ivan Lebedev designed, performed and analyzed all of the biochemical and biophysical experiments.

Dr. Michael Tong helped perform and analyze the NMR experiments.

Dr. Alice Nemajerova helped carry out and analyze pulldown assays.

Maja Kornaj helped with protein denaturation and CypD activity assays.

Dr. Franz Schmidt and Dr. Philipp Schmidpeter designed the CypD activity assay and helped with data interpretation and writing feedback.

Dr. Markus Seeliger and Dr. Ute Moll advised the design, techniques and analysis of the biochemical experiments.

4.1 Introduction

Ischemia/Reperfusion (IR) injury can cause irreversible tissue damage and necrosis in vital organs such as brain (ischemic or hemorrhagic stroke) and heart (myocardial infarction), and reperfusion injury is a leading cause of permanent disability and death worldwide [14]. Ischemia/Reperfusion injury leads to increased intracellular concentrations of reactive oxygen species (ROS) and increased cytosolic Ca^{2+} influx into the mitochondrial matrix [298]. Together, these events lead to dissipation and collapse of the actively maintained electrochemical proton gradient ($\Delta\Psi m$) across the inner mitochondrial membrane due to the sudden opening of the mitochondrial permeability transition pore (mPTP) in the inner mitochondrial membrane. The mPTP is an elusive non-selective pore for small solutes and water that is impermeable under normal physiological conditions but opens abruptly in response to prolonged oxidative stress, an event called mitochondrial permeability transition (mPT) [60], [298]. This causes ion influx that dissipates $\Delta\Psi m$ and shuts down oxidative phosphorylation and ATP production, ending in catastrophic energetic failure [60]. Concomitantly, water influx causes matrix swelling, rupture of the rigid outer mitochondrial membrane (OMM) and release of all sequestered cell death factors from the intermembranous space. Recent studies identified several key players involved in mitochondrial permeability transition. They include the central regulatory protein cyclophilin D (CypD, gene name PPIF, UniProt: P30405, PDB: 2Z6W, not to be confused with the larger 40 kD nuclear and cytosolic CypD otherwise known as CyP40), an exclusively mitochondrial matrix prolyl-isomerase whose enzymatic activity is essential to trigger mPT [8]–[10] , and the stress sensor p53 (TP53) under conditions of oxidative damage [2]–[7]. Structural pore

components encompass the c-subunit ring [85], [299] and the oligomycin-sensitivity conferring protein (OSCP) [148] of the F1Fo-ATP synthase, and more recently the product of the Spastic Paraplegia 7 gene (SPG7) [300]. Despite these advances, the full assembly of the mPTP is not understood and more importantly, the mechanism by which pore opening is triggered remains unknown.

p53 is an extensively studied nuclear transcription factor that acts as a potent tumor suppressor by rapidly and broadly responding to DNA damage signals *via* activating genes involved in cell cycle arrest or senescence, DNA repair and apoptosis as effective anti-cancer mechanisms. Moreover, wildtype p53 protein has additional pro-death functions directly at the mitochondria, including driving transcription-independent apoptosis [192].

Recent work has shown that a fraction of stress-induced p53 protein translocates to mitochondria to interact with multiple members of the Bcl2 family and directly drive apoptosis through permeabilization of the outer mitochondrial membrane [191]. A long-standing paradigm had been that p53 controls apoptosis but plays no role in necrosis. However, in response to oxidative stress Vaseva *et al.* recently established a necrotic mitochondrial p53 program, in addition to the well-characterized apoptotic mitochondrial p53 program [2]. The authors showed that upon hypoxia and oxidative stress, cytoplasmic p53 translocates into the mitochondrial matrix and participates in necrosis by triggering mPT through interaction with CypD [2]. Purified p53 protein opens the PTP pore in isolated mitochondria independent of Bax and Bak but dependent on CypD. Conversely, $p53^{-/-}$ MEFs are protected from oxidative stress-induced mPT and mPTP opening. Direct targeting of p53 to mitochondrial matrix induces mPT and necrosis in a

CypD-dependent manner, and oxidative stress- induced PTP opening and necrosis is largely transcription-independent. Intriguingly, a robust p53-CypD complex forms during mouse brain ischemia/reperfusion injury (stroke model). In contrast, reduction of p53 levels or cyclosporine A pretreatment of mice prevents this complex and correlates with effective stroke protection [2]. However, details of the p53•CypD interaction and the mechanism by which p53 triggers opening of the mPTP have yet to be investigated.

The major event during ischemia/reperfusion injury leading to sudden collapse of mitochondrial function and energy catastrophe is the formation and prolonged opening of the mPTP following the insult by ROS and/or Ca^{2+}. While it has been shown that the mPTP can be transiently opened and closed to serve as a physiologic Ca^{2+} release channel [301], it is the prolonged opening of the pore that is required for necrotic cell death [58]. The exact proteins that make up the mPTP have evaded researchers for over two decades and the only genetically proven and consistently indispensable component has been the obligatory regulatory factor CypD [8]–[10]. Genetic deletion of CypD [79], [151], [152] or inhibition of CypD with the highly specific pan-cyclophilin inhibitor cyclosporine A (CsA) [2], [150] prevents mPTP opening and mPT *in vivo*. It is thought that the structural pore component of the mPTP itself is composed of the c-subunit ring of the F1Fo-ATP synthase [299] and that CypD binds distally to the OSCP subunit of the F1Fo-ATP synthase [85]. Binding of CypD to OSCP is hypothesized to increase the PTP's apparent affinity for Ca^{2+}, in turn sensitizing the pore to opening [58].

Over 1500 different proteins can be found in mammalian mitochondria [302]. However, the mitochondrial genome only harbors 13 protein-coding genes [258], indicating that the vast majority of mitochondrial proteins including p53 and CypD are

encoded in the nucleus and imported from the cytosol. As such, mitochondria heavily depend on chaperone proteins to maintain proper protein-folding homeostasis [303]. These mitochondrial chaperones are also regulators of mitochondrial permeability transition, contributing to a cytoprotective chaperone network that antagonizes CypD-dependent cell death [12], [269], [273], [276], [304]. Conversely, and consistent with this vital role, mitochondrial chaperones are involved in the mitochondrial unfolded protein response (mtUPR) [305] that is triggered by a variety of mitochondrial stressors including ROS [306]. Of note, both CypD and p53 interact with members of the mtUPR including mitochondrial mtHSP60 [269], [270], mtHSP90 [272] and the mitochondrial HSP90 homologue Trap1 [12]. These interactions beckon the question of whether or not mitochondrial chaperones may also be involved in p53-mediated mPT.

To better understand the mechanism how p53 is involved in oxidative stress-induced opening of the mPTP, complementary biophysical methods were employed here to explore the p53•CypD interaction. NMR and biochemical methods were used to identify catalytic CypD residues directly involved in aggregation of p53. Two assays were developed to monitor the aggregation of p53 in a CypD activity-dependent manner *in vitro*. We explored the nature of the insoluble p53 aggregates formed by interaction with CypD using transmission electron microscopy (TEM). To explore the involvement of Trap1 in p53-mediated mPT, mitochondrial calcein retention assays were used to directly monitor opening of the mPTP in WT, $p53^{-/-}$ and $CypD^{-/-}$ MEFs by FACS in the presence or absence of H_2O_2 stress and gamitrinib, a specific Trap1 inhibitor. We find that CypD causes aggregation of p53 into amyloid-like fibrils and that inhibition of Trap1 sensitizes cells to mPT in a p53-dependent manner. This suggests that stress-imported

matrix p53 is responsible for modulating mPT by cooperating with members of the mtUPR, possibly activating CypD by its competitive displacement from chaperone interaction.

4.2 Methods

The work in this chapter employs some of the general methods described in chapter 2 including expression and purification of CypD and p53DBD from both *E.coli* and SF9 sources, urea denaturation assays, thermal denaturation assays, pulldown assays, CypD activity assays and NMR.

4.2.1 Co-aggregation assays

p53 co-aggregation assays follow the same protocol as standard pulldown assays with the addition of an additional condition containing bead-bound GST in the presence of soluble CypD (not the GST-CypD fusion).

4.2.2 Transmission Electron Microscopy

Transmission electron microscopy images of p53DBD aggregates were obtained by letting aggregates of the different conditions settle on a copper grid for 30 seconds, wicking away remaining buffer followed by negative staining with 2% uranyl acetate. Images were taken on a Tecnai BioTwinG2 microscope (FEI).

4.2.3 Calcein Retention Assay

Mitochondrial permeability transition pore opening was assessed using the calcein assay with $CoCl_2$ quenching (LifeTechnologies) where loss of calcein fluorescence directly indicates opening of the mPTP. Where specified, MEFs were pre-treated with 0.4 mM H_2O_2 for 8 hr in the absence or presence of 2 μM CsA as previously described [2] and the absence or presence of 10 μM Gamitrinib. The cells

were labeled with calcein for 30 min at 37 °C in Hanks' balanced salt solution with 10 mM Hepes pH 7.4 and 0.1 μM calcein as described [197]. Fluorescence was detected by an EMD Millipore Amnis FlowSight Imaging Flow Cytometer using the manufacturer's instructions and the supplied IDEAS analysis software. The fluorescent signal was normalized to $CoCl_2$ bleached, unstressed untreated cells as maximum signal.

4.3 Results

4.3.1 NMR slow exchange behavior reveals that catalytic CypD residues are responsible for p53 aggregation

We previously showed by pulldown of GST-tagged proteins and co-immunoprecipitation experiments that p53 and CypD interact in mouse embryonic fibroblasts (MEFs), human HCT116 colon cancer cell lines and in acutely infarcted mouse brain tissue [2]. Mapping experiments by using a truncation series of p53 proteins in pulldown experiments with CypD showed that CypD interacts with p53 residues 80-220, corresponding to the N-terminal portion of the DNA Binding Domain of p53 (p53DBD, residues 94-312) [2]. To further characterize the interaction and identify the key residues of CypD responsible for interacting with p53DBD, we compared the chemical shift changes of isotopically-labeled CypD, recombinantly expressed and purified from *E.coli*, upon addition of unlabeled baculoviral p53DBD purified from Sf9 cells using ^{1}H- ^{15}N HSQC NMR spectroscopy (Figure 4.1 a-b). Since NMR chemical shifts are sensitive to changes in the chemical environment, chemical shift perturbations can be used to determine the binding interface. Upon addition of p53DBD to ^{15}N-CypD,

NMR crosspeaks shifted, peaks split and new crosspeaks emerged (summarized in Figure 4.1 a-b) due to the effect that p53DBD binding has on CypD (Figures 4.2 a-c).

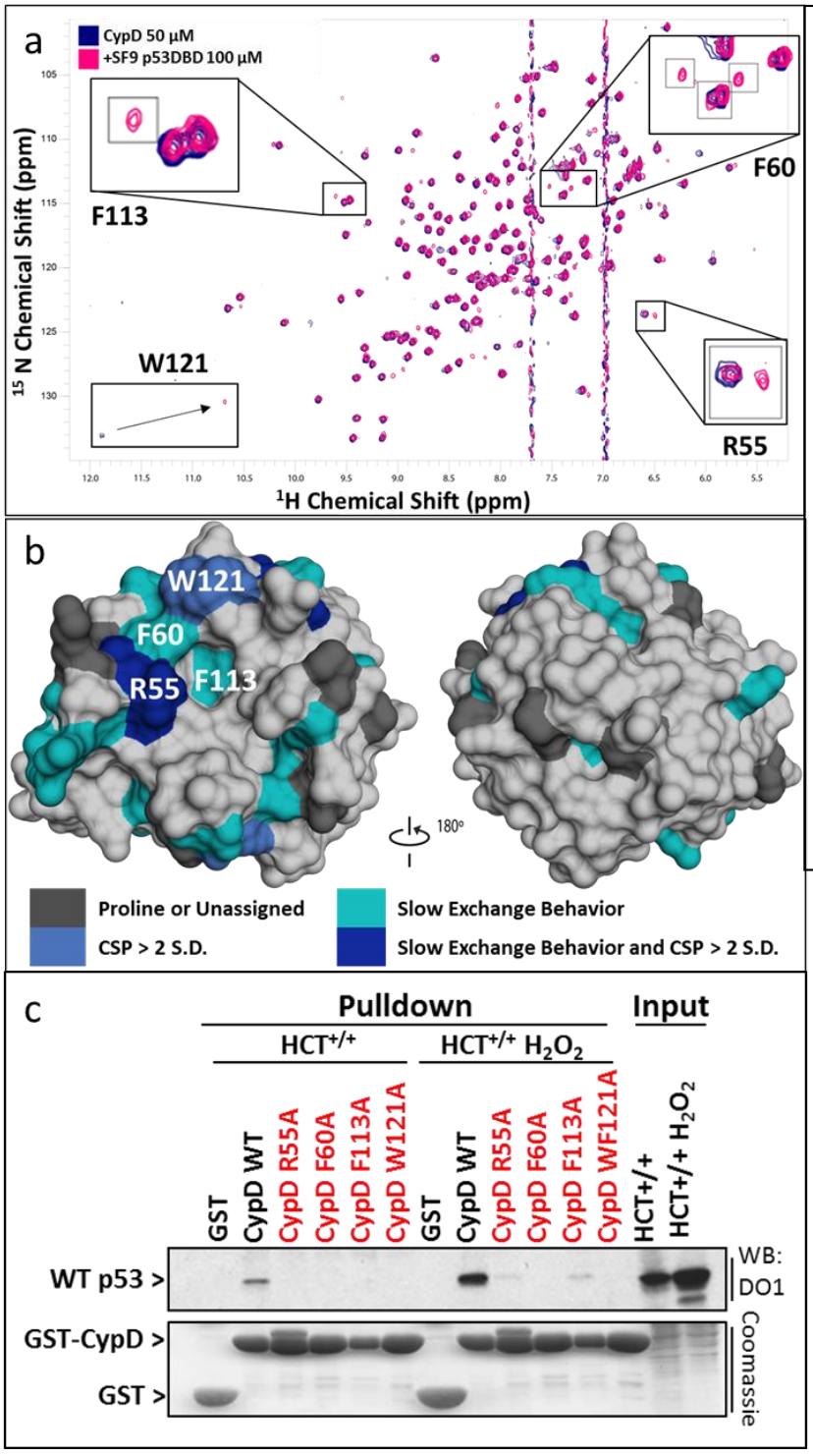

Figure 4.1 NMR reveals CypD active site residues required for interaction with p53. a) ^{1}H, ^{15}N HSQC spectra containing 50 µM isotopically labeled CypD in the presence of 100 µM p53DBD at 25 °C. Doubling of peaks indicates slow exchange behavior characteristic of a dynamic protein-protein interaction. Key active-site residues are highlighted and enlarged. b) Map of the significant chemical shift perturbations (>2 standard deviations) and residues participating in slow-exchange behavior colored in the structure of CypD (PDB:2Z6W). c) Pulldown of endogenous wildtype p53+/+ from H2O2-stressed and unstressed HCT116 cells by wildtype (WT) CypD and the CypD active-site mutants R55A, F60A, F113A and W121A expressed as GST-fusion proteins and immobilized on glutathione

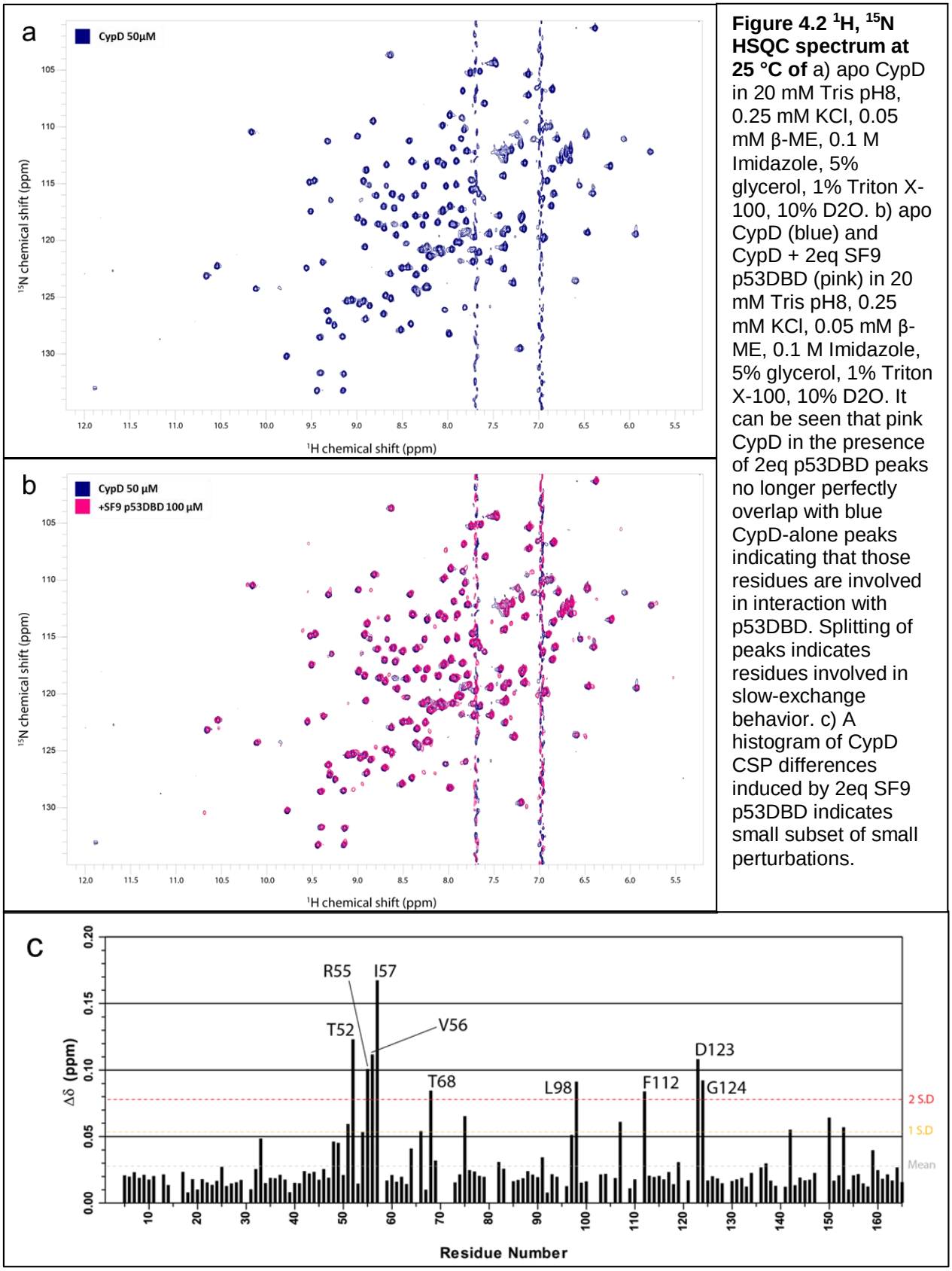

Figure 4.2 ^{1}H, ^{15}N HSQC spectrum at 25 °C of a) apo CypD in 20 mM Tris pH8, 0.25 mM KCl, 0.05 mM β-ME, 0.1 M Imidazole, 5% glycerol, 1% Triton X-100, 10% D2O. b) apo CypD (blue) and CypD + 2eq SF9 p53DBD (pink) in 20 mM Tris pH8, 0.25 mM KCl, 0.05 mM β-ME, 0.1 M Imidazole, 5% glycerol, 1% Triton X-100, 10% D2O. It can be seen that pink CypD in the presence of 2eq p53DBD peaks no longer perfectly overlap with blue CypD-alone peaks indicating that those residues are involved in interaction with p53DBD. Splitting of peaks indicates residues involved in slow-exchange behavior. c) A histogram of CypD CSP differences induced by 2eq SF9 p53DBD indicates small subset of small perturbations.

These changes indicate slow-exchange behavior, characteristic of a dynamic process such as a proline cis-trans isomerization event [307], and are strikingly similar to that of the cytosolic pSer/pThr specific prolyl-isomerase Pin1 interacting with one of its substrates, Amyloid Precursor Protein (APP) [308]. Interestingly, Pin1 has been shown to also bind to p53 and to isomerize multiple sites on p53 [309], causing several downstream effects including dissociation of p53 from interacting proteins [310], translocation of p53 into the mitochondria [311], and stabilization and transcriptional activation of p53 [310], [312], [313]. These diverse interactions help highlight and motivate the importance of understanding the dynamic interactions between p53 and prolyl-isomerases such as CypD in this study. Of note, upon completion of the 4-hour NMR experiment, we observed severe visible aggregation in the NMR tube. We found that p53DBD was quantitatively precipitated from the NMR sample, while no CypD was found among the aggregated fraction (Figure 4.3). To eliminate the possibility that p53DBD aggregation might be responsible for the observed CypD peak shifts, we repeated the experiment in the presence of 2 M urea to prevent aggregation. Under these conditions CypD remained folded and we again observed slow-exchange behavior including peak shifts, peak doubling, and the emergence of new peaks (Figure 4.4). However, no protein precipitation was observed in this condition, confirming that CypD was indeed interacting with soluble p53 and not with p53 aggregates. We tested the enzymatic activity of CypD in the presence or absence of 2 M urea using a fluorescent peptide cis/trans isomerization assay [281] which shows that the addition of 2 M urea does not reduce the activity of CypD (Figures 4.5 a-b). A thermal shift assay tracking changes in intrinsic protein fluorescence upon heating was conducted on WT

CypD and CypD with the addition of 2 M urea to confirm that 2 M urea did not unfold CypD (Figure 4.6 a-b). Taken together, these results indicate that a dynamic interaction exists between CypD and p53DBD which leads to the aggregation of p53.

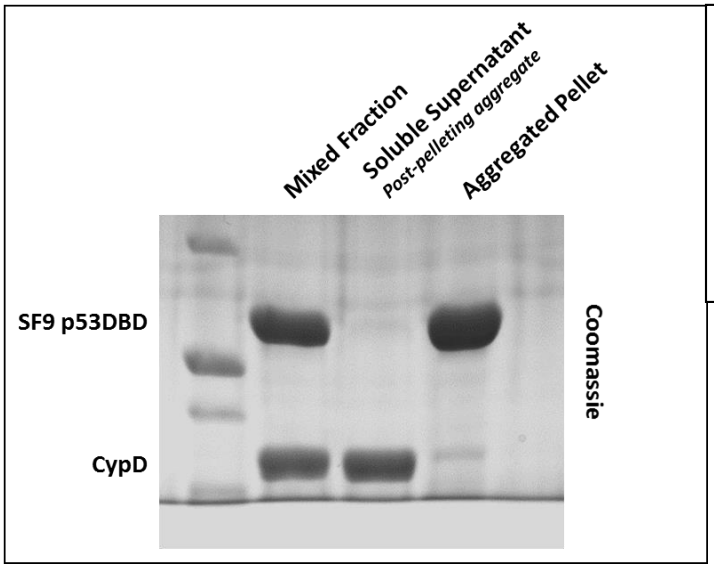

Figure 4.3 Coomassie staining of mixed, soluble and precipitated fractions of NMR sample ^{1}H, ^{15}N HSQC spectrum of apo CypD + 2eq SF9 p53DBD from Figure 4.2 b. It can be seen that no p53DBD remains in solution after interaction with CypD and that CypD does not aggregate with p53DBD.

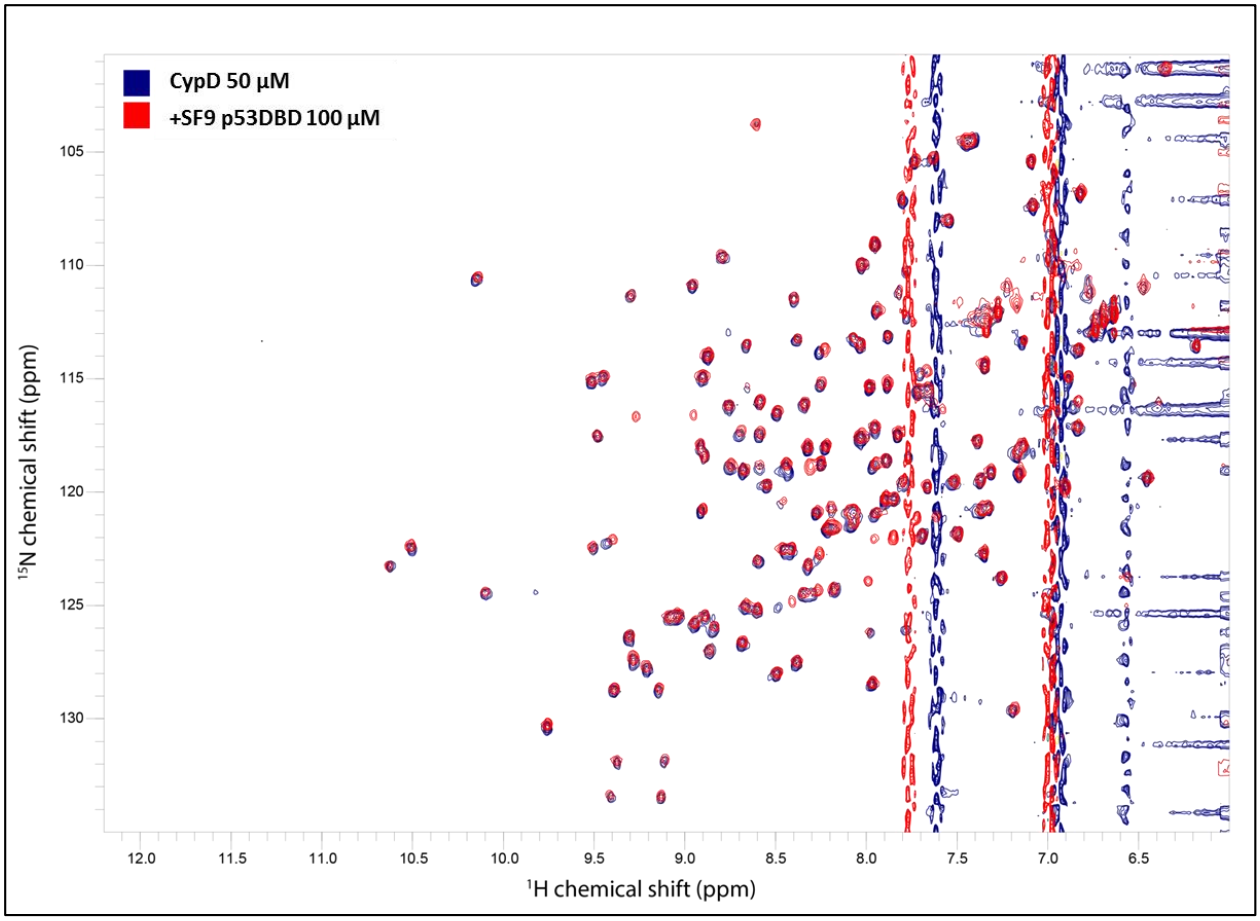

Figure 4.4 ^{1}H, ^{15}N HSQC spectrum at 25 °C of apo CypD (blue) and CypD + 2eq SF9 p53DBD + 2 M Urea (red) in 20 mM Tris pH8, 0.25 mM KCl, 0.05 mM β-ME, 0.1 M Imidazole, 5% glycerol, 1% Triton X-100, 10% D2O, 2 M Urea. It can be seen that red peaks (CypD in the presence of 2eq p53DBD) no longer perfectly overlap with blue CypD-alone peaks indicating that those residues are involved in interaction with p53DBD. Splitting of peaks indicates residues involved in slow-exchange behavior. The presence of 2 M urea prevented any visible aggregates from forming however the slow-exchange behavior remains indicating that CypD does indeed interact dynamically with soluble p53DBD and not p53DBD aggregates as was observed in the absence of 2 M urea.

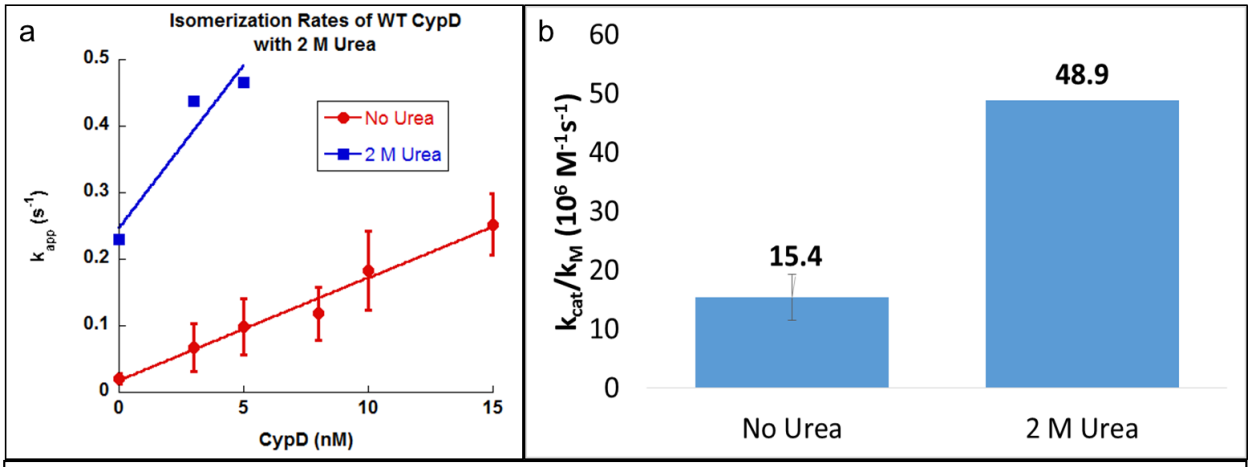

Figure 4.5 Activity of CypD in 2 M urea. a) AFPF peptide-isomerization activity of WT CypD in 50 mM NaH2PO4+5 mM DTT compared to 50 mM NaH_2PO_4+5 mM DTT+2 M urea. b) Specific activity of WT CypD in the presence of 2 M urea.

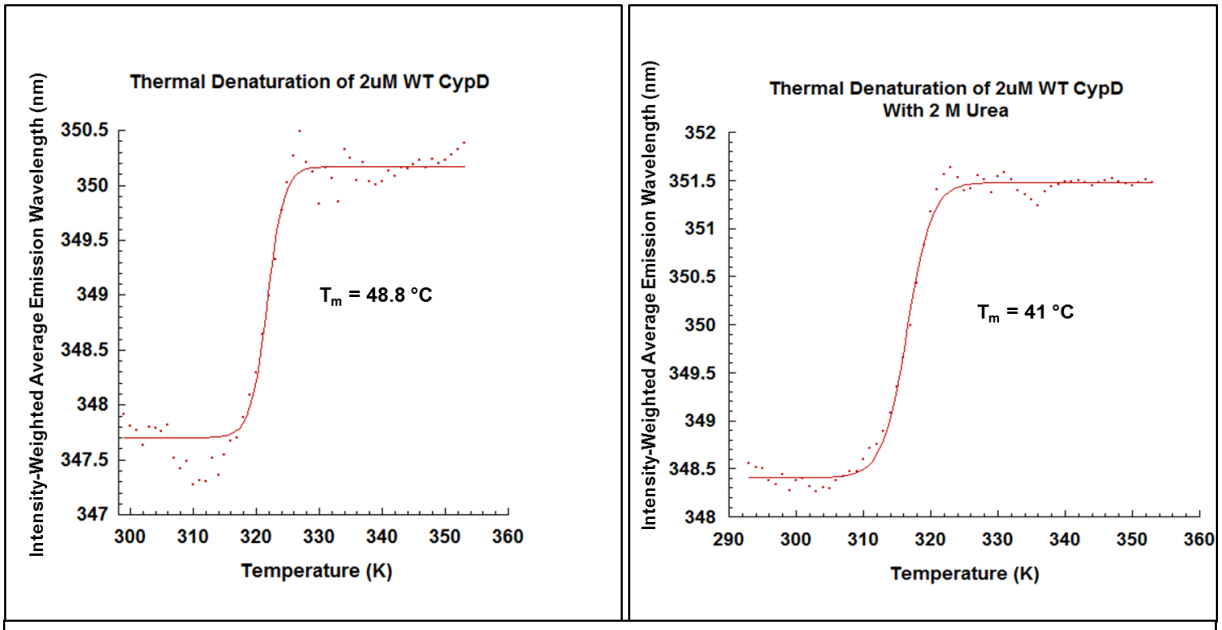

Figure 4.6 Thermal denaturation of CypD. a) 2 µM CypD in 50 mM NaH_2PO_4+5 mM DTT. b) 2 µM CypD in 50 mM NaH_2PO_4 + 5 mM DTT + 2 M urea.

The NMR experiment also reveals that CypD active-site residues R55, F60 and F113, known to be involved in binding to the CypD inhibitor CsA [163], exhibit slow exchange behavior with p53. Similarly, CypD active-site residue W121, which is also part of the CsA binding site[163], showed a significant chemical cross-peak shift (Figure 4.2 c). To validate the importance of these residues for p53 interaction, we individually mutated them to alanines and tested for pulldown of endogenous p53 from HCT116 cells (Figure 4.1 c). Mutant proteins F60A and W121A had lost all ability to pull down p53, while R55A and F113A showed severely reduced ability to pull down p53. Next, we tested the enzymatic activity of CypD variants using a fluorescent peptide cis/trans isomerization assay [281]. We found that in contrast to CypD WT, the CypD active-site mutants R55A, F60A, F113A and W121A had completely lost isomerization activity (Figures 4.7 a-b) as would be expected for similar active site mutations described previously [314]. A thermal shift assay confirmed all CypD mutants were folded at room temperature (Figures 4.8 a-c). Since W121 is the sole tryptophan in CypD, making intrinsic protein fluorescence difficult to monitor, the fluorescence of the unfolding reporter dye Sypro Orange was used instead (Figure 4.9).

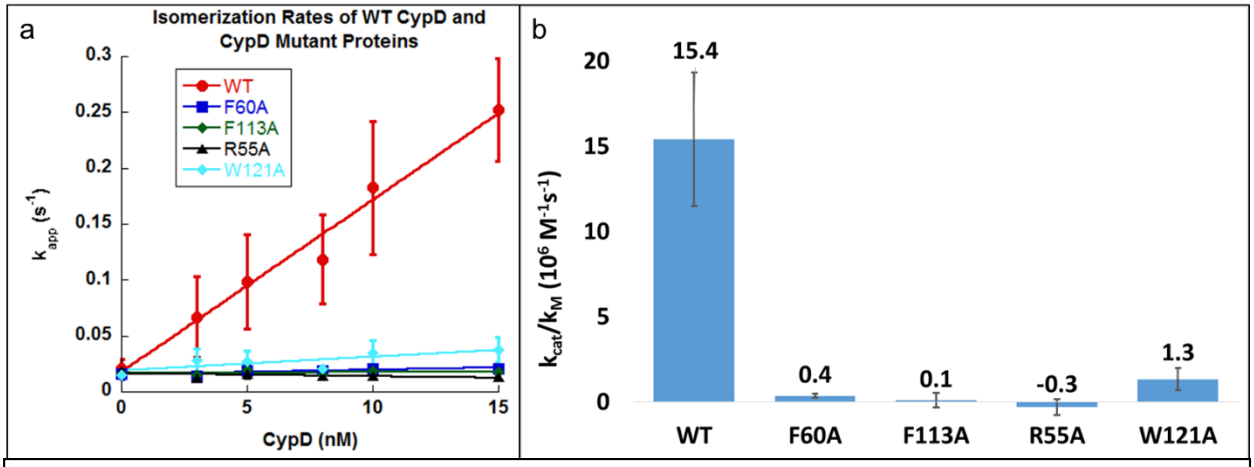

Figure 4.7 CypD activity assays with CypD active-site mutants R55A, F60A, F113A and W121A. a) AFPF peptide-isomerization activity of WT CypD compared to active site mutants F60A, F113A, R55A and W121A. It can be seen that all CypD mutants are inactive and can no longer catalyze the isomerization of AFPF peptide. These mutants also do not interact with p53 by pulldown (Figure 4.1 c). b) Specific activity of WT CypD and CypD mutant proteins R55A, F60A, F113A, and W121A.

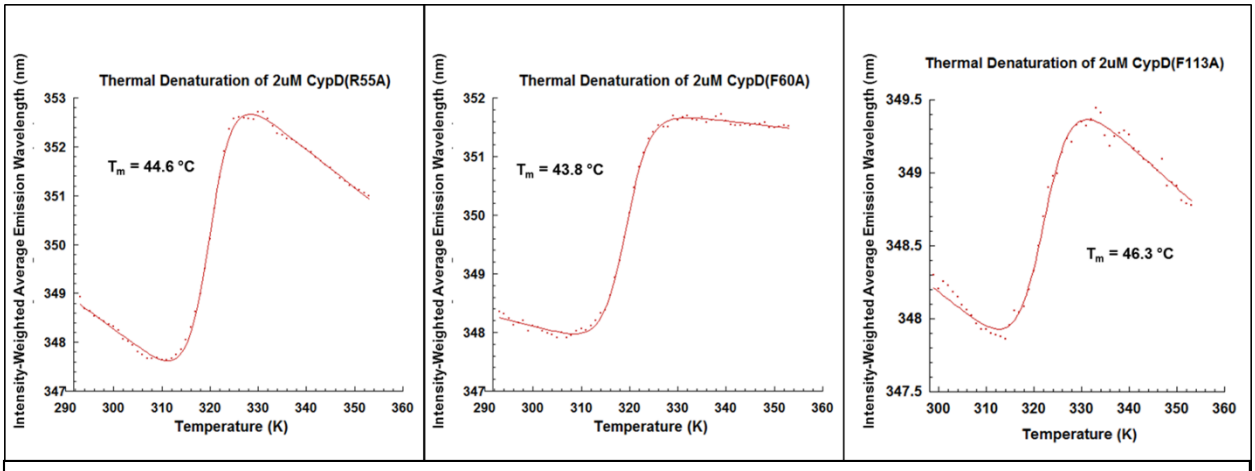

Figure 4.8 Thermal denaturation of CypD active-site mutants determined from NMR. a) CypD mutant R55A has a T_m of 44.6 ^{0}C. b) CypD mutant F60A has a T_m of 43.8 ^{0}C. c) CypD mutant F113A has a T_m of 46.3 ^{0}C.

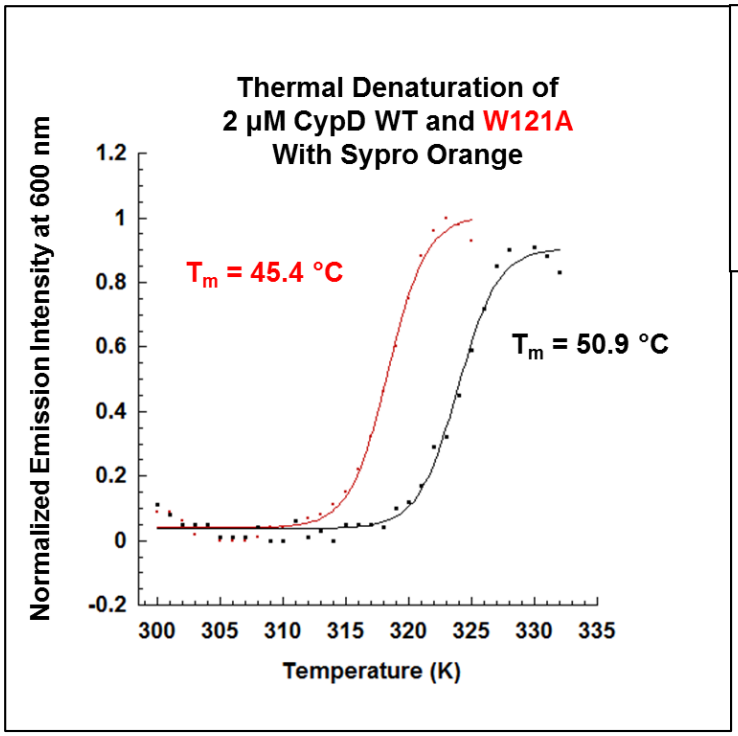

Figure 4.9 Thermal denaturation of CypD WT and mutant W121A monitored by changes in the fluorescence of Sypro Orange. Thermal denaturation of WT CypD in black, T_m = 50.9 °C and thermal denaturation of CypD W121A in red, T_m = 45.4 °C.

4.3.2 p53 aggregates in the presence of active CypD

In light of the propensity of p53 to form insoluble aggregates in the presence of CypD, a modified pulldown assay was designed. Previously, we immobilized GST-CypD on glutathione beads as the bait to capture soluble p53. However, in this scenario, it is impossible to distinguish p53 that has bound to and is pulled down by CypD from insoluble p53 aggregates that sediment together with the glutathione beads. To understand whether or not the pulldown was a binding event or p53 was aggregating and settling with glutathione beads as the NMR results suggested, we compared the initial pulldown condition, i.e. GST-CypD capturing soluble p53, to a control with soluble CypD instead of CypD immobilized on the glutathione beads. In the latter condition, one would expect that if CypD was binding p53, the soluble co-complex would be washed away in subsequent washing steps and we would not detect p53 in the pellet. However, if CypD was causing p53 to aggregate, we would be able to detect p53 in the pellet

since the aggregates will sediment together with the glutathione beads. Indeed, CypD causes both highly purified full-length human p53 as well as recombinant Sf9 p53DBD to aggregate and sediment with the beads (Figure 4.10 a). Moreover, endogenous p53 from H_2O_2-stressed and unstressed human HCT116 cells also aggregates and sediments with the glutathione beads in the presence of soluble CypD, but fails to aggregate when CypD is inhibited by CsA (Figure 4.10 b). Taken together, these results indicate that CypD must be active to interact with p53. Moreover, enzymatically active CypD causes the formation of insoluble p53 aggregates even at the low concentrations of the pulldown assays.

To better understand how the stability and folded state of p53DBD affects the interaction with CypD, we generated a set of common cancer-associated p53 missense mutations which were previously shown to be completely unstructured in the p53DBD at 25 °C [215]. Mutant p53 proteins R175H, L194V, R248Q, R249S, R273H and R282P were expressed in $p53^{-/-}$ HCT cells in the absence of stress and standard biochemical pulldowns were performed (Figure 4.10 c). Structural destabilization of the p53DBD does not reduce p53's ability to interact with CypD; on the contrary it appears to enhance it, indicating that p53 does not require a folded state in order to interact with CypD. Furthermore, the Sf9 p53DBD protein, which we show is insolubally aggregated by CypD, only posesses marginal thermodynamic stability (Figure 3.11 b, Table 4.1). Taken together, these results indicate that CypD interacts with an unstructured region of p53DBD which leads to insoluble aggregation. It should also be noted that the previously mapped p53 minimal construct (amino acids 80-220 [2]) that interacts with CypD by pulldown excludes three β-strands from the core of the p53DBD which would

be critical for proper folding of the protein (Figure 1.2). This supports the idea that CypD does not interact with a folded state of p53.

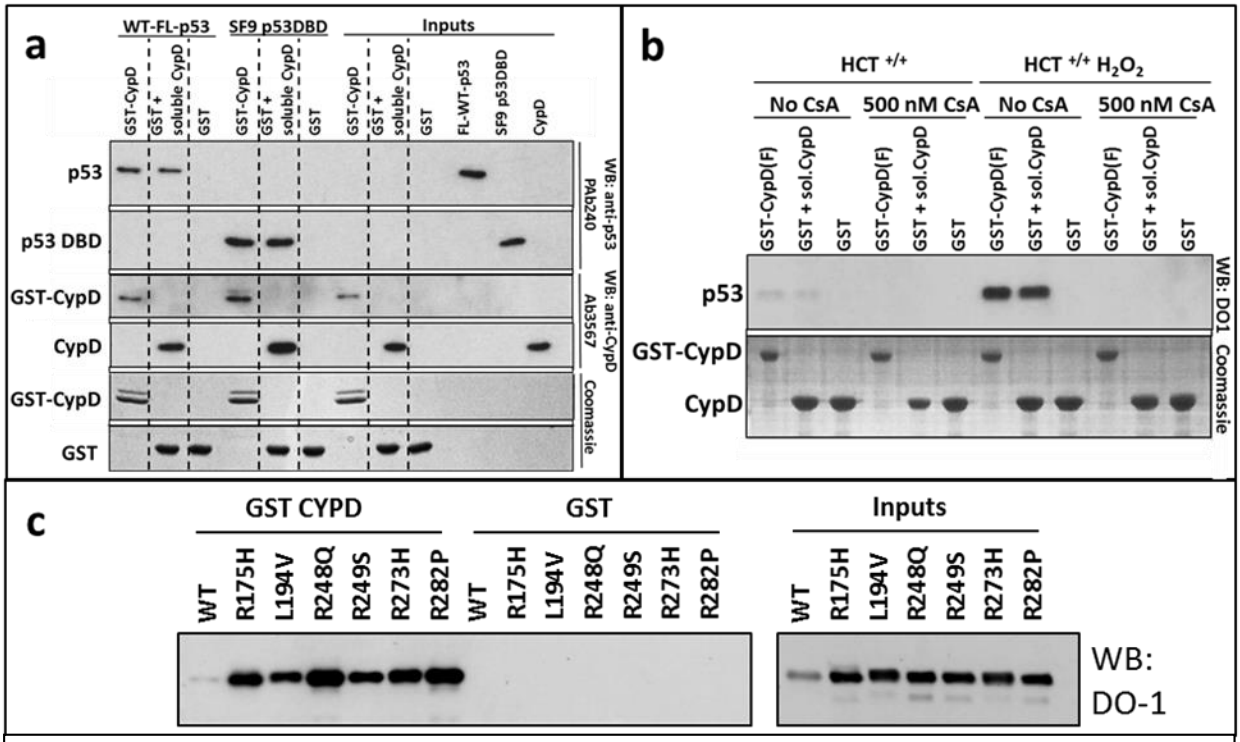

Figure 4.10: p53 is aggregated by active CypD and sediments with beads in pulldown experiment. a) Co-precipitation of commercial WT full-length p53 and SF9 p53DBD by GST-CypD and soluble CypD (between dashed lines) in the presence of GST but not GST alone. Whether CypD is soluble (between dashed lines) or GST-CypD is immobilized on glutathione beads, commercially purified WT-full-length-p53 or recombinant SF9 p53DBD will co precipitate with the glutathione beads only in the presence of CypD. **b)** Co-precipitation of endogenous p53 from H_2O_2 stressed and unstressed HCT116 whole cell lysates by GST-CypD and soluble CypD in the presence of GST but not GST alone. Whether CypD is soluble or GST-CypD is immobilized on glutathione beads, endogenous WT-p53 from H_2O_2- stressed or unstressed HCT116 cells will co-precipitates with glutathione beads in the presence of CypD. **c)** Pulldown of common cancer-associated p53DBD missense mutant proteins. Mutant proteins R175H, R248Q, R249S and R273H are structurally destabilized [215]-(Table 4.1), yet can be readily precipitated by CypD, indicating that proper folding of p53 is not required for interaction with CypD.

Table 4.1 Thermodynamic stability of p53DBD and common cancer-associated p53DBD mutant proteins. All indicated p53 mutant proteins from transfected $p53^{-/-}$ HCT cells are pulled down by CypD (Figure 4.10 2c) yet R175H, R248Q, R249S and R273H have previously been determined to be structurally destabilized [2] indicating that proper folding of p53 is not required for interaction with CypD. SF9 p53DBD is slightly structurally destabilized but interacts with CypD as shown by NMR (Figure 4.1 a-b) and in aggregation assays (Figure 4.10 a). N/D indicates experiments that were not performed. The source of recombinant p53 is indicated in parenthesis.

p53 Construct	CypD Interaction (Source of Recombinant p53)	ΔG (kcal/mol) at 10 °C	ΔG (kcal/mol) At 25 °C
p53DBD	**+** (SF9)	***N/D***	**-3.46** (SF9)
p53DBD	**+** (HCT116)	***N/D***	***N/D***
p53DBD	**-** (*E.coli*)	**-9.76** [215] (*E.coli*)	**-5.96** [215] (*E.coli*)
R175H	**+** (HCT116)	**-2.59** [215] (*E.coli*)	***N/D***
L194V	**+** (HCT116)	***N/D***	***N/D***
R248Q	**+** (HCT116)	**-2.91** [215] (*E.coli*)	***N/D***
R249S	**+** (HCT116)	**-3.09** [215] (*E.coli*)	***N/D***
R273H	**+** (HCT116)	**-3.11** [215] (*E.coli*)	***N/D***
R282P	**+** (HCT116)	***N/D***	***N/D***

4.3.3 CypD causes p53 to self-aggregate into amyloid-like fibrils in vitro

There has been extensive research into the formation of p53 amyloid-like, fibrillar self-aggregates brought on by stress or mutation [315]–[318]. It is thought that p53 residues 252-258 within the p53DBD are highly aggregation prone and a recent study has shown that targeting this region with the small residue 252-258-derived peptide ReACp53 can prevent aggregation and amyloid formation of p53 *in vivo* [319], [320] . Thus, we investigated the nature of the p53DBD aggregates that were generated by CypD during our NMR experiments. It has been shown that thermal denaturation of p53DBD causes non-specific *granular* aggregation of p53DBD. In contrast, mild denaturation, such as the use of pressure, causes the formation of amyloid-like fibrils [315]. We generated p53DBD aggregates by either incubating 50 μM CypD with 100 μM

p53DBD overnight at 25 ºC, or by thermally unfolding 100 µM p53DBD at 55 ºC for 30 minutes in the absence of CypD. Following negative staining of aggregates by 2% uranyl acetate, visualization by transmission electron microscopy (TEM) revealed that p53DBD aggregates generated in the presence of CypD readily formed numerous elongated amyloid-like fibrillar structures, as well as non-specific granular aggregates (Figure 4.11 a-c and Figure 4.12 a-c). It is generally accepted that amyloid fibrils begin as diffuse aggregates that transform into more stable fibrillary forms with time, suggesting that the fibrils act as a slow kinetic trap [321], [322]. In contrast, thermally denatured p53DBD aggregates formed only non-specific large granular precipitates but no fibrillar amyloid-like structures, as expected (Figure 4.13a-b). As additional control, p53DBD that had been incubated overnight at 25 ºC in the absence of CypD formed some granular aggregates albeit to a lesser degree than thermally denatured p53DBD, and, importantly, no amyloid-like fibrils were detected (Figure 4.14 a-b). Finally, p53DBD was incubated overnight at 25 ºC with the catalytically dead CypD mutants F60A and W121A. Again, the degree of precipitation was much less than when p53DBD was incubated with WT CypD and importantly, no amyloid-like fibrils were observed (Figure 4.15 a-d).

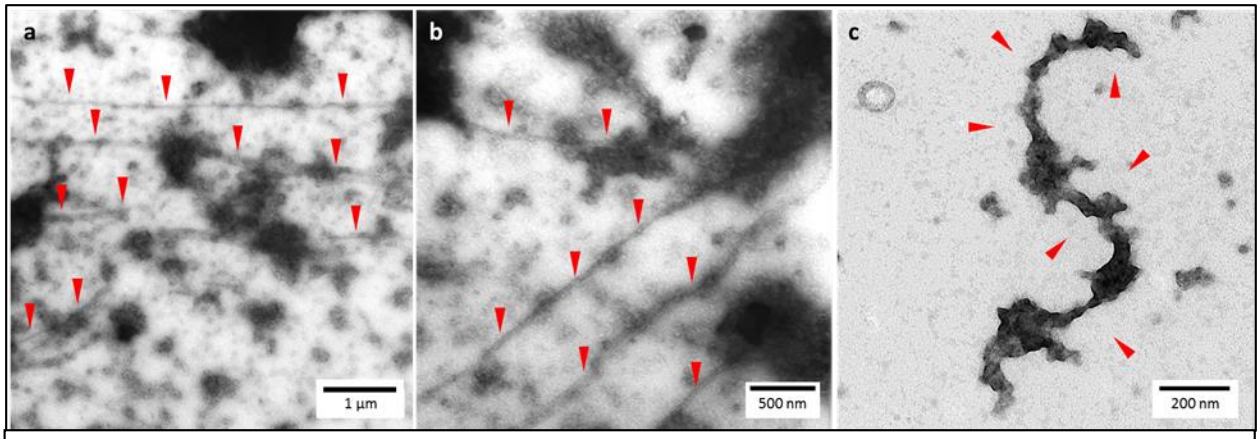

Figure 4.11 TEM of p53DBD incubated with WT CypD ~16 hours at 25 ^{0}C under conditions identical to NMR experiments, negative staining with 2% uranyl acetate. Red arrows indicate amyloid-like fibrils among large diffuse aggregates. a) Elongated fibrils at 30,000x magnification. b) Elongated fibrils at 68,000x magnification. c) Short, individual fibril at 98,000x magnification.

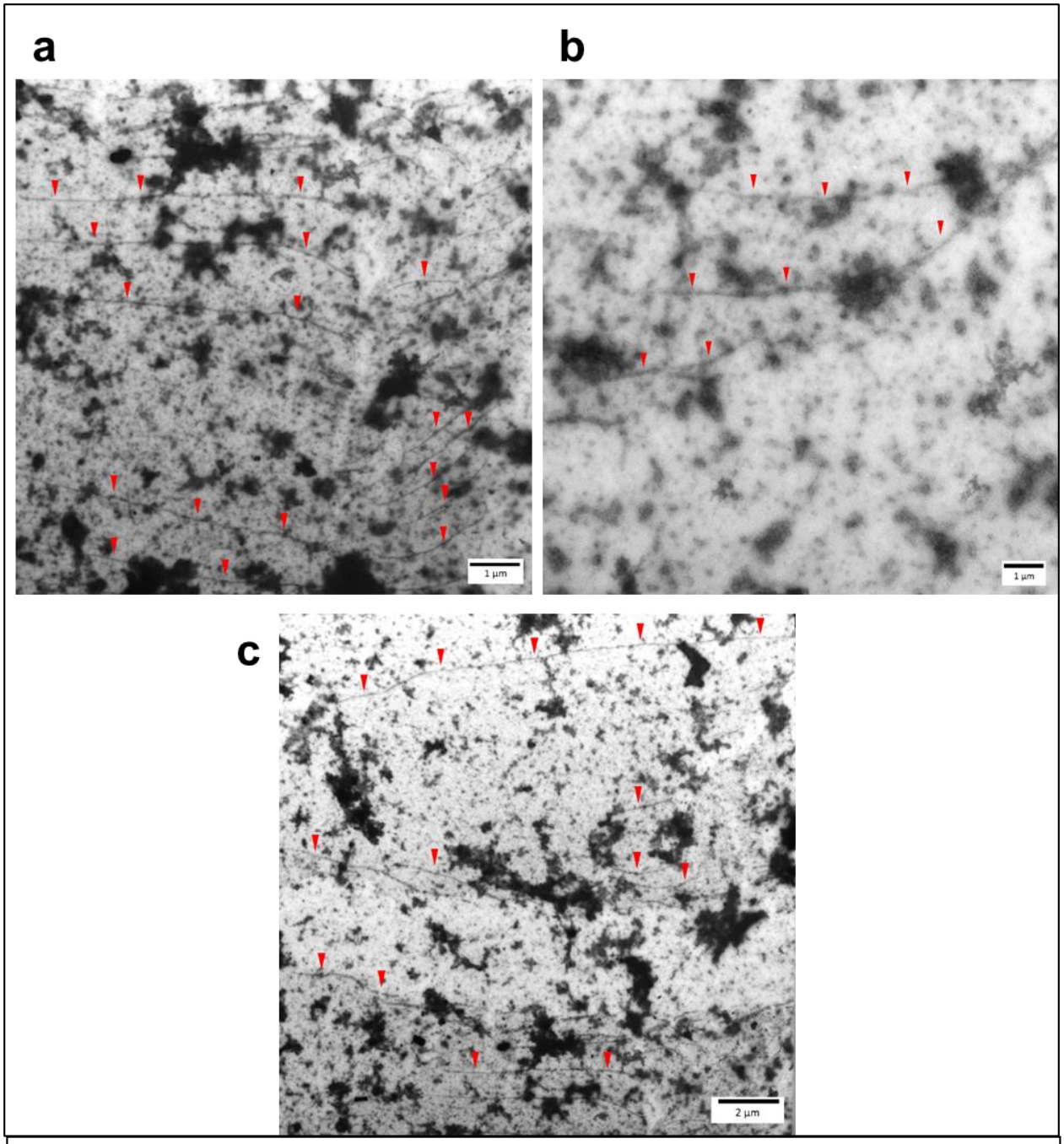

Figure 4.12 a-c) TEM of p53DBD incubated with WT CypD ~16 hours at 25 ^{0}C under conditions identical to NMR experiments, negative staining with 2% uranyl acetate at different magnifications. Red arrows indicate amyloid-like fibrils among large diffuse aggregates.

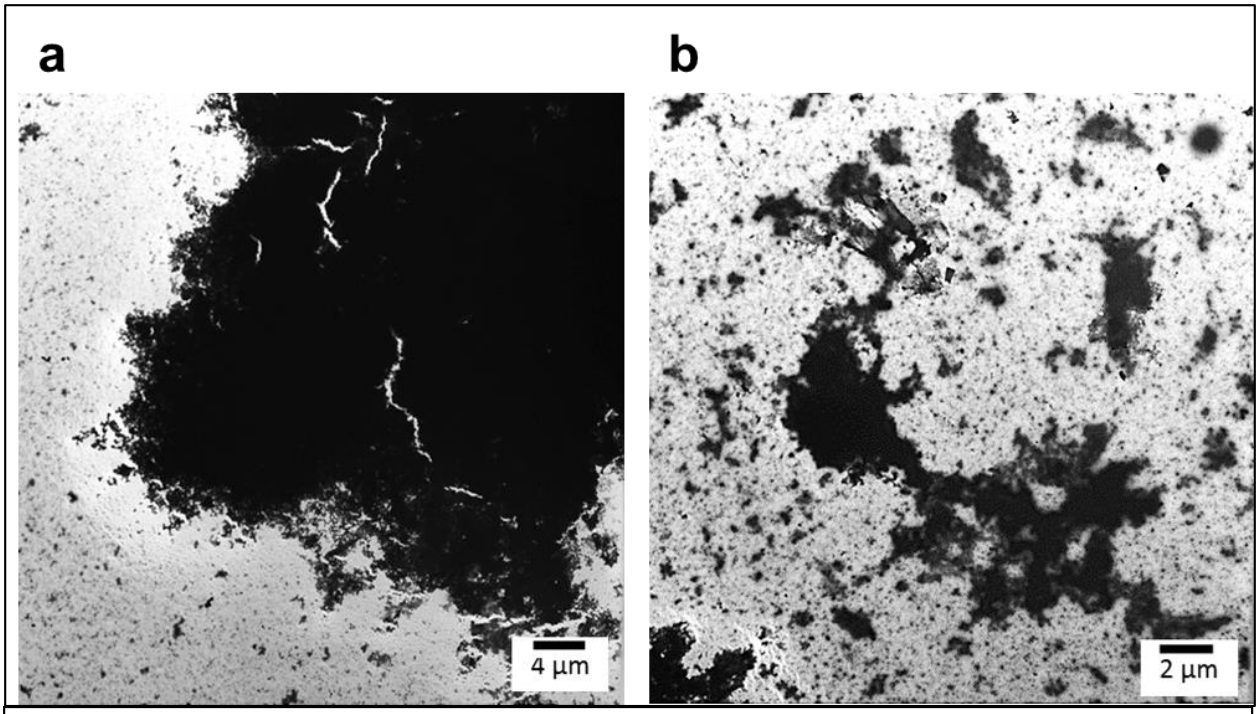

Figure 4.13 a-c) TEM of p53DBD heat denatured 30 min at 55 ^{0}C under conditions identical to NMR experiments, negative staining with 2% uranyl acetate at different magnifications. Only large densities of granular, non-specific, precipitate can be seen; no elongated amyloid-like fibrils.

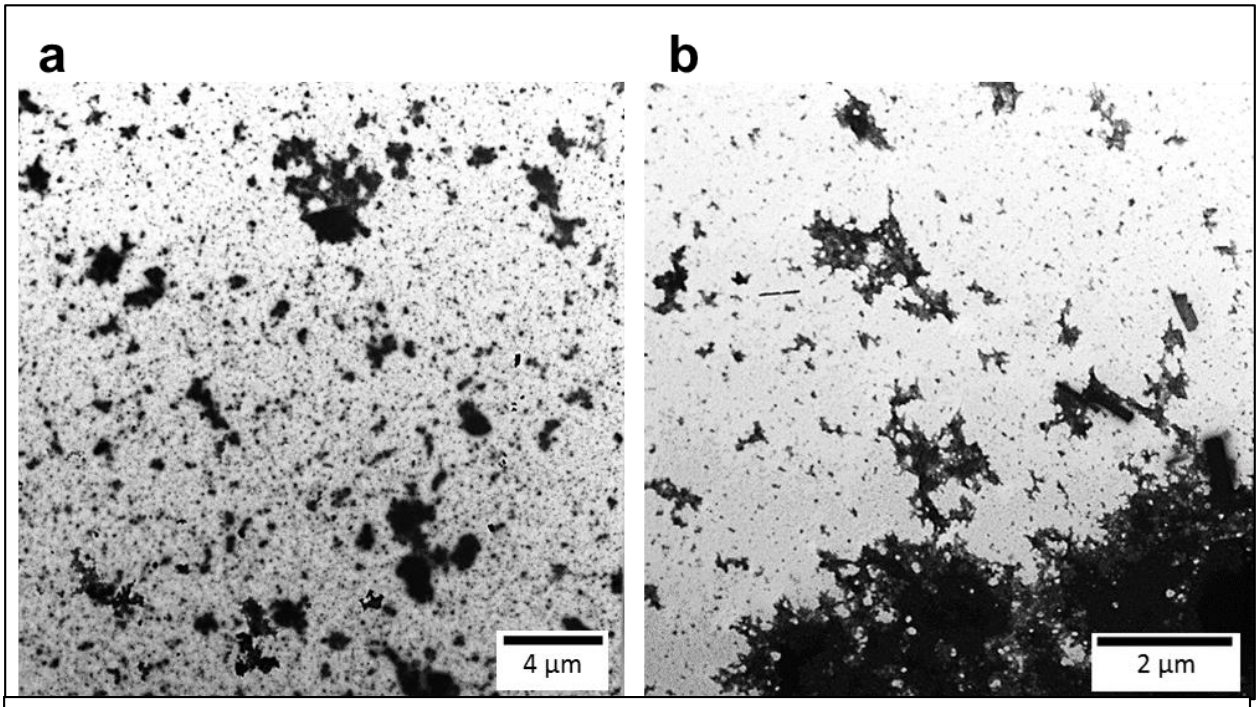

Figure 4.14 a-c) TEM of p53DBD incubated on its own for ~16 hours at 25 ^{0}C under conditions identical to NMR experiments, negative staining with 2% uranyl acetate at different magnifications. Only granular, non-specific, precipitate can be seen; no elongated amyloid-like fibrils.

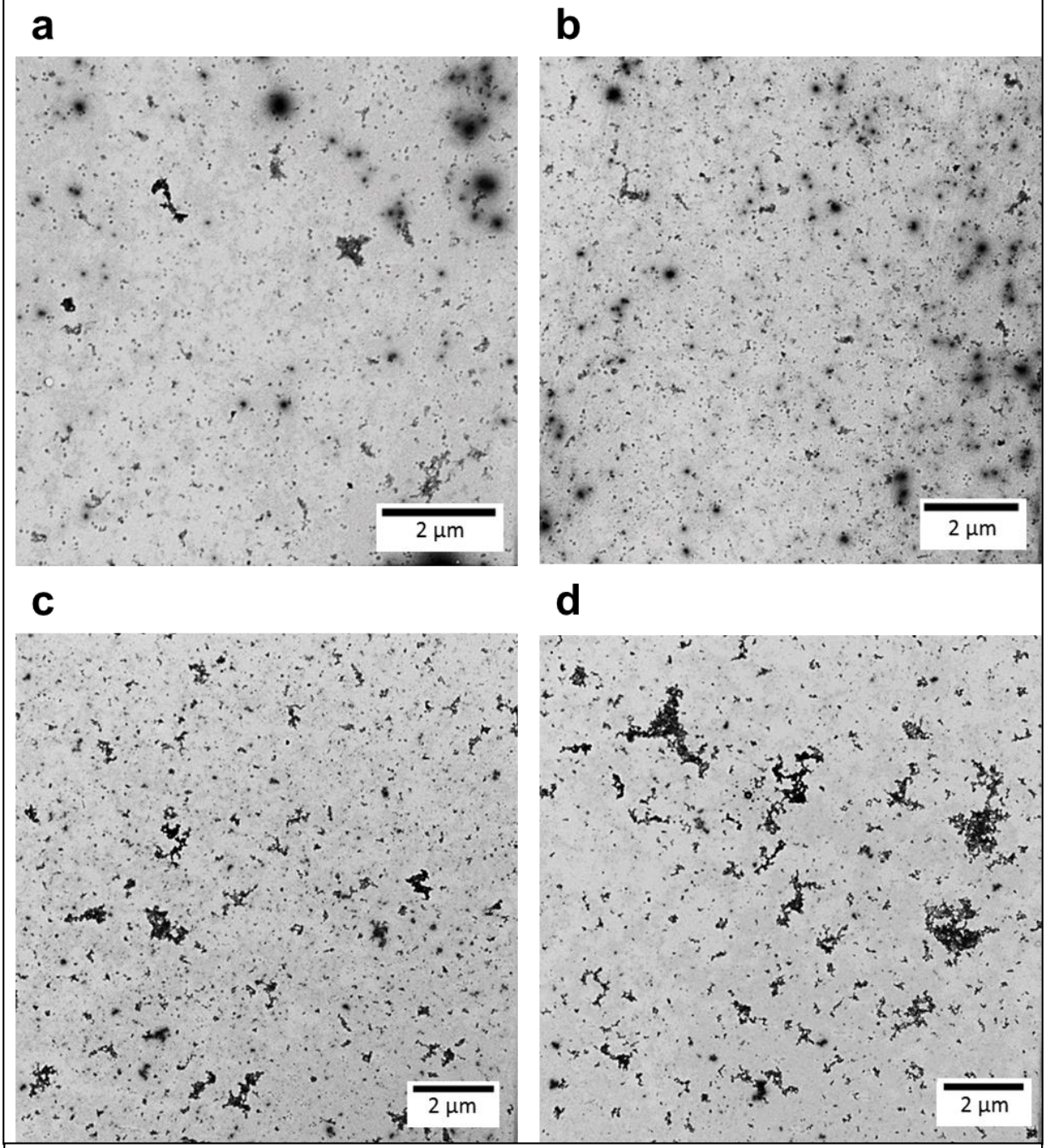

Figure 4.15 a-d) TEM of p53DBD incubated with catalytically-dead CypD mutant proteins ~16 hours at 25 ^{0}C under conditions identical to NMR experiments, negative staining with 2% uranyl acetate at different magnifications.. a-b) p53DBD incubated with CypD mutant protein F60A. c-d) p53DBD incubated with CypD mutant protein W121A. Markedly less granular, non-specific, precipitate can be seen compared to p53DBD in the presence of WT CypD or heat denatured p53DBD. Importantly, no elongated amyloid-like fibrils are present indicating that CypD activity is necessary to form p53DBD amyloid fibrils.

4.3.4 Inhibition of Trap1 sensitizes MEFs to mPT and mPTP pore opening in a p53-dependent manner

It has been shown that aggregation of p53 upregulates the expression of heat-shock proteins including HSP70 [224], [323] and HSP90 [272], [320], [323], [324]. Inhibition of HSP70 using the small inhibitor pifithrin-μ prevents translocation of p53 into the mitochondria [214], [325], [326]. We and others have previously shown that hypoxic and other stress-induced mitochondrial p53 physically associates with the mitochondrial matrix-located protein import and folding chaperones mtHSP60 [2], [193], [269], [270] and mtHSP70 [2], [193], [222] (also known as GRP75, UniProtKB: P38646). Furthermore, we and others have shown that in order to prevent aggregation, mutant p53 in cancer cells forms a stable interaction with the cytosolic HSP90 chaperone [327] and that the HSP90 inhibitor 17-AAG disrupts this complex [221], [222], [246], [272], [328]–[330]. Strikingly, the inhibitor gamitrinib, a specific mitochondria-targeted 17-AAG analogue, inhibits a mitochondrial HSP90 homologue, Trap1, as well as the mitochondrial pool of HSP90. This leads to sensitization of cells to mPTP opening in a CypD dependent manner [11]–[13]. Conversely, overexpression of Trap1 protects cardiomyocytes and rat brains from I/R injury and mPT [266], [273], [276]. Importantly, it has been demonstrated that CypD can form stable complexes with both HSP60 and Trap1 [12], [269].

In order to understand the role of p53 in the context of Trap1-mediated protection from mPT, we performed calcein release assays in WT, $p53^{-/-}$ and $CypD^{-/-}$ MEFs using FACS. In this assay, healthy, mitochondria retain green fluorescence from calcein dye in the presence of the quencher $CoCl_2$ which can only enter the mitochondria and

quench calcein fluorescence upon opening of the mitochondrial permeability transition pore. Experiments were performed in the presence or absence of H_2O_2 stress, with and without the selective Trap1 inhibitor Gamitrinib and in the presence or absence of the CypD inhibitor CsA (Figure 4.16). Inhibition of Trap1 in unstressed WT MEFs caused marked mPTP opening, and further addition of H_2O_2 stress caused WT MEFs to undergo complete mPT opening. As expected, no mPT could be detected in WT MEFs in the presence of the CypD inhibitor CsA or in CypD$^{-/-}$ MEFs under any condition (except for the positive control with the calcium ionophore ionomycin), confirming the role of CypD as an indispensable component of mPT and the mPTP. Importantly, however, inhibition of Trap1 only minimally sensitized p53$^{-/-}$ MEFs to mPTP, and addition of H_2O_2 stress failed to yield further sensitization. These results indicate that p53 plays a major role in triggering mPT opening. Moreover, p53 acts through a novel mechanism involving Trap1, a member of the mitochondrial unfolded protein response (mtUPR) pathway.

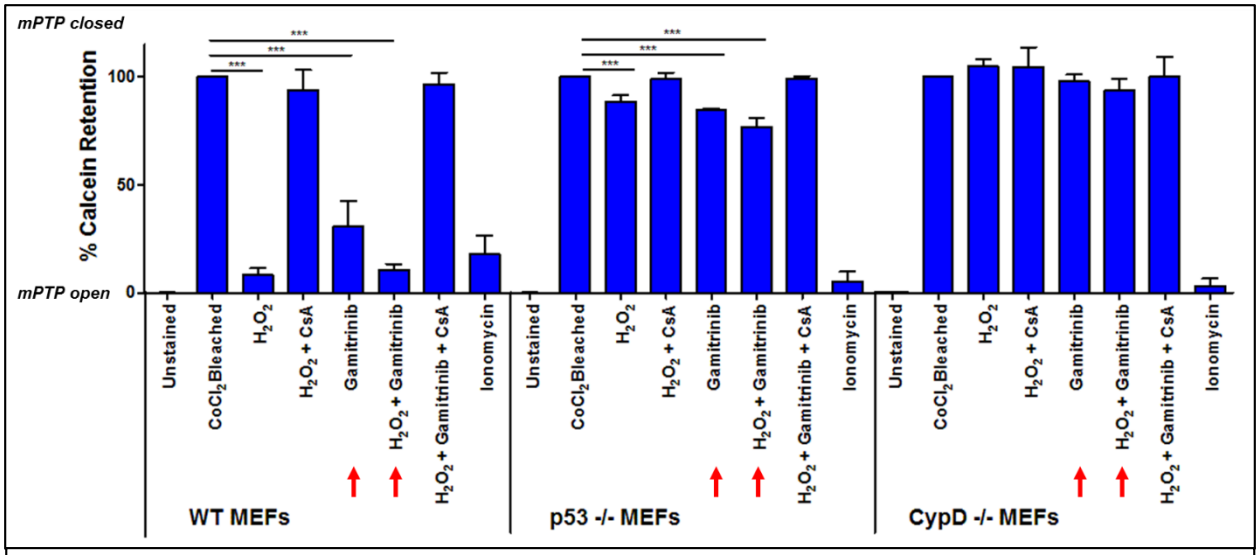

Figure 4.16: Inhibition of Trap1 sensitizes MEFs to mPT in a p53-dependent manner. Retention of calcein fluorescence within the mitochondrial matrix in MEFs is a direct reflection of mPTP opening, measured by FACS in the presence or absence of H_2O_2 oxidative stress, with and without the Trap1 inhibitor gamitrinib and in the presence or absence of the CypD inhibitor CsA. High values of retained calcein fluorescence indicate that the mPTP is closed while low values of retained calcein fluorescence indicate opening of the mPTP. H_2O_2 and gamitrinib greatly sensitize WT MEFs (red arrows) to mPT but only minimally sensitize in $p53^{-/-}$ MEFs. mPT does not occur in the absence of CypD. Data from 3 independent biological replicas, mean +/- SD are shown.

4.4 Discussion

There is a great interest in uncovering the full structural and functional details of the mitochondrial permeability transition pore, and particularly the regulation of this process. Modulation of the mPTP has been implicated as a therapeutic target for multiple diseases including ischemia-reperfusion injury [2], [60], Alzheimer dementia [10] and cancer [11]. Here we investigated the role of p53 in mPT, which in this context acts as an oxidative stress signaling molecule locally in the mitochondrial matrix. Our results provide new details of the potential mechanism how p53 regulates mPTP opening. We previously showed that in response to oxidative stress and in I/R brain injury (stroke), accumulation of p53 in the mitochondrial matrix causes activation of CypD, triggering the opening of the mPTP and necrotic death[2]–[7]. This novel effector pathway of necrotic rather than apoptotic death *via* the mitochondrial p53-mPTP axis,

mediated by CypD interaction, was subsequently confirmed in the context of oxidative damage-, dexamethasone-, cisplatin- and doxorubicin-induced necrotic death in cancer cells, osteoblasts and neurons [2]–[7]. Proteins translocated across the outer and inner mitochondrial membranes need to be refolded when they arrive in the matrix, a process requiring one or more molecular chaperones [331]. Upon translocation, mitochondrial matrix p53 is stabilized by a variety of molecular chaperones including HSP60, HSP70 and HSP90 under stress and non-stress conditions [221], [222], [332]. Notably, in unstressed healthy cells CypD can also interact with the matrix chaperones HSP60, HSP90 and Trap1 [9], [12], [332], [333]. Moreover, CypD can assemble into a higher-order complex consisting of CypD, HSP60, and either HSP90 or Trap1 [12], [269].

Our *in vitro* experiments reveal that a dynamic interaction occurs between CypD and the DNA binding domain of p53, as shown *via* NMR by slow-exchange behavior of catalytically active CypD residues. This slow exchange behavior is similar to that previously characterized for another prolyl-isomerase, Pin1, with its substrate APP [308] indicating that p53 may be a substrate of CypD. More importantly, we show that WT p53 interaction with CypD causes robust aggregation of WT p53 derived from various sources, including recombinant baculoviral human p53DBD, endogenous full-length human p53 from H_2O_2 -stressed and unstressed HCT116 colon cancer cells and purified human full-length p53. These results suggest that CypD activity causes destabilization of the imported unfolded p53, which leads to its irreversible aggregation in the matrix. This is supported by an additional control NMR experiment in the presence of urea where we continue to observe dynamic slow-exchange behavior but do not detect formation of insoluble aggregates because they are solubilized by urea.

The fact that CypD retains its ability to interact with structurally destabilized *mutant* p53 proteins supports the hypothesis that CypD interacts with unfolded WT p53 entering the mitochondrial matrix upon stress. Intriguingly, we find that the insoluble p53 aggregates formed by interaction with CypD are not amorphic but tend to be long, amyloid-like fibrillary structures.

The physiological significance of stress-induced p53 aggregation in the mitochondrial matrix is not yet clear. However, there is growing literature about the role of the mitochondrial unfolded protein response [303], [305], [334]. It has been shown that the refolding of p53DBD is slow [215], [335] which makes it vulnerable to off-target interactions and processes [323] including proline cis-trans isomerization. mtUPR could play an important role in stabilizing the influx of the unfolded p53, since p53 will require refolding upon entry into the matrix. We had shown previously that CypD and p53 from cellular extracts interact with each other in immunoprecipitations [2], but it was not clear whether this is a direct interaction or whether this interaction between p53 and CypD is mediated by a bridging factor. Here, we propose a model where p53 enters into the matrix upon cellular stress and binds to the Trap1/HSP60/HSP90 chaperone complexes. These chaperones complexes are present in the matrix of unstressed cells and keep CypD inactive with respect to mPT [11]–[13], [270]. According to this model, p53 binding to Trap1/HSP60/HSP90 releases CypD from the chaperones. The ensuing CypD liberation activates its enzymatic isomerase activity. Active CypD then acts on structural mPTP proteins as isomerization substrates, thereby inducing opening of the mPT pores. Importantly, active CypD also isomerizes p53 (and possibly other proteins), thereby causing p53 aggregation (Figure 4.17). The driving force for a change in the

prolyl cis/trans isomerization of p53 could be that the aggregate and fibril forming unit of p53 may require a cis-proline. Preferential aggregation of a cis-prolyl p53 would remove cis-prolyl p53 from the equilibrium of soluble p53 and drive the isomerization [336]. Moreover, it is possible that aggregated p53 sequesters Trap1/HSP60/HSP90, in turn leading to the activation of additional CypD. This generates a positive feed-forward loop for CypD activation and the cell undergoes prolonged mPT, thereby reaching the point of no return towards necrotic death. Our FACS data support this model where the inhibition of Trap1 sensitizes p53-proficient WT MEFs to mPT and pore opening in a p53- and CypD-dependent manner. This implies that p53 serves as a major mitochondrial stress signal transducer that requires Trap1 to impinge on, thereby activating CypD. This working model can now be tested in the future.

Necrosis has long been considered a completely unregulated form of cell death. However, there is a growing body of evidence implicating a variety of regulated necrosis pathways. These pathways have taken on different names including the necrosome signaling complex, ferroptosis, oxytosis, NETosis, ETosis, parthanatos, pyroptosis, pyronecrosis and finally CypD-mediated necrosis [55], [56]. Globally, these various regulated necrosis pathways fall under the newly-coined term necroptosis. Our work supports the notion of a regulated necrosis in the condition of oxidative stress, and implicates p53 as an important signaling molecule within the CypD-mediated necrotic pathway. This work motivates additional research into modulation of p53-mediated necrosis as an inhibitory or activating target for the treatment of various diseases.

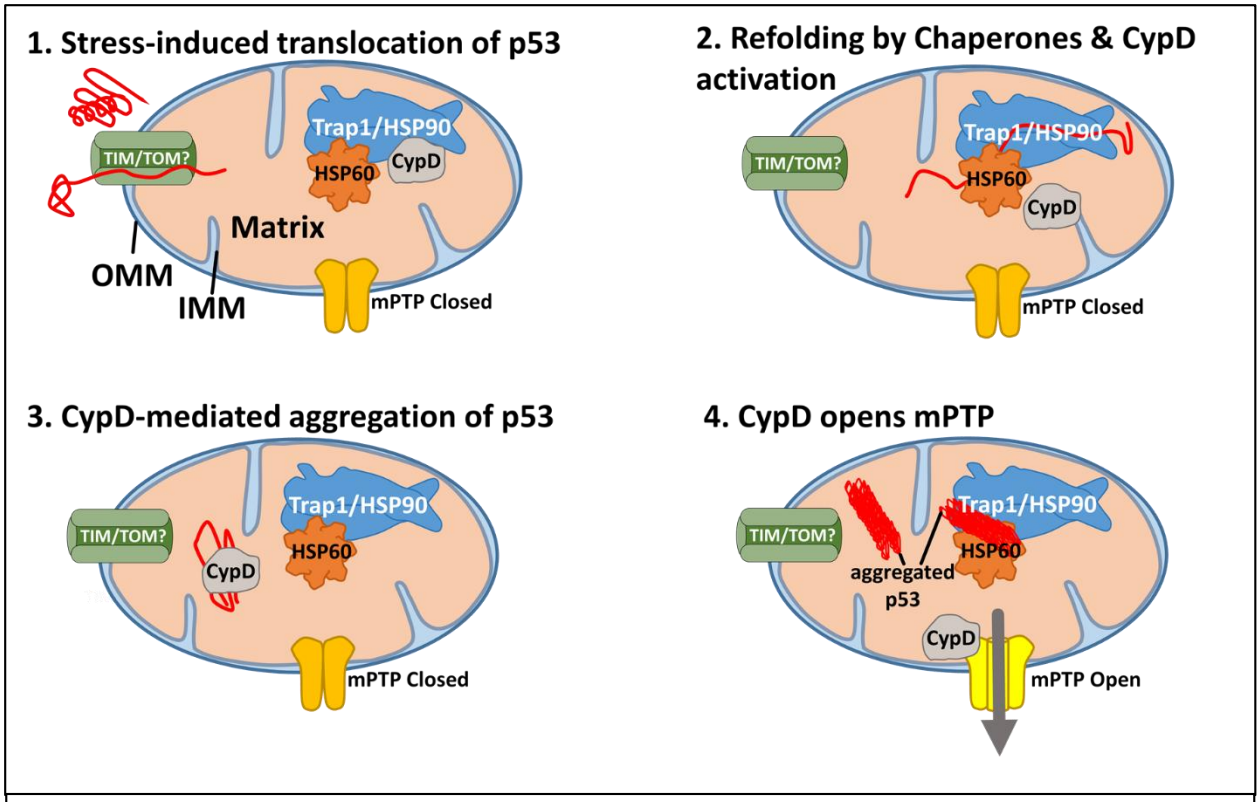

Figure 4.17: Proposed model of stress-induced p53 activating CypD upon p53's entry into the mitochondrial matrix. This leads to mPT. 1) Stress-induced p53 is imported into the mitochondrial matrix, unfolding in the process. 2) Chaperones Trap 1 and HSP60/90 are recruited to refold p53, which competes off CypD, normally held inactive by complexation with Trap1/HSP60/90. Release of CypD activates its isomerase activity. 3) Liberated CypD then isomerizes multiple proteins including p53 (causing p53 aggregation). 4) CypD is recruited to the structural components of the mPTP pore and induces pore opening, leading to energetic breakdown and necrotic cell death.

Chapter 5: General Discussion and Future Directions

Stroke and myocardial infarction are among the leading causes of death and permanent disability worldwide [1]. The underlying cause of major tissue damage comes from reperfusion injury after a period of ischemia [16], [18], [30]. Currently, no pharmacological treatments for reperfusion injury exist though several drugs are currently awaiting clinical trial outcomes [101], [162]. One major cell-death pathway associated with reperfusion injury is necrosis, which was recently shown to be dependent on the opening of the mitochondrial permeability transition pore (mPTP) and is ultimately regulated by the sole mitochondrial cyclophilin *cis/trans* prolyl-isomerase family member CypD [8], [211], [333], [337]. Further regulation of mPTP opening is proposed to be facilitated by translocation of p53 protein into the mitochondrial matrix, which activates CypD and drives mPT [2]. The work presented in this thesis explores the biophysical interaction of CypD and p53 from two perspectives and concludes with the proposition of a new model. This model proposes that p53 activates CypD through displacement of CypD from a constitutively inactive complex with mitochondrial chaperone proteins Trap1 and HSP60/90.

The initial model for how p53 activates CypD to trigger mPTP opening and subsequent necrosis hypothesized that CypD binds directly to p53 and forms a stable protein-protein complex. The model was supported by pulldown and immunoprecipitation experiments which suggested a protein-protein complex could exist [2]. Extensive *in vitro* efforts to detect the binding of CypD to p53 to support this model however, were largely unsuccessful when working with recombinant p53 protein purified from *E.coli* bacteria as is primarily discussed in Chapter 3. Expression of p53 in *E.coli*

was chosen because it yields large amounts of protein for biophysical experiments such as X-ray crystallography and allows isotopical labeling for NMR experiments. Furthermore, an efficient protocol for the expression and purification of the DNA-binding domain of p53 exists [215] and this construct has been shown to interact with CypD in mammalian cells [2]. We and others [215], [227] show through denaturation experiments and NMR that both p53DBD and CypD expressed in *E.coli* are folded and mass spec analysis indicates the correct proteins are being expressed in our system. A functional assay of CypD indicates that CypD is an active enzyme which can catalyze the isomerization of a substrate peptide. Despite all of the quality controls pointing to both CypD and p53DBD being properly expressed and folded, no single biophysical experiment is able to detect any indication of binding including gel filtration, fluorescence anisotropy, isothermal calorimetry and NMR. Potential explanations for why no direct binding of *E.coli* p53DBD to CypD could be detected include the potential requirement of a post-translational modification or the requirement of a bridging protein that is not present in *E.coli*.

The second half of Chapter 3 focuses on comparing p53DBD expressed in *E.coli* to p53DBD expressed in SF9 insect cells. SF9 cells were chosen as an alternate expression system because they can post-translationally modify proteins, have chaperone proteins that may affect protein folding and yield sufficiently high quantities of protein for biophysical experiments. I found that SF9 p53DBD is thermodynamically destabilized compared to *E.coli* p53DBD. The degree of thermodynamic destabilization is of the same order of magnitude that certain, known, structurally-destabilizing p53DBD cancer mutations confer onto p53 [215], [229]. However, the SF9 p53DBD protein does

interact with CypD by the classical pulldown experiments which is consistent with the behavior of mammalian p53DBD as previously described [2]. This led to the speculation that perhaps CypD interacts with completely or partially unfolded p53. This could be rationalized by the fact that proteins like p53 enter the mitochondrial matrix unfolded via channel proteins. Upon entering the mitochondrial matrix newly imported proteins can refold (often with the help of chaperones, such as heat shock proteins or prolyl isomerases). Presumably, the translocation of p53 into the mitochondrial matrix occurs through the TIM/TOM complex. However, without a mitochondrial localization signal on p53, the exact details of how p53 enters the mitochondria are not known today. What is the signal for p53 import into the mitochondria? Which proteins facilitate delivery and import of p53 into the mitochondria? Does p53 refold in the mitochondria or remain unfolded? Does p53 need to be post-translationally modified for mitochondrial import and do the PTMs change once imported into the matrix? Addressing these question would allow for a better understanding of what other proteins influence p53 signaling in the mitochondria and during which p53-signaling stages pharmaceutical intervention could help protect tissues from IR-injury.

The remainder of Chapter 3 discusses the effects of detergents on the stability of p53DBD. We used 1% Triton X-100 during the purification of SF9 p53DBD to improve protein solubility and yield. Specifically, we wanted to know if Triton X-100 affected the thermodynamic stability of p53DBD and thereby helped to facilitate an interaction with CypD. Using two methods, we found that the presence of detergents reduced the melting temperature of p53DBD. Firstly, tracking changes in the intrinsic protein fluorescence spectrum of *E.coli* p53DBD upon heating, we found that the detergent

Tween 20 decreased the melting temperature of *E.coli* p53DBD by 3 °C and the thermodynamic stability by 3.47 kcal/mol from -5.96 kcal/mol in the absence of Tween 20 to -2.49 kcal/mol in the presence of 0.1% Tween 20. Substitution of Tween 20 for Triton X-100 in the fluorescence assays was necessary because of the strong absorbance of Triton X-100 at 280 nm, which corresponds to the excitation wavelength necessary for the fluorescence assay [292]. A direct effect of Triton X-100 on p53DBD stability was determined by DSC, which also showed a 4.5 °C reduction in the T_m of *E.coli* p53DBD. Triton X-100 was always present in the previously described pulldown of endogenous p53 from cells [2]. This, paired with our finding that Triton X-100 destabilizes p53DBD, supports the hypothesis that CypD likely interacts with a structurally destabilized form of p53 protein. This is consistent with our finding that thermodynamically destabilized SF9 p53DBD does interact with CypD by classic pulldowns while more stable *E.coli* p53DBD does not interact with CypD. Based upon these conclusions, thermodynamic destabilization of p53DBD is necessary for interaction with CypD, but we cannot conclude that it is sufficient. Previous literature and the results of calcein release assays in Chapter 4 support a model where p53 indirectly activates CypD rather than forming a direct, stable protein-protein complex. This implies that the *in vitro* observations where CypD causes SF9 p53DBD, but not *E.coli* p53DBD, to aggregate could be due to decreased solubility of SF9 p53DBD compared to *E.coli* p53DBD. To test whether or not thermodynamic destabilization of p53DBD is sufficient to facilitate an interaction with CypD, some of the biophysical experiments could be repeated in the presence of mild denaturants such as urea or zinc chelators. It has been established that CypD is active in the presence of 2 M urea and

NMR detects chemical shift perturbations and slow exchange behavior of CypD residues upon titration of SF9 p53DBD in 2 M urea. Since Figure 3.11a shows that the unfolding transition of *E.coli* p53DBD by urea titration begins at an approximate concentration of 2 M urea, the NMR experiment in the presence of 2 M urea should be repeated with titration of *E.coli* p53DBD to CypD. The expected result, if thermodynamic destabilization of p53DBD is sufficient to facilitate an interaction with CypD, would be that thermodynamically destabilized *E.coli* p53DBD should now be able to induce chemical shift perturbations and slow exchange behavior of CypD residues by NMR in the presence of 2 M urea similar to what was observed upon titration of SF9 p53DBD.

To fully validate the role of thermodynamic stabilization of p53 for interaction with CypD, it could be useful to repeat the classical pulldown experiments and NMR experiments with some of the known structurally destabilizing p53-cancer point mutations. Previous work [2] and pulldowns discussed in Chapter 4 show that deletion constructs (e.g. minimal construct residues 80-220) of p53 that are expected to be unfolded and unstructured p53 point mutant proteins, still interact with CypD by pulldown. However, these constructs were all expressed in transfected $p53^{-/-}$ mammalian cell lines therefore the presence of a bridging protein such as heat shock proteins or the requirement for specific post-translational modifications of p53 cannot be excluded as the requirement for interaction with CypD. For future work, structurally-destabilized p53 point mutant proteins, such as R175H or C242S, should be purified from *E.coli* and analyzed for post-translational modifications by mass spectrometry. We expect that these mutant proteins are unmodified because WT p53 is also not modified when expressed in *E.coli*. Next, we would determine the thermodynamic stability of the

mutant proteins by equilibrium urea denaturation and compare it to the literature values. The mutant proteins can then be tested for CypD interaction by pulldown and NMR. We expect that only non-PTM, but thermodynamically *destabilized* p53 mutant protein, would interact with CypD. These could be compared to known p53 hyperstabilizing mutations, such as N239Y or the M133L/V203A/N239Y/N268D quadrimutant which are thermodynamically stabilized by -1.49 and -2.6 kcal/mol respectively [217]. We expect that non-PTM but thermodynamically *stabilized E.coli* p53DBD, would no longer interact with CypD by pulldown or NMR.

Chapter 4 of this thesis discusses the aggregation behavior of SF9 p53DBD in the presence of active CypD and establishes a new hypothesis for how CypD and p53 could interact. We detected changes in the chemical environment of CypD backbone amide protons upon addition of 2 molar excess of SF9 p53DBD by NMR (Figure 4.1). Some CypD residues show significant chemical shifts while others exhibit slow-exchange behavior upon addition of SF9 p53DBD, as is commonly observed in dynamic interactions such as that of prolyl isomerization [308]. Furthermore, a 4-hour incubation of SF9 p53DBD with CypD results in complete aggregation of SF9 p53DBD. This lead us to hypothesize that CypD activity is responsible for driving aggregation of SF9 p53DBD. This is tested in classic pulldowns where key CypD active-site residues R55, F60, F113 and W121 are mutated to alanines. These CypD mutant proteins can no longer pulldown endogenous WT p53 from HCT cell lysates. These mutant proteins are also no longer able to catalyze the isomerization of the CypD substrate peptide Abz-AFPF-pNA in activity assays. Taken together, the results indicate that CypD activity is required for interaction with p53 and the result of the interaction is irreversible

aggregation of p53. These findings do not support the original model where it was expected that CypD and p53 would form a stable protein-protein complex. Support for the new model, where CypD leads to aggregation of p53, was further obtained from the co-aggregation assays where p53 can still be detected among the sedimented GST beads in the presence of soluble, non bead-bound, CypD but not in the absence of CypD. Had a stable complex been formed, soluble CypD and p53 would have been washed away during wash steps in the experiment. Final evidence in support of this model was found through TEM analysis of SF9 p53DBD aggregates that form elongated amyloid-like fibrils, but only in the presence of active CypD. Neither catalytically-dead CypD mutants nor heat denaturation or incubation of SF9 p53DBD alone lead to the formation of amyloid-like fibrils.

The CypD-dependence of SF9 p53DBD aggregation could be further quantified in light scattering assays [338]. This assay would monitor the amount of light scattered upon aggregation of p53 by monitoring a wavelength independent of protein absorption or interference of buffer constituents. As more protein aggregates, more light will be scattered and the aggregation rate can be determined. Here, it would be expected that under conditions identical to NMR and TEM, active CypD would increase the rate of the aggregation of SF9 p53DBD compared to SF9 p53DBD alone. Catalytically dead CypD or CsA-inhibited CypD is not expected to increase the rate of p53DBD aggregation. It would be important to verify the protein concentration requirements for these assays as both NMR and TEM were conducted at 75x and 40x respectively higher concentrations of SF9 p53DBD than what was used in pulldown and co-aggregation assays. Since p53 protein in solution exists at equilibrium between folded and partially unfolded states, and

it is expected that addition of CypD drives aggregation of the unfolded state, high concentrations of p53 protein would aggregate more readily in a CypD dependent manner.

As shown by TEM, incubation of SF9 p53DBD in the presence of active CypD leads to the formation of amyloid fibrils *in vitro*. Amyloid formation could also be tracked in real time by monitoring the fluorescence of Thioflavin T (ThT) binding to SF9 p53DBD amyloid fibrils in a CypD dependent manner. ThT is a reporter dye for amyloid formation by monitoring its increase in fluorescence at 482 nm (excitation 440 nm) upon ThT binding to amyloid fibrils [339]. The same protein concentration requirements, as for 90 º light scattering assays, would need to be explored here as literature reports of ThT binding to amyloid are typically performed at 10-20 µM concentrations of protein [251], [340]–[342] while amyloid fibrils reported in Chapter 4 were formed at 150 µM of SF9 p53DBD. Similarly, to understand whether or not the amyloid fibrils detected *in vitro* have any physiological relevance *in vivo*, tissue sections of necrosed mouse brains from the previously reported stroke model [2] could be stained with ThT or Congo Red (CR). This would allow us to determine whether amyloid fibrils in WT, $p53^{-/-}$ and $CypD^{-/-}$ tissues exist in necrotic brain tissue [342], [343]. Another approach, using the same tissues, could be to investigate the co-localization of a p53 antibody with an aggregate-specific antibody such as A11. A11 binds to amyloid fibrils and has been shown to co-localize with p53 mutant protein in breast cancer cell lines, tumor biopsy samples and purified p53 R248Q mutant protein [251], [344]–[346]. While it is not necessarily required for p53 to form amyloid fibrils in the mitochondrial matrix in the context of activating CypD for regulation of the mPTP, it would help distinguish the *in vitro*

observations of the CypD interaction with p53 from the actual *in vivo* mechanism by which p53 regulates CypD activity and mPTP opening.

The future experiments of greatest interest would be to fully characterize how influx of p53 into the mitochondrial matrix upon stress displaces CypD from a constitutively inactive complex with Trap1 and HSP60/90. The literature reports several binary interactions between CypD and chaperones HSP60 [269] and Trap1 [12], as well as p53 with CypD [2] and HSP60 [2], [270], [271]. However, the full set of interactions have not yet been shown in one study. As such, the first experiment should be to immunoprecipitate p53, as has been done before [2], and probe for co-precipitation of HSP60, HSP90, Trap1 and CypD to show a complete set of interactions.

Calcein release assays and FACS analysis in Chapter 4 shows that inhibition of mitochondrial HSP90 and Trap1 using the inhibitor gamitrinib, sensitizes cells to mPT and is highly dependent on p53. We postulate that this is due to displacement of CypD from Trap1 and HSP60/90. This is plausible since $p53^{-/-}$ cells are still sensitized to mPT with gamitrinib as would be expected for simple CypD displacement from Trap1 and HSP60/90. However, the effect of gamitrinib inhibition is compounded when p53 and furthermore p53 with H_2O_2 stress is present. In these instances, the majority of cells undergo mPT indicating that p53 and gamitrinib have a synergistic effect in sensitizing cells to mPT. It is still unclear what the necessary and required steps for CypD displacement are. FACS data in $p53^{-/-}$ cells indicates that inhibition of Trap1 and HSP90 is sufficient for mild mPT sensitization. If p53 and gamitrinib are both the target of Trap1 and sequestering Trap1 is sufficient to release CypD for mPTP formation, then increasing gamitrinib concentrations in $p53^{-/-}$ cells should be able to recapitulate the

greater mPT sensitivity observed by FACS calcein release assays in WT cells (containing p53) upon H_2O_2 stress. Similarly, it should be possible to immunoprecipitate Trap1 from H_2O_2 stressed cells, which should co-precipitate p53 along with the expected components HSP60/90 and, when compared to unstressed cells, relatively less CypD.

However, it is possible that Trap1 is not the target of p53 upon translocation into the mitochondria. In such a model, it could be hypothesized that the observed compounding effects of gamitrinib and p53 are due to sequestering of all the chaperones that keep CypD constitutively inactive. That is, p53 could bind HSP60, perhaps as a client protein for refolding, while gamitrinib inhibits Trap1 and HSP90; the combination of which allows CypD to freely participate in mPTP regulation. This hypothesis could be tested in the calcein release assay by FACS, where mitochondrial targeting of an HSP60 inhibitor such as Mizoribine [347], EC3016 [348], or Epolactaene [349] would serve as a surrogate for p53 in $p53^{-/-}$ cells. The mitochondria-targeted HSP60 inhibitor, in tandem with gamitrinib, should recapitulate the greater mPT sensitization effects seen in WT cells containing p53 and H_2O_2 stress.

The displacement of CypD from Trap1 and HSP60/90 by p53 could also be tested biophysically as expression protocols for Trap1 [350], HSP60 [351] and HSP90 [352] have been established. Much like the biophysical experiments described in chapter 3, the combination of fluorescence anisotropy, analytical gel filtration or pulldowns could be used to show the formation of the CypD-inactivating complex with Trap1 and HSP60/90, followed by disruption of that complex by the addition of p53. Working with purified proteins could also serve to validate or motivate testing of the two

aforementioned models to better understand the individual interactions necessary for CypD displacement. Paired with the availability of inhibitors that no longer need to be mitochondrial targeted, the use of an HSP60 inhibitor as a surrogate for p53 could help answer whether CypD release is primarily dictated by sequestering Trap1, HSP90, HSP60 or all three. Similarly, competition assays using p53 and gamitrinib could help determine whether p53 is ultimately a Trap1 target or not.

In conclusion, the work in this thesis has provided a model framework that can be tested to further understand how p53 is involved in regulation of the mitochondrial permeability transition pore. My model suggests that p53 displacement of CypD from a constitutively inactive complex with Trap1 and HSP60/90 is responsible for activating CypD to open the mitochondrial permeability transition pore. In parallel, my work shows that the thermodynamic stability of p53 plays an important role in its ability to interact with CypD. Specifically that structural destabilization of p53 is necessary for interaction with CypD. This supports my model which implicates the mitochondrial chaperone proteins Trap1 and HSP60/90 as important regulatory components in CypD activation, opening of the mitochondrial permeability transition pore and subsequent cell death by necrosis. Therefore, these proteins can now be tested as potential therapeutic targets to prevent tissue necrosis in response to ischemia-reperfusion injury.

Literature Cited

[1] "WHO | The world health report 2002 - Reducing Risks, Promoting Healthy Life."

[2] A. V. Vaseva, N. D. Marchenko, K. Ji, S. E. Tsirka, S. Holzmann, and U. M. Moll, "p53 Opens the Mitochondrial Permeability Transition Pore to Trigger Necrosis," *Cell*, vol. 149, no. 7, pp. 1536–1548, 2012.

[3] Y.-F. Zhen, G.-D. Wang, L.-Q. Zhu, S.-P. Tan, F.-Y. Zhang, X.-Z. Zhou, and X.-D. Wang, "P53 dependent mitochondrial permeability transition pore opening is required for dexamethasone-induced death of osteoblasts.," *J. Cell. Physiol.*, vol. 229, no. 10, pp. 1475–83, Oct. 2014.

[4] B. Chen, M. Xu, H. Zhang, J. Wang, P. Zheng, L. Gong, G. Wu, and T. Dai, "Cisplatin-induced non-apoptotic death of pancreatic cancer cells requires mitochondrial cyclophilin-D-p53 signaling.," *Biochem. Biophys. Res. Commun.*, vol. 437, no. 4, pp. 526–31, Aug. 2013.

[5] X. Guo, H. Sesaki, and X. Qi, "Drp1 stabilizes p53 on the mitochondria to trigger necrosis under oxidative stress conditions in vitro and in vivo.," *Biochem. J.*, vol. 461, no. 1, pp. 137–46, Jul. 2014.

[6] L.-P. Zhao, C. Ji, P.-H. Lu, C. Li, B. Xu, and H. Gao, "Oxygen glucose deprivation (OGD)/re-oxygenation-induced in vitro neuronal cell death involves mitochondrial cyclophilin-D/P53 signaling axis.," *Neurochem. Res.*, vol. 38, no. 4, pp. 705–13, Apr. 2013.

[7] J.-H. Lu, Z.-F. Shi, and H. Xu, "The mitochondrial cyclophilin D/p53 complexation mediates doxorubicin-induced non-apoptotic death of A549 lung cancer cells.," *Mol. Cell. Biochem.*, vol. 389, no. 1–2, pp. 17–24, Apr. 2014.

[8] A. C. Schinzel, O. Takeuchi, Z. Huang, J. K. Fisher, Z. Zhou, J. Rubens, C. Hetz, N. N. Danial, M. A. Moskowitz, and S. J. Korsmeyer, "Cyclophilin D is a component of mitochondrial permeability transition and mediates neuronal cell death after focal cerebral ischemia.," *Proc. Natl. Acad. Sci. U. S. A.*, vol. 102, no. 34, pp. 12005–10, Aug. 2005.

[9] C. P. Baines, R. A. Kaiser, N. H. Purcell, N. S. Blair, H. Osinska, M. A. Hambleton, E. W. Brunskill, M. R. Sayen, R. A. Gottlieb, G. W. Dorn, J. Robbins, and J. D. Molkentin, "Loss of cyclophilin D reveals a critical role for mitochondrial permeability transition in cell death.," *Nature*, vol. 434, no. 7033, pp. 658–62, Mar. 2005.

[10] H. Du, L. Guo, F. Fang, D. Chen, A. A Sosunov, G. M McKhann, Y. Yan, C. Wang, H. Zhang, J. D. Molkentin, F. J. Gunn-Moore, J. P. Vonsattel, O. Arancio, J. X. Chen, and S. Du Yan, "Cyclophilin D deficiency attenuates mitochondrial and neuronal perturbation and ameliorates learning and memory in Alzheimer's disease," *Nat. Med.*, vol. 14, no. 10, pp. 1097–1105, 2008.

[11] B. H. Kang, J. Plescia, H. Y. Song, M. Meli, G. Colombo, K. Beebe, B. Scroggins, L. Neckers, and D. C. Altieri, “Combinatorial drug design targeting multiple cancer signaling networks controlled by mitochondrial Hsp90,” *J. Clin. Invest.*, vol. 119, no. 3, pp. 454–464, Mar. 2009.

[12] B. H. Kang, J. Plescia, T. Dohi, J. Rosa, S. J. Doxsey, and D. C. Altieri, “Regulation of Tumor Cell Mitochondrial Homeostasis by an Organelle-Specific Hsp90 Chaperone Network,” *Cell*, vol. 131, no. 2, pp. 257–270, Oct. 2007.

[13] D. C. Altieri, “Hsp90 regulation of mitochondrial protein folding: from organelle integrity to cellular homeostasis.,” *Cell. Mol. Life Sci.*, vol. 70, no. 14, pp. 2463–72, Jul. 2013.

[14] D. Mozaffarian, E. J. Benjamin, A. S. Go, D. K. Arnett, M. J. Blaha, M. Cushman, S. de Ferranti, J.-P. Després, H. J. Fullerton, V. J. Howard, M. D. Huffman, S. E. Judd, B. M. Kissela, D. T. Lackland, J. H. Lichtman, L. D. Lisabeth, S. Liu, R. H. Mackey, D. B. Matchar, D. K. McGuire, E. R. Mohler, C. S. Moy, P. Muntner, M. E. Mussolino, K. Nasir, R. W. Neumar, G. Nichol, L. Palaniappan, D. K. Pandey, M. J. Reeves, C. J. Rodriguez, P. D. Sorlie, J. Stein, A. Towfighi, T. N. Turan, S. S. Virani, J. Z. Willey, D. Woo, R. W. Yeh, and M. B. Turner, “Heart Disease and Stroke Statistics-2015 Update: A Report From the American Heart Association.,” *Circulation*, vol. 131, no. 4, pp. e29–322, Dec. 2014.

[15] S. Z. Goldhaber, “Pulmonary Embolism and Deep Vein Thrombosis,” *Circulation*, vol. 106, no. 12, pp. 1436–1438, Sep. 2002.

[16] T. Kalogeris, C. P. Baines, M. Krenz, and R. J. Korthuis, “Cell biology of ischemia/reperfusion injury.,” *Int. Rev. Cell Mol. Biol.*, vol. 298, pp. 229–317, Jan. 2012.

[17] R. B. JENNINGS, H. M. SOMMERS, G. A. SMYTH, H. A. FLACK, and H. LINN, “Myocardial necrosis induced by temporary occlusion of a coronary artery in the dog.,” *Arch. Pathol.*, vol. 70, pp. 68–78, Jul. 1960.

[18] D. M. Yellon and D. J. Hausenloy, “Myocardial Reperfusion Injury,” *N. Engl. J. Med.*, vol. 357, no. 11, pp. 1121–1135, Sep. 2007.

[19] J. M. Ordy, T. M. Wengenack, P. Bialobok, P. D. Coleman, P. Rodier, R. B. Baggs, W. P. Dunlap, and B. Kates, “Selective vulnerability and early progression of hippocampal CA1 pyramidal cell degeneration and GFAP-positive astrocyte reactivity in the rat four-vessel occlusion model of transient global ischemia.,” *Exp. Neurol.*, vol. 119, no. 1, pp. 128–39, Jan. 1993.

[20] J. M. Bond, B. Herman, and J. J. Lemasters, “Protection by acidotic pH against anoxia/reoxygenation injury to rat neonatal cardiac myocytes.,” *Biochem. Biophys. Res. Commun.*, vol. 179, no. 2, pp. 798–803, Oct. 1991.

[21] S. R. Mehta, S. Yusuf, R. Díaz, J. Zhu, P. Pais, D. Xavier, E. Paolasso, R.

Ahmed, C. Xie, K. Kazmi, J. Tai, A. Orlandini, J. Pogue, and L. Liu, “Effect of glucose-insulin-potassium infusion on mortality in patients with acute ST-segment elevation myocardial infarction: the CREATE-ECLA randomized controlled trial.,” *JAMA*, vol. 293, no. 4, pp. 437–46, Jan. 2005.

[22] T. H. after C. A. S. Group, “Mild therapeutic hypothermia to improve the neurologic outcome after cardiac arrest.,” *N. Engl. J. Med.*, vol. 346, no. 8, pp. 549–56, Feb. 2002.

[23] C. W. Christensen, M. A. Rieder, E. L. Silverstein, and N. E. Gencheff, “Magnesium sulfate reduces myocardial infarct size when administered before but not after coronary reperfusion in a canine model.,” *Circulation*, vol. 92, no. 9, pp. 2617–21, Dec. 1995.

[24] E. Bluhmki, A. Chamorro, A. Dávalos, T. Machnig, C. Sauce, N. Wahlgren, J. Wardlaw, and W. Hacke, “Stroke treatment with alteplase given 3.0-4.5 h after onset of acute ischaemic stroke (ECASS III): additional outcomes and subgroup analysis of a randomised controlled trial.,” *Lancet. Neurol.*, vol. 8, no. 12, pp. 1095–102, Dec. 2009.

[25] M. R. Litt, R. W. Jeremy, H. F. Weisman, J. A. Winkelstein, and L. C. Becker, “Neutrophil depletion limited to reperfusion reduces myocardial infarct size after 90 minutes of ischemia. Evidence for neutrophil-mediated reperfusion injury.,” *Circulation*, vol. 80, no. 6, pp. 1816–27, Dec. 1989.

[26] R. J. Gumina, E. Buerger, C. Eickmeier, J. Moore, J. Daemmgen, and G. J. Gross, “Inhibition of the Na(+)/H(+) exchanger confers greater cardioprotection against 90 minutes of myocardial ischemia than ischemic preconditioning in dogs.,” *Circulation*, vol. 100, no. 25, pp. 2519–26; discussion 2469–72, Jan. .

[27] M. M. Carry, R. E. Mrak, M. L. Murphy, C. F. Peng, K. D. Straub, and E. P. Fody, “Reperfusion injury in ischemic myocardium: protective effects of ruthenium red and of nitroprusside.,” *Am. J. Cardiovasc. Pathol.*, vol. 2, no. 4, pp. 335–44, Jan. 1989.

[28] H. H. Klein, S. Pich, S. Lindert, K. Nebendahl, G. Warneke, and H. Kreuzer, “Treatment of reperfusion injury with intracoronary calcium channel antagonists and reduced coronary free calcium concentration in regionally ischemic, reperfused porcine hearts.,” *J. Am. Coll. Cardiol.*, vol. 13, no. 6, pp. 1395–401, May 1989.

[29] P. W. Armstrong, C. B. Granger, P. X. Adams, C. Hamm, D. Holmes, W. W. O’Neill, T. G. Todaro, A. Vahanian, and F. Van de Werf, “Pexelizumab for acute ST-elevation myocardial infarction in patients undergoing primary percutaneous coronary intervention: a randomized controlled trial.,” *JAMA*, vol. 297, no. 1, pp. 43–51, Jan. 2007.

[30] J.-F. Tanguay, M. W. Krucoff, R. J. Gibbons, E. Chavez, A. S. Liprandi, V. Molina-

Viamonte, P. E. Aylward, J. L. Lopez-Sendon, D. S. Holloway, K. Shields, J. S. Yu, E. Loh, K. W. Baran, V. K. Bethala, A. Vahanian, and H. D. White, “Efficacy of a novel P-selectin antagonist, rPSGL-Ig for reperfusion therapy in acute myocardial infarction: The RAPSODY trial,” *J. Am. Coll. Cardiol.*, vol. 41, no. 6, pp. 404–405, Mar. 2003.

[31] D. P. Faxon, R. J. Gibbons, N. A. F. Chronos, P. A. Gurbel, and F. Sheehan, “The effect of blockade of the CD11/CD18 integrin receptor on infarct size in patients with acute myocardial infarction treated with direct angioplasty: the results of the HALT-MI study.,” *J. Am. Coll. Cardiol.*, vol. 40, no. 7, pp. 1199–204, Oct. 2002.

[32] M. Avkiran and M. S. Marber, “Na+/h+ exchange inhibitors for cardioprotective therapy: progress, problems and prospects,” *J. Am. Coll. Cardiol.*, vol. 39, no. 5, pp. 747–753, Mar. 2002.

[33] U. Zeymer, H. Suryapranata, J. P. Monassier, G. Opolski, J. Davies, G. Rasmanis, G. Linssen, U. Tebbe, R. Schröder, R. Tiemann, T. Machnig, and K. L. Neuhaus, “The Na(+)/H(+) exchange inhibitor eniporide as an adjunct to early reperfusion therapy for acute myocardial infarction. Results of the evaluation of the safety and cardioprotective effects of eniporide in acute myocardial infarction (ESCAMI) trial.,” *J. Am. Coll. Cardiol.*, vol. 38, no. 6, pp. 1644–50, Dec. 2001.

[34] H. Ono, T. Osanai, H. Ishizaka, H. Hanada, T. Kamada, H. Onodera, N. Fujita, S. Sasaki, T. Matsunaga, and K. Okumura, “Nicorandil improves cardiac function and clinical outcome in patients with acute myocardial infarction undergoing primary percutaneous coronary intervention: role of inhibitory effect on reactive oxygen species formation.,” *Am. Heart J.*, vol. 148, no. 4, p. E15, Oct. 2004.

[35] K. W. Baran, M. Nguyen, G. R. McKendall, C. T. Lambrew, G. Dykstra, S. T. Palmeri, R. J. Gibbons, S. Borzak, B. E. Sobel, S. G. Gourlay, A. C. Rundle, C. M. Gibson, and H. V Barron, “Double-blind, randomized trial of an anti-CD18 antibody in conjunction with recombinant tissue plasminogen activator for acute myocardial infarction: limitation of myocardial infarction following thrombolysis in acute myocardial infarction (LIMIT AMI) stu,” *Circulation*, vol. 104, no. 23, pp. 2778–83, Dec. 2001.

[36] J. M. Downey, “Free radicals and their involvement during long-term myocardial ischemia and reperfusion.,” *Annu. Rev. Physiol.*, vol. 52, pp. 487–504, Jan. 1990.

[37] J. T. Flaherty, B. Pitt, J. W. Gruber, R. R. Heuser, D. A. Rothbaum, L. R. Burwell, B. S. George, D. J. Kereiakes, D. Deitchman, and N. Gustafson, “Recombinant human superoxide dismutase (h-SOD) fails to improve recovery of ventricular function in patients undergoing coronary angioplasty for acute myocardial infarction.,” *Circulation*, vol. 89, no. 5, pp. 1982–91, May 1994.

[38] R. C. Taylor, S. P. Cullen, and S. J. Martin, “Apoptosis: controlled demolition at the cellular level.,” *Nat. Rev. Mol. Cell Biol.*, vol. 9, no. 3, pp. 231–41, Mar. 2008.

[39] G. Kroemer and S. J. Martin, “Caspase-independent cell death.,” *Nat. Med.*, vol. 11, no. 7, pp. 725–30, Jul. 2005.

[40] A. Kaczmarek, P. Vandenabeele, and D. V Krysko, “Necroptosis: the release of damage-associated molecular patterns and its physiological relevance.,” *Immunity*, vol. 38, no. 2, pp. 209–23, Feb. 2013.

[41] S. J. Martin, C. M. Henry, and S. P. Cullen, “A perspective on mammalian caspases as positive and negative regulators of inflammation.,” *Mol. Cell*, vol. 46, no. 4, pp. 387–97, May 2012.

[42] B. Alberts, A. Johnson, J. Lewis, M. Raff, K. Roberts, and P. Walter, “Programmed Cell Death (Apoptosis).” Garland Science, 2002.

[43] S. Elmore, “Apoptosis: a review of programmed cell death.,” *Toxicol. Pathol.*, vol. 35, no. 4, pp. 495–516, Jun. 2007.

[44] S. J. Martin and C. M. Henry, “Distinguishing between apoptosis, necrosis, necroptosis and other cell death modalities.,” *Methods*, vol. 61, no. 2, pp. 87–9, Jun. 2013.

[45] W. Fiers, R. Beyaert, W. Declercq, and P. Vandenabeele, “More than one way to die: apoptosis, necrosis and reactive oxygen damage.,” *Oncogene*, vol. 18, no. 54, pp. 7719–30, Dec. 1999.

[46] C. J. Zeiss, “The apoptosis-necrosis continuum: insights from genetically altered mice.,” *Vet. Pathol.*, vol. 40, no. 5, pp. 481–95, Sep. 2003.

[47] M. Leist, B. Single, A. F. Castoldi, S. Kühnle, and P. Nicotera, “Intracellular adenosine triphosphate (ATP) concentration: a switch in the decision between apoptosis and necrosis.,” *J. Exp. Med.*, vol. 185, no. 8, pp. 1481–6, Apr. 1997.

[48] S. Chung, T. L. Gumienny, M. O. Hengartner, and M. Driscoll, “A common set of engulfment genes mediates removal of both apoptotic and necrotic cell corpses in C. elegans.,” *Nat. Cell Biol.*, vol. 2, no. 12, pp. 931–7, Dec. 2000.

[49] P. Nicotera, M. Leist, and E. Ferrando-May, “Intracellular ATP, a switch in the decision between apoptosis and necrosis.,” *Toxicol. Lett.*, vol. 102–103, pp. 139–42, Dec. 1998.

[50] G. Majno and I. Joris, “Apoptosis, oncosis, and necrosis. An overview of cell death.,” *Am. J. Pathol.*, vol. 146, no. 1, pp. 3–15, Jan. 1995.

[51] B. F. Trump, I. K. Berezesky, S. H. Chang, and P. C. Phelps, “The pathways of cell death: oncosis, apoptosis, and necrosis.,” *Toxicol. Pathol.*, vol. 25, no. 1, pp. 82–8, Jan. .

[52] R. W. Oppenheim, R. A. Flavell, S. Vinsant, D. Prevette, C. Y. Kuan, and P.

Rakic, “Programmed cell death of developing mammalian neurons after genetic deletion of caspases.,” *J. Neurosci.*, vol. 21, no. 13, pp. 4752–60, Jul. 2001.

[53] M. Chautan, G. Chazal, F. Cecconi, P. Gruss, and P. Golstein, “Interdigital cell death can occur through a necrotic and caspase-independent pathway.,” *Curr. Biol.*, vol. 9, no. 17, pp. 967–70, Sep. 1999.

[54] T. Vanden Berghe, N. Vanlangenakker, E. Parthoens, W. Deckers, M. Devos, N. Festjens, C. J. Guerin, U. T. Brunk, W. Declercq, and P. Vandenabeele, “Necroptosis, necrosis and secondary necrosis converge on similar cellular disintegration features.,” *Cell Death Differ.*, vol. 17, no. 6, pp. 922–30, Jun. 2010.

[55] P. Vandenabeele, L. Galluzzi, T. Vanden Berghe, and G. Kroemer, “Molecular mechanisms of necroptosis: an ordered cellular explosion.,” *Nat. Rev. Mol. Cell Biol.*, vol. 11, no. 10, pp. 700–14, Oct. 2010.

[56] T. Vanden Berghe, A. Linkermann, S. Jouan-Lanhouet, H. Walczak, and P. Vandenabeele, “Regulated necrosis: the expanding network of non-apoptotic cell death pathways.,” *Nat. Rev. Mol. Cell Biol.*, vol. 15, no. 2, pp. 135–47, Feb. 2014.

[57] M. Conrad, J. P. F. Angeli, P. Vandenabeele, and B. R. Stockwell, “Regulated necrosis: disease relevance and therapeutic opportunities.,” *Nat. Rev. Drug Discov.*, vol. advance on, Jan. 2016.

[58] P. Bernardi, “The mitochondrial permeability transition pore: a mystery solved?,” *Front. Physiol.*, vol. 4, p. 95, Jan. 2013.

[59] M. Gutiérrez-Aguilar and C. P. Baines, “Structural mechanisms of cyclophilin D-dependent control of the mitochondrial permeability transition pore,” *Biochim. Biophys. Acta - Gen. Subj.*, vol. 1850, no. 10, pp. 2041–2047, Oct. 2015.

[60] G. Morciano, C. Giorgi, M. Bonora, S. Punzetti, R. Pavasini, M. R. Wieckowski, G. Campo, and P. Pinton, “Molecular identity of the mitochondrial permeability transition pore and its role in ischemia-reperfusion injury,” *J. Mol. Cell. Cardiol.*, vol. 78, pp. 142–153, 2015.

[61] A. P. Halestrap, “What is the mitochondrial permeability transition pore?,” *J. Mol. Cell. Cardiol.*, vol. 46, no. 6, pp. 821–31, Jun. 2009.

[62] R. A. Haworth and D. R. Hunter, “The Ca2+-induced membrane transition in mitochondria,” *Arch. Biochem. Biophys.*, vol. 195, no. 2, pp. 460–467, Jul. 1979.

[63] D. R. Hunter and R. A. Haworth, “The Ca2+-induced membrane transition in mitochondria,” *Arch. Biochem. Biophys.*, vol. 195, no. 2, pp. 453–459, Jul. 1979.

[64] M. Crompton, A. Costi, and L. Hayat, “Evidence for the presence of a reversible Ca2+-dependent pore activated by oxidative stress in heart mitochondria.,” *Biochem. J.*, vol. 245, no. 3, pp. 915–8, Aug. 1987.

[65] D. J. Hausenloy, M. R. Duchen, and D. M. Yellon, “Inhibiting mitochondrial permeability transition pore opening at reperfusion protects against ischaemia-reperfusion injury.,” *Cardiovasc. Res.*, vol. 60, no. 3, pp. 617–25, Dec. 2003.

[66] L. Argaud, O. Gateau-Roesch, D. Muntean, L. Chalabreysse, J. Loufouat, D. Robert, and M. Ovize, “Specific inhibition of the mitochondrial permeability transition prevents lethal reperfusion injury.,” *J. Mol. Cell. Cardiol.*, vol. 38, no. 2, pp. 367–74, Feb. 2005.

[67] E. J. Griffiths and A. P. Halestrap, “Mitochondrial non-specific pores remain closed during cardiac ischaemia, but open upon reperfusion.,” *Biochem. J.*, vol. 307 (Pt 1, pp. 93–8, Apr. 1995.

[68] A. Leyssens, A. V Nowicky, L. Patterson, M. Crompton, and M. R. Duchen, “The relationship between mitochondrial state, ATP hydrolysis, [Mg2+]i and [Ca2+]i studied in isolated rat cardiomyocytes.,” *J. Physiol.*, vol. 496 (Pt 1, pp. 111–28, Oct. 1996.

[69] F. Di Lisa and P. Bernardi, “Mitochondria and ischemia-reperfusion injury of the heart: fixing a hole.,” *Cardiovasc. Res.*, vol. 70, no. 2, pp. 191–9, May 2006.

[70] M. Crompton and A. Costi, “Kinetic evidence for a heart mitochondrial pore activated by Ca2+, inorganic phosphate and oxidative stress. A potential mechanism for mitochondrial dysfunction during cellular Ca2+ overload.,” *Eur. J. Biochem.*, vol. 178, no. 2, pp. 489–501, Dec. 1988.

[71] F. Ichas, L. S. Jouaville, and J. P. Mazat, “Mitochondria are excitable organelles capable of generating and conveying electrical and calcium signals.,” *Cell*, vol. 89, no. 7, pp. 1145–53, Jun. 1997.

[72] P. Bernardi and V. Petronilli, “The permeability transition pore as a mitochondrial calcium release channel: a critical appraisal.,” *J. Bioenerg. Biomembr.*, vol. 28, no. 2, pp. 131–8, Apr. 1996.

[73] T. E. Gunter and D. R. Pfeiffer, “Mechanisms by which mitochondria transport calcium.,” *Am. J. Physiol.*, vol. 258, no. 5 Pt 1, pp. C755–86, May 1990.

[74] V. Petronilli, G. Miotto, M. Canton, M. Brini, R. Colonna, P. Bernardi, and F. Di Lisa, “Transient and long-lasting openings of the mitochondrial permeability transition pore can be monitored directly in intact cells by changes in mitochondrial calcein fluorescence.,” *Biophys. J.*, vol. 76, no. 2, pp. 725–34, Feb. 1999.

[75] J. J. Lemasters, T. P. Theruvath, Z. Zhong, and A.-L. Nieminen, “Mitochondrial calcium and the permeability transition in cell death.,” *Biochim. Biophys. Acta*, vol. 1787, no. 11, pp. 1395–401, Nov. 2009.

[76] J.-S. Kim, L. He, and J. J. Lemasters, “Mitochondrial permeability transition: a

common pathway to necrosis and apoptosis," *Biochem. Biophys. Res. Commun.*, vol. 304, no. 3, pp. 463–470, May 2003.

[77] L. Biasutto, M. Azzolini, I. Szabò, and M. Zoratti, "The mitochondrial permeability transition pore in AD 2016: An update.," *Biochim. Biophys. Acta*, Feb. 2016.

[78] J. Karch and J. D. Molkentin, "Identifying the components of the elusive mitochondrial permeability transition pore," *Proc. Natl. Acad. Sci.*, vol. 111, no. 29, pp. 10396–10397, 2014.

[79] J. W. Elrod, R. Wong, S. Mishra, R. J. Vagnozzi, B. Sakthievel, S. A. Goonasekera, J. Karch, S. Gabel, J. Farber, T. Force, J. H. Brown, E. Murphy, and J. D. Molkentin, "Cyclophilin D controls mitochondrial pore-dependent Ca(2+) exchange, metabolic flexibility, and propensity for heart failure in mice.," *J. Clin. Invest.*, vol. 120, no. 10, pp. 3680–7, Oct. 2010.

[80] M. J. Hansson, S. Morota, L. Chen, N. Matsuyama, Y. Suzuki, S. Nakajima, T. Tanoue, A. Omi, F. Shibasaki, M. Shimazu, Y. Ikeda, H. Uchino, and E. Elmér, "Cyclophilin D-Sensitive Mitochondrial Permeability Transition in Adult Human Brain and Liver Mitochondria," *J. Neurotrauma*, vol. 28, no. 1, pp. 143–153, 2011.

[81] C. P. Baines, R. A. Kaiser, T. Sheiko, W. J. Craigen, and J. D. Molkentin, "Voltage-dependent anion channels are dispensable for mitochondrial-dependent cell death," *Nat. Cell Biol.*, vol. 9, no. 5, pp. 550–555, Apr. 2007.

[82] J. E. Kokoszka, K. G. Waymire, S. E. Levy, J. E. Sligh, J. Cai, D. P. Jones, G. R. MacGregor, and D. C. Wallace, "The ADP/ATP translocator is not essential for the mitochondrial permeability transition pore.," *Nature*, vol. 427, no. 6973, pp. 461–5, Jan. 2004.

[83] M. Gutiérrez-Aguilar, D. L. Douglas, A. K. Gibson, T. L. Domeier, J. D. Molkentin, and C. P. Baines, "Genetic manipulation of the cardiac mitochondrial phosphate carrier does not affect permeability transition.," *J. Mol. Cell. Cardiol.*, vol. 72, pp. 316–25, Jul. 2014.

[84] J. Šileikytė, E. Blachly-Dyson, R. Sewell, A. Carpi, R. Menabò, F. Di Lisa, F. Ricchelli, P. Bernardi, and M. Forte, "Regulation of the mitochondrial permeability transition pore by the outer membrane does not involve the peripheral benzodiazepine receptor (Translocator Protein of 18 kDa (TSPO))," *J. Biol. Chem.*, vol. 289, no. 20, pp. 13769–81, May 2014.

[85] V. Giorgio, S. von Stockum, M. Antoniel, A. Fabbro, F. Fogolari, M. Forte, G. D. Glick, V. Petronilli, M. Zoratti, I. Szabo, G. Lippe, and P. Bernardi, "Dimers of mitochondrial ATP synthase form the permeability transition pore," *Proc. Natl. Acad. Sci.*, vol. 110, no. 15, pp. 5887–5892, Mar. 2013.

[86] P. Bernardi, A. Rasola, M. Forte, and G. Lippe, "The Mitochondrial Permeability Transition Pore: Channel Formation by F-ATP Synthase, Integration in Signal

Transduction, and Role in Pathophysiology.," *Physiol. Rev.*, vol. 95, no. 4, pp. 1111–55, Oct. 2015.

[87] S. Nesci, F. Trombetti, V. Ventrella, and A. Pagliarani, "The c-Ring of the F1FO-ATP Synthase: Facts and Perspectives.," *J. Membr. Biol.*, Nov. 2015.

[88] A. P. Halestrap, "The C Ring of the F1Fo ATP Synthase Forms the Mitochondrial Permeability Transition Pore: A Critical Appraisal.," *Front. Oncol.*, vol. 4, p. 234, Jan. 2014.

[89] C. Gerle, "On the structural possibility of pore-forming mitochondrial FoF1 ATP synthase.," *Biochim. Biophys. Acta*, Mar. 2016.

[90] Q. Long, K. Yang, and Q. Yang, "Regulation of mitochondrial ATP synthase in cardiac pathophysiology.," *Am. J. Cardiovasc. Dis.*, vol. 5, no. 1, pp. 19–32, Jan. 2015.

[91] P. Bernardi and F. Di Lisa, "The mitochondrial permeability transition pore: molecular nature and role as a target in cardioprotection.," *J. Mol. Cell. Cardiol.*, vol. 78, pp. 100–6, Jan. 2015.

[92] S. F. Göthel and M. A. Marahiel, "Peptidyl-prolyl cis-trans isomerases, a superfamily of ubiquitous folding catalysts.," *Cell. Mol. Life Sci.*, vol. 55, no. 3, pp. 423–36, Mar. 1999.

[93] A. Galat, "Peptidylprolyl cis/trans isomerases (immunophilins): biological diversity--targets--functions.," *Curr. Top. Med. Chem.*, vol. 3, no. 12, pp. 1315–47, Jan. 2003.

[94] U. Reidt, K. Reuter, T. Achsel, D. Ingelfinger, R. Lührmann, and R. Ficner, "Crystal structure of the human U4/U6 small nuclear ribonucleoprotein particle-specific SnuCyp-20, a nuclear cyclophilin.," *J. Biol. Chem.*, vol. 275, no. 11, pp. 7439–42, Mar. 2000.

[95] G. Bernstein, W. Tempel, T. Davis, E. . Newman, F. Jr, P.J, F. Mackenzie, J. Weigelt, M. Sundstrom, C. . Arrowsmith, A. . Edwards, A. Bochkarev, S. Dhe-Paganon, and S. G. C. (SGC), "Crystal structure of the peptidyl-prolyl isomerase domain of human cyclophilin G," *To be Publ.*

[96] J. Chen, S. Chen, J. Wang, M. Zhang, Z. Gong, Y. Wei, L. Li, Y. Zhang, X. Zhao, S. Jiang, and L. Yu, "Cyclophilin J is a novel peptidyl-prolyl isomerase and target for repressing the growth of hepatocellular carcinoma.," *PLoS One*, vol. 10, no. 5, p. e0127668, Jan. 2015.

[97] P. Wang and J. Heitman, "The cyclophilins.," *Genome Biol.*, vol. 6, no. 7, p. 226, Jan. 2005.

[98] S. Kumari, S. Roy, P. Singh, S. L. Singla-Pareek, and A. Pareek, "Cyclophilins:

proteins in search of function.," *Plant Signal. Behav.*, vol. 8, no. 1, p. e22734, Jan. 2013.

[99] S. Barik, "Immunophilins: for the love of proteins.," *Cell. Mol. Life Sci.*, vol. 63, no. 24, pp. 2889–900, Dec. 2006.

[100] A. R. Marks, "Cellular functions of immunophilins.," *Physiol. Rev.*, vol. 76, no. 3, pp. 631–49, Jul. 1996.

[101] Z. K. Sweeney, J. Fu, and B. Wiedmann, "From chemical tools to clinical medicines: nonimmunosuppressive cyclophilin inhibitors derived from the cyclosporin and sanglifehrin scaffolds.," *J. Med. Chem.*, vol. 57, no. 17, pp. 7145–59, Sep. 2014.

[102] T. L. Davis, J. R. Walker, V. Campagna-Slater, P. J. Finerty, R. Paramanathan, G. Bernstein, F. MacKenzie, W. Tempel, H. Ouyang, W. H. Lee, E. Z. Eisenmesser, and S. Dhe-Paganon, "Structural and biochemical characterization of the human cyclophilin family of peptidyl-prolyl isomerases.," *PLoS Biol.*, vol. 8, no. 7, p. e1000439, Jan. 2010.

[103] P. Nigro, G. Pompilio, and M. C. Capogrossi, "Cyclophilin A: a key player for human disease.," *Cell Death Dis.*, vol. 4, p. e888, Jan. 2013.

[104] J. Luban, "Absconding with the chaperone: essential cyclophilin-Gag interaction in HIV-1 virions.," *Cell*, vol. 87, no. 7, pp. 1157–9, Dec. 1996.

[105] D. A. Bosco, E. Z. Eisenmesser, S. Pochapsky, W. I. Sundquist, and D. Kern, "Catalysis of cis/trans isomerization in native HIV-1 capsid by human cyclophilin A.," *Proc. Natl. Acad. Sci. U. S. A.*, vol. 99, no. 8, pp. 5247–52, Apr. 2002.

[106] S. A. Helekar, D. Char, S. Neff, and J. Patrick, "Prolyl isomerase requirement for the expression of functional homo-oligomeric ligand-gated ion channels.," *Neuron*, vol. 12, no. 1, pp. 179–89, Jan. 1994.

[107] S. A. Helekar and J. Patrick, "Peptidyl prolyl cis-trans isomerase activity of cyclophilin A in functional homo-oligomeric receptor expression.," *Proc. Natl. Acad. Sci. U. S. A.*, vol. 94, no. 10, pp. 5432–7, May 1997.

[108] B. Steinmann, P. Bruckner, and A. Superti-Furga, "Cyclosporin A slows collagen triple-helix formation in vivo: indirect evidence for a physiologic role of peptidyl-prolyl cis-trans-isomerase.," *J. Biol. Chem.*, vol. 266, no. 2, pp. 1299–303, Jan. 1991.

[109] H. F. Lodish and N. Kong, "Cyclosporin A inhibits an initial step in folding of transferrin within the endoplasmic reticulum.," *J. Biol. Chem.*, vol. 266, no. 23, pp. 14835–8, Aug. 1991.

[110] S. Schneuwly, R. D. Shortridge, D. C. Larrivee, T. Ono, M. Ozaki, and W. L. Pak,

"Drosophila ninaA gene encodes an eye-specific cyclophilin (cyclosporine A binding protein).," *Proc. Natl. Acad. Sci. U. S. A.*, vol. 86, no. 14, pp. 5390–4, Jul. 1989.

[111] B. H. Shieh, M. A. Stamnes, S. Seavello, G. L. Harris, and C. S. Zuker, "The ninaA gene required for visual transduction in Drosophila encodes a homologue of cyclosporin A-binding protein.," *Nature*, vol. 338, no. 6210, pp. 67–70, Mar. 1989.

[112] C. Zhu, X. Wang, J. Deinum, Z. Huang, J. Gao, N. Modjtahedi, M. R. Neagu, M. Nilsson, P. S. Eriksson, H. Hagberg, J. Luban, G. Kroemer, and K. Blomgren, "Cyclophilin A participates in the nuclear translocation of apoptosis-inducing factor in neurons after cerebral hypoxia-ischemia.," *J. Exp. Med.*, vol. 204, no. 8, pp. 1741–8, Aug. 2007.

[113] H. Tanaka, H. Shimazaki, M. Kimura, H. Izuta, K. Tsuruma, M. Shimazawa, and H. Hara, "Apoptosis-inducing factor and cyclophilin A cotranslocate to the motor neuronal nuclei in amyotrophic lateral sclerosis model mice.," *CNS Neurosci. Ther.*, vol. 17, no. 5, pp. 294–304, Oct. 2011.

[114] H. Pan, C. Luo, R. Li, A. Qiao, L. Zhang, M. Mines, A. M. Nyanda, J. Zhang, and G.-H. Fan, "Cyclophilin A is required for CXCR4-mediated nuclear export of heterogeneous nuclear ribonucleoprotein A2, activation and nuclear translocation of ERK1/2, and chemotactic cell migration.," *J. Biol. Chem.*, vol. 283, no. 1, pp. 623–37, Jan. 2008.

[115] V. Yurchenko, T. Pushkarsky, J.-H. Li, W. W. Dai, B. Sherry, and M. Bukrinsky, "Regulation of CD147 cell surface expression: involvement of the proline residue in the CD147 transmembrane domain.," *J. Biol. Chem.*, vol. 280, no. 17, pp. 17013–9, Apr. 2005.

[116] T. Huang, H. Deng, A. W. Wolkoff, and R. J. Stockert, "Phosphorylation-dependent interaction of the asialoglycoprotein receptor with molecular chaperones.," *J. Biol. Chem.*, vol. 277, no. 40, pp. 37798–803, Oct. 2002.

[117] C. R. Brown, D. Y. Cui, G. G. Hung, and H. L. Chiang, "Cyclophilin A mediates Vid22p function in the import of fructose-1,6-bisphosphatase into Vid vesicles.," *J. Biol. Chem.*, vol. 276, no. 51, pp. 48017–26, Dec. 2001.

[118] H. Ansari, G. Greco, and J. Luban, "Cyclophilin A peptidyl-prolyl isomerase activity promotes ZPR1 nuclear export.," *Mol. Cell. Biol.*, vol. 22, no. 20, pp. 6993–7003, Oct. 2002.

[119] Z.-G. Jin, A. O. Lungu, L. Xie, M. Wang, C. Wong, and B. C. Berk, "Cyclophilin A is a proinflammatory cytokine that activates endothelial cells.," *Arterioscler. Thromb. Vasc. Biol.*, vol. 24, no. 7, pp. 1186–91, Jul. 2004.

[120] W. M. Flanagan, B. Corthésy, R. J. Bram, and G. R. Crabtree, "Nuclear

association of a T-cell transcription factor blocked by FK-506 and cyclosporin A.," *Nature*, vol. 352, no. 6338, pp. 803–7, Aug. 1991.

[121] E. A. Emmel, C. L. Verweij, D. B. Durand, K. M. Higgins, E. Lacy, and G. R. Crabtree, "Cyclosporin A specifically inhibits function of nuclear proteins involved in T cell activation.," *Science*, vol. 246, no. 4937, pp. 1617–20, Dec. 1989.

[122] P. Stocki, D. C. Chapman, L. A. Beach, and D. B. Williams, "Depletion of cyclophilins B and C leads to dysregulation of endoplasmic reticulum redox homeostasis.," *J. Biol. Chem.*, vol. 289, no. 33, pp. 23086–96, Aug. 2014.

[123] E. R. Price, M. Jin, D. Lim, S. Pati, C. T. Walsh, and F. D. McKeon, "Cyclophilin B trafficking through the secretory pathway is altered by binding of cyclosporin A.," *Proc. Natl. Acad. Sci. U. S. A.*, vol. 91, no. 9, pp. 3931–5, Apr. 1994.

[124] F. Pirkl and J. Buchner, "Functional analysis of the Hsp90-associated human peptidyl prolyl cis/trans isomerases FKBP51, FKBP52 and Cyp40.," *J. Mol. Biol.*, vol. 308, no. 4, pp. 795–806, May 2001.

[125] M. S. Park, F. Chu, J. Xie, Y. Wang, P. Bhattacharya, and W. K. Chan, "Identification of cyclophilin-40-interacting proteins reveals potential cellular function of cyclophilin-40.," *Anal. Biochem.*, vol. 410, no. 2, pp. 257–65, Mar. 2011.

[126] M. L. Mucenski, K. McLain, A. B. Kier, S. H. Swerdlow, C. M. Schreiner, T. A. Miller, D. W. Pietryga, W. J. Scott, and S. S. Potter, "A functional c-myb gene is required for normal murine fetal hepatic hematopoiesis.," *Cell*, vol. 65, no. 4, pp. 677–89, May 1991.

[127] J. D. Leverson and S. A. Ness, "Point Mutations in v-Myb Disrupt a Cyclophilin-Catalyzed Negative Regulatory Mechanism," *Mol. Cell*, vol. 1, no. 2, pp. 203–211, Jan. 1998.

[128] I. Kuraoka, S. Ito, T. Wada, M. Hayashida, L. Lee, M. Saijo, Y. Nakatsu, M. Matsumoto, T. Matsunaga, H. Handa, J. Qin, Y. Nakatani, and K. Tanaka, "Isolation of XAB2 complex involved in pre-mRNA splicing, transcription, and transcription-coupled repair.," *J. Biol. Chem.*, vol. 283, no. 2, pp. 940–50, Jan. 2008.

[129] H. Mi, O. Kops, E. Zimmermann, A. Jäschke, and M. Tropschug, "A nuclear RNA-binding cyclophilin in human T cells," *FEBS Lett.*, vol. 398, no. 2–3, pp. 201–205, Dec. 1996.

[130] C. L. Lin, S. Leu, M. C. Lu, and P. Ouyang, "Over-expression of SR-cyclophilin, an interaction partner of nuclear pinin, releases SR family splicing factors from nuclear speckles.," *Biochem. Biophys. Res. Commun.*, vol. 321, no. 3, pp. 638–47, Aug. 2004.

[131] D. S. Horowitz, E. J. Lee, S. A. Mabon, and T. Misteli, “A cyclophilin functions in pre-mRNA splicing.,” *EMBO J.*, vol. 21, no. 3, pp. 470–80, Feb. 2002.

[132] Z. Zhou, K. Ying, J. Dai, R. Tang, W. Wang, Y. Huang, W. Zhao, Y. Xie, and Y. Mao, “Molecular cloning and characterization of a novel peptidylprolyl isomerase (cyclophilin)-like gene (PPIL3) from human fetal brain.,” *Cytogenet. Cell Genet.*, vol. 92, no. 3–4, pp. 231–6, Jan. 2001.

[133] S. K. Anderson, S. Gallinger, J. Roder, J. Frey, H. A. Young, and J. R. Ortaldo, “A cyclophilin-related protein involved in the function of natural killer cells.,” *Proc. Natl. Acad. Sci. U. S. A.*, vol. 90, no. 2, pp. 542–6, Jan. 1993.

[134] A. Rinfret, C. Collins, R. Ménard, and S. K. Anderson, “The N-terminal cyclophilin-homologous domain of a 150-kilodalton tumor recognition molecule exhibits both peptidylprolyl cis-trans-isomerase and chaperone activities.,” *Biochemistry*, vol. 33, no. 7, pp. 1668–73, Feb. 1994.

[135] N. Johnson, A. Khan, S. Virji, J. M. Ward, and M. Crompton, “Import and processing of heart mitochondrial cyclophilin D,” *Eur. J. Biochem.*, vol. 263, no. 2, pp. 353–359, Jul. 1999.

[136] W. Neupert, “Protein import into mitochondria.,” *Annu. Rev. Biochem.*, vol. 66, pp. 863–917, Jan. 1997.

[137] J. W. Elrod and J. D. Molkentin, “Physiologic Functions of Cyclophilin D and the Mitochondrial Permeability Transition Pore,” *Circ. J.*, vol. 77, no. 5, pp. 1111–1122, Apr. 2013.

[138] R. A. Eliseev, J. Malecki, T. Lester, Y. Zhang, J. Humphrey, and T. E. Gunter, “Cyclophilin D interacts with Bcl2 and exerts an anti-apoptotic effect.,” *J. Biol. Chem.*, vol. 284, no. 15, pp. 9692–9, Apr. 2009.

[139] A. Schubert and S. Grimm, “Cyclophilin D, a component of the permeability transition-pore, is an apoptosis repressor.,” *Cancer Res.*, vol. 64, no. 1, pp. 85–93, Jan. 2004.

[140] K. Machida, Y. Ohta, and H. Osada, “Suppression of apoptosis by cyclophilin D via stabilization of hexokinase II mitochondrial binding in cancer cells.,” *J. Biol. Chem.*, vol. 281, no. 20, pp. 14314–20, May 2006.

[141] R. S. Carreira, Y. Lee, M. Ghochani, Å. B. Gustafsson, and R. A. Gottlieb, “Cyclophilin D is required for mitochondrial removal by autophagy in cardiac cells.,” *Autophagy*, vol. 6, no. 4, pp. 462–72, May 2010.

[142] M. Tavecchio, S. Lisanti, A. Lam, J. C. Ghosh, N. M. Martin, M. O’Connell, A. T. Weeraratna, A. V Kossenkov, L. C. Showe, and D. C. Altieri, “Cyclophilin D extramitochondrial signaling controls cell cycle progression and chemokine-directed cell motility.,” *J. Biol. Chem.*, vol. 288, no. 8, pp. 5553–61, Feb. 2013.

[143] K. Boengler, D. Hilfiker-Kleiner, G. Heusch, and R. Schulz, “Inhibition of permeability transition pore opening by mitochondrial STAT3 and its role in myocardial ischemia/reperfusion.,” *Basic Res. Cardiol.*, vol. 105, no. 6, pp. 771–85, Nov. 2010.

[144] E. J. Griffiths and A. P. Halestrap, “Further evidence that cyclosporin A protects mitochondria from calcium overload by inhibiting a matrix peptidyl-prolyl cis-trans isomerase. Implications for the immunosuppressive and toxic effects of cyclosporin.,” *Biochem. J.*, vol. 274 (Pt 2, pp. 611–4, Mar. 1991.

[145] A. Nicolli, E. Basso, V. Petronilli, R. M. Wenger, and P. Bernardi, “Interactions of cyclophilin with the mitochondrial inner membrane and regulation of the permeability transition pore, and cyclosporin A-sensitive channel.,” *J. Biol. Chem.*, vol. 271, no. 4, pp. 2185–92, Jan. 1996.

[146] S. J. Clarke, G. P. McStay, and A. P. Halestrap, “Sanglifehrin A acts as a potent inhibitor of the mitochondrial permeability transition and reperfusion injury of the heart by binding to cyclophilin-D at a different site from cyclosporin A.,” *J. Biol. Chem.*, vol. 277, no. 38, pp. 34793–9, Sep. 2002.

[147] V. Giorgio, E. Bisetto, M. E. Soriano, F. Dabbeni-Sala, E. Basso, V. Petronilli, M. A. Forte, P. Bernardi, and G. Lippe, “Cyclophilin D modulates mitochondrial F0F1-ATP synthase by interacting with the lateral stalk of the complex.,” *J. Biol. Chem.*, vol. 284, no. 49, pp. 33982–8, Dec. 2009.

[148] M. Antoniel, V. Giorgio, F. Fogolari, G. Glick, P. Bernardi, and G. Lippe, “The Oligomycin-Sensitivity Conferring Protein of Mitochondrial ATP Synthase: Emerging New Roles in Mitochondrial Pathophysiology,” *Int. J. Mol. Sci.*, vol. 15, no. 5, pp. 7513–7536, Apr. 2014.

[149] K. N. Alavian, G. Beutner, E. Lazrove, S. Sacchetti, H. -a. Park, P. Licznerski, H. Li, P. Nabili, K. Hockensmith, M. Graham, G. a. Porter, and E. a. Jonas, “An uncoupling channel within the c-subunit ring of the F1FO ATP synthase is the mitochondrial permeability transition pore,” *Proc. Natl. Acad. Sci.*, vol. 111, no. 29, pp. 10580–10585, 2014.

[150] R. A. Altschuld, C. M. Hohl, L. C. Castillo, A. A. Garleb, R. C. Starling, and G. P. Brierley, “Cyclosporin inhibits mitochondrial calcium efflux in isolated adult rat ventricular cardiomyocytes,” *Am J Physiol Hear. Circ Physiol*, vol. 262, no. 6, pp. H1699–1704, Jun. 1992.

[151] A. Barsukova, A. Komarov, G. Hajnóczky, P. Bernardi, D. Bourdette, and M. Forte, “Activation of the mitochondrial permeability transition pore modulates Ca2+ responses to physiological stimuli in adult neurons,” *Eur. J. Neurosci.*, vol. 33, no. 5, pp. 831–842, Mar. 2011.

[152] P. A. Parone, S. Da Cruz, J. S. Han, M. McAlonis-Downes, A. P. Vetto, S. K. Lee, E. Tseng, and D. W. Cleveland, “Enhancing mitochondrial calcium buffering

capacity reduces aggregation of misfolded SOD1 and motor neuron cell death without extending survival in mouse models of inherited amyotrophic lateral sclerosis.," *J. Neurosci.*, vol. 33, no. 11, pp. 4657–71, Mar. 2013.

[153] M. P. Y. Lam, E. Lau, D. A. Liem, and P. Ping, "Cyclophilin D and acetylation: a new link in cardiac signaling.," *Circ. Res.*, vol. 113, no. 12, pp. 1268–9, Dec. 2013.

[154] A. V Hafner, J. Dai, A. P. Gomes, C.-Y. Xiao, C. M. Palmeira, A. Rosenzweig, and D. A. Sinclair, "Regulation of the mPTP by SIRT3-mediated deacetylation of CypD at lysine 166 suppresses age-related cardiac hypertrophy.," *Aging (Albany. NY).*, vol. 2, no. 12, pp. 914–23, Dec. 2010.

[155] N. Shulga, R. Wilson-Smith, and J. G. Pastorino, "Sirtuin-3 deacetylation of cyclophilin D induces dissociation of hexokinase II from the mitochondria.," *J. Cell Sci.*, vol. 123, no. Pt 6, pp. 894–902, Mar. 2010.

[156] A. Vassilopoulos, J. D. Pennington, T. Andresson, D. M. Rees, A. D. Bosley, I. M. Fearnley, A. Ham, C. R. Flynn, S. Hill, K. L. Rose, H.-S. Kim, C.-X. Deng, J. E. Walker, and D. Gius, "SIRT3 deacetylates ATP synthase F1 complex proteins in response to nutrient- and exercise-induced stress.," *Antioxid. Redox Signal.*, vol. 21, no. 4, pp. 551–64, Aug. 2014.

[157] A. Rasola, M. Sciacovelli, F. Chiara, B. Pantic, W. S. Brusilow, and P. Bernardi, "Activation of mitochondrial ERK protects cancer cells from death through inhibition of the permeability transition.," *Proc. Natl. Acad. Sci. U. S. A.*, vol. 107, no. 2, pp. 726–31, Jan. 2010.

[158] F. Chiara, A. Gambalunga, M. Sciacovelli, A. Nicolli, L. Ronconi, D. Fregona, P. Bernardi, A. Rasola, and A. Trevisan, "Chemotherapeutic induction of mitochondrial oxidative stress activates GSK-3α/β and Bax, leading to permeability transition pore opening and tumor cell death.," *Cell Death Dis.*, vol. 3, p. e444, Jan. 2012.

[159] T. T. Nguyen, M. V Stevens, M. Kohr, C. Steenbergen, M. N. Sack, and E. Murphy, "Cysteine 203 of cyclophilin D is critical for cyclophilin D activation of the mitochondrial permeability transition pore.," *J. Biol. Chem.*, vol. 286, no. 46, pp. 40184–92, Nov. 2011.

[160] K. Heusler and A. Pletscher, "The controversial early history of cyclosporin.," *Swiss Med. Wkly.*, vol. 131, no. 21–22, pp. 299–302, Jun. 2001.

[161] J. F. Borel, F. Di Padova, J. Mason, V. Quesniaux, B. Ryffel, and R. Wenger, "Pharmacology of cyclosporine (sandimmune). I. Introduction.," *Pharmacol. Rev.*, vol. 41, no. 3, pp. 239–42, Sep. 1990.

[162] D. Tedesco and L. Haragsim, "Cyclosporine: a review.," *J. Transplant.*, vol. 2012, p. 230386, Jan. 2012.

[163] K. Kajitani, M. Fujihashi, Y. Kobayashi, S. Shimizu, Y. Tsujimoto, and K. Miki, “Crystal structure of human cyclophilin D in complex with its inhibitor, cyclosporin A at 0.96-Å resolution,” *Proteins Struct. Funct. Bioinforma.*, vol. 70, no. 4, pp. 1635–1639, Dec. 2007.

[164] G. Ikeda, T. Matoba, Y. Nakano, K. Nagaoka, A. Ishikita, K. Nakano, D. Funamoto, K. Sunagawa, and K. Egashira, “Nanoparticle-Mediated Targeting of Cyclosporine A Enhances Cardioprotection Against Ischemia-Reperfusion Injury Through Inhibition of Mitochondrial Permeability Transition Pore Opening.,” *Sci. Rep.*, vol. 6, p. 20467, Jan. 2016.

[165] S. Kochi, H. Takanaga, H. Matsuo, M. Naito, T. Tsuruo, and Y. Sawada, “Effect of cyclosporin A or tacrolimus on the function of blood-brain barrier cells.,” *Eur. J. Pharmacol.*, vol. 372, no. 3, pp. 287–95, May 1999.

[166] K. Meissner, M. J. Avram, V. Yermolenka, A. M. Francis, J. Blood, and E. D. Kharasch, “Cyclosporine-inhibitable blood-brain barrier drug transport influences clinical morphine pharmacodynamics.,” *Anesthesiology*, vol. 119, no. 4, pp. 941–53, Oct. 2013.

[167] S. Dohgu, N. Sumi, T. Nishioku, F. Takata, T. Watanabe, M. Naito, H. Shuto, A. Yamauchi, and Y. Kataoka, “Cyclosporin A induces hyperpermeability of the blood-brain barrier by inhibiting autocrine adrenomedullin-mediated up-regulation of endothelial barrier function.,” *Eur. J. Pharmacol.*, vol. 644, no. 1–3, pp. 5–9, Oct. 2010.

[168] J. M. Gijtenbeek, M. J. van den Bent, and C. J. Vecht, “Cyclosporine neurotoxicity: a review.,” *J. Neurol.*, vol. 246, no. 5, pp. 339–46, May 1999.

[169] A. Busauschina, P. Schnuelle, and F. J. van der Woude, “Cyclosporine nephrotoxicity.,” *Transplant. Proc.*, vol. 36, no. 2 Suppl, p. 229S–233S, Mar. 2004.

[170] P. Fioretto, B. Najafian, D. E. R. Sutherland, and M. Mauer, “Tacrolimus and cyclosporine nephrotoxicity in native kidneys of pancreas transplant recipients.,” *Clin. J. Am. Soc. Nephrol.*, vol. 6, no. 1, pp. 101–6, Jan. 2011.

[171] N. Taniai, K. Akimaru, Y. Ishikawa, T. Kanada, D. Kakinuma, Y. Mizuguchi, Y. Mamada, H. Yoshida, and T. Tajiri, “Hepatotoxicity caused by both tacrolimus and cyclosporine after living donor liver transplantation.,” *J. Nippon Med. Sch.*, vol. 75, no. 3, pp. 187–91, Jun. 2008.

[172] M. Murozono, S. Matsumoto, E. Matsumoto, A. Isshiki, and Y. Watanabe, “Neuroprotective and neurotoxic effects of cyclosporine A on transient focal ischemia in mdr1a knockout mice.,” *Eur. J. Pharmacol.*, vol. 498, no. 1–3, pp. 115–8, Sep. 2004.

[173] N. Nighoghossian, Y. Berthezène, L. Mechtouff, L. Derex, T. H. Cho, T. Ritzenthaler, S. Rheims, F. Chauveau, Y. Béjot, A. Jacquin, M. Giroud, F. Ricolfi,

F. Philippeau, C. Lamy, G. Turc, E. Bodiguel, V. Domigo, V. Guiraud, J.-L. Mas, C. Oppenheim, P. Amarenco, S. Cakmak, M. Sevin-Allouet, B. Guillon, H. Desal, H. Hosseini, I. Sibon, M.-H. Mahagne, E. Ong, N. Mewton, and M. Ovize, “Cyclosporine in acute ischemic stroke.,” *Neurology*, vol. 84, no. 22, pp. 2216–23, Jun. 2015.

[174] P. A. Gallay, “Cyclophilin inhibitors: a novel class of promising host-targeting anti-HCV agents.,” *Immunol. Res.*, vol. 52, no. 3, pp. 200–10, Jun. 2012.

[175] R. Flisiak, J. Jaroszewicz, I. Flisiak, and T. Łapiński, “Update on alisporivir in treatment of viral hepatitis C.,” *Expert Opin. Investig. Drugs*, vol. 21, no. 3, pp. 375–82, Mar. 2012.

[176] S. Phillips, S. Chokshi, U. Chatterji, A. Riva, M. Bobardt, R. Williams, P. Gallay, and N. V Naoumov, “Alisporivir inhibition of hepatocyte cyclophilins reduces HBV replication and hepatitis B surface antigen production.,” *Gastroenterology*, vol. 148, no. 2, pp. 403–14.e7, Feb. 2015.

[177] G. Quarato, A. D’Aprile, B. Gavillet, G. Vuagniaux, D. Moradpour, N. Capitanio, and C. Piccoli, “The cyclophilin inhibitor alisporivir prevents hepatitis C virus-mediated mitochondrial dysfunction.,” *Hepatology*, vol. 55, no. 5, pp. 1333–43, May 2012.

[178] J. J. Sanglier, V. Quesniaux, T. Fehr, H. Hofmann, M. Mahnke, K. Memmert, W. Schuler, G. Zenke, L. Gschwind, C. Maurer, and W. Schilling, “Sanglifehrins A, B, C and D, novel cyclophilin-binding compounds isolated from Streptomyces sp. A92-308110. I. Taxonomy, fermentation, isolation and biological activity.,” *J. Antibiot. (Tokyo).*, vol. 52, no. 5, pp. 466–73, May 1999.

[179] G. Zenke, U. Strittmatter, S. Fuchs, V. F. J. Quesniaux, V. Brinkmann, W. Schuler, M. Zurini, A. Enz, A. Billich, J.-J. Sanglier, and T. Fehr, “Sanglifehrin A, a Novel Cyclophilin-Binding Compound Showing Immunosuppressive Activity with a New Mechanism of Action,” *J. Immunol.*, vol. 166, no. 12, pp. 7165–7171, Jun. 2001.

[180] Z. Chvojkova, L. Skarka, I. Ostadalova, M. Budilova, P. Stavek, and B. Ostadal, “Sanglifehrin A inhibits opening of mitochondrial permeability transition pore (MPTP) during ischemia/reperfusion in the adult but not in the immature heart,” *J. Mol. Cell. Cardiol.*, vol. 40, no. 6, pp. 955–955, Jun. 2006.

[181] D. P. Lane, “Cancer. p53, guardian of the genome.,” *Nature*, vol. 358, no. 6381, pp. 15–6, Jul. 1992.

[182] J. T. Zilfou and S. W. Lowe, “Tumor suppressive functions of p53.,” *Cold Spring Harb. Perspect. Biol.*, vol. 1, no. 5, p. a001883, Nov. 2009.

[183] K. T. Bieging, S. S. Mello, and L. D. Attardi, “Unravelling mechanisms of p53-mediated tumour suppression.,” *Nat. Rev. Cancer*, vol. 14, no. 5, pp. 359–70, May

2014.

[184] A. J. Levine, “p53, the cellular gatekeeper for growth and division.,” *Cell*, vol. 88, no. 3, pp. 323–31, Mar. 1997.

[185] A. J. Levine and M. Oren, “The first 30 years of p53: growing ever more complex,” *Nat. Rev. Cancer*, vol. 9, no. 10, pp. 749–758, Oct. 2009.

[186] T. Soussi, “The history of p53. A perfect example of the drawbacks of scientific paradigms.,” *EMBO Rep.*, vol. 11, no. 11, pp. 822–6, Nov. 2010.

[187] C. A. Brady and L. D. Attardi, “p53 at a glance,” *J. Cell Sci.*, vol. 123, no. 15, pp. 2527–2532, Jul. 2010.

[188] U. M. Moll, S. Wolff, D. Speidel, and W. Deppert, “Transcription-independent pro-apoptotic functions of p53.,” *Curr. Opin. Cell Biol.*, vol. 17, no. 6, pp. 631–6, Dec. 2005.

[189] D. Speidel, “Transcription-independent p53 apoptosis: an alternative route to death.,” *Trends Cell Biol.*, vol. 20, no. 1, pp. 14–24, Jan. 2010.

[190] K. S. Yee and K. H. Vousden, “Complicating the complexity of p53.,” *Carcinogenesis*, vol. 26, no. 8, pp. 1317–22, Aug. 2005.

[191] A. V Vaseva and U. M. Moll, “The mitochondrial p53 pathway.,” *Biochim. Biophys. Acta*, vol. 1787, no. 5, pp. 414–20, May 2009.

[192] D. R. Green and G. Kroemer, “Cytoplasmic functions of the tumour suppressor p53.,” *Nature*, vol. 458, no. 7242, pp. 1127–30, Apr. 2009.

[193] N. D. Marchenko, “Death Signal-induced Localization of p53 Protein to Mitochondria. A POTENTIAL ROLE IN APOPTOTIC SIGNALING,” *J. Biol. Chem.*, vol. 275, no. 21, pp. 16202–16212, May 2000.

[194] L. Qin, P. Jia, Z. Zhang, and S. Zhang, “ROS-p53-cyclophilin-D signaling mediates salinomycin-induced glioma cell necrosis.,” *J. Exp. Clin. Cancer Res.*, vol. 34, p. 57, Jan. 2015.

[195] D. B. Wang, C. Kinoshita, Y. Kinoshita, and R. S. Morrison, “p53 and mitochondrial function in neurons.,” *Biochim. Biophys. Acta*, vol. 1842, no. 8, pp. 1186–97, Aug. 2014.

[196] R. Elkholi and J. E. Chipuk, “How do I kill thee? Let me count the ways: p53 regulates PARP-1 dependent necrosis.,” *Bioessays*, vol. 36, no. 1, pp. 46–51, Jan. 2014.

[197] S. Wolff, S. Erster, G. Palacios, and U. M. Moll, “p53’s mitochondrial translocation and MOMP action is independent of Puma and Bax and severely disrupts

mitochondrial membrane integrity.," *Cell Res.*, vol. 18, no. 7, pp. 733–44, Jul. 2008.

[198] J. E. Chipuk, T. Kuwana, L. Bouchier-Hayes, N. M. Droin, D. D. Newmeyer, M. Schuler, and D. R. Green, "Direct activation of Bax by p53 mediates mitochondrial membrane permeabilization and apoptosis.," *Science*, vol. 303, no. 5660, pp. 1010–4, Feb. 2004.

[199] M. Mihara, S. Erster, A. Zaika, O. Petrenko, T. Chittenden, P. Pancoska, and U. M. Moll, "p53 has a direct apoptogenic role at the mitochondria.," *Mol. Cell*, vol. 11, no. 3, pp. 577–90, Mar. 2003.

[200] J. I.-J. Leu, P. Dumont, M. Hafey, M. E. Murphy, and D. L. George, "Mitochondrial p53 activates Bak and causes disruption of a Bak-Mcl1 complex.," *Nat. Cell Biol.*, vol. 6, no. 5, pp. 443–50, May 2004.

[201] U. M. Moll, N. Marchenko, and X.-K. Zhang, "p53 and Nur77/TR3 - transcription factors that directly target mitochondria for cell death induction.," *Oncogene*, vol. 25, no. 34, pp. 4725–43, Aug. 2006.

[202] C. Du, M. Fang, Y. Li, L. Li, and X. Wang, "Smac, a mitochondrial protein that promotes cytochrome c-dependent caspase activation by eliminating IAP inhibition.," *Cell*, vol. 102, no. 1, pp. 33–42, Jul. 2000.

[203] A. M. Verhagen, P. G. Ekert, M. Pakusch, J. Silke, L. M. Connolly, G. E. Reid, R. L. Moritz, R. J. Simpson, and D. L. Vaux, "Identification of DIABLO, a mammalian protein that promotes apoptosis by binding to and antagonizing IAP proteins.," *Cell*, vol. 102, no. 1, pp. 43–53, Jul. 2000.

[204] A. MacKenzie and E. LaCasse, "Inhibition of IAP's protection by Diablo/Smac: new therapeutic opportunities?," *Cell Death Differ.*, vol. 7, no. 10, pp. 866–7, Oct. 2000.

[205] Q.-H. Yang, R. Church-Hajduk, J. Ren, M. L. Newton, and C. Du, "Omi/HtrA2 catalytic cleavage of inhibitor of apoptosis (IAP) irreversibly inactivates IAPs and facilitates caspase activity in apoptosis.," *Genes Dev.*, vol. 17, no. 12, pp. 1487–96, Jun. 2003.

[206] L. M. Martins, I. Iaccarino, T. Tenev, S. Gschmeissner, N. F. Totty, N. R. Lemoine, J. Savopoulos, C. W. Gray, C. L. Creasy, C. Dingwall, and J. Downward, "The serine protease Omi/HtrA2 regulates apoptosis by binding XIAP through a reaper-like motif.," *J. Biol. Chem.*, vol. 277, no. 1, pp. 439–44, Jan. 2002.

[207] L. Vande Walle, M. Lamkanfi, and P. Vandenabeele, "The mitochondrial serine protease HtrA2/Omi: an overview.," *Cell Death Differ.*, vol. 15, no. 3, pp. 453–60, Mar. 2008.

[208] G. Kroemer, L. Galluzzi, and C. Brenner, “Mitochondrial membrane permeabilization in cell death.,” *Physiol. Rev.*, vol. 87, no. 1, pp. 99–163, Jan. 2007.

[209] J. E. Chipuk, L. Bouchier-Hayes, T. Kuwana, D. D. Newmeyer, and D. R. Green, “PUMA couples the nuclear and cytoplasmic proapoptotic function of p53.,” *Science*, vol. 309, no. 5741, pp. 1732–5, Oct. 2005.

[210] E. Basso, L. Fante, J. Fowlkes, V. Petronilli, M. A. Forte, and P. Bernardi, “Properties of the permeability transition pore in mitochondria devoid of Cyclophilin D.,” *J. Biol. Chem.*, vol. 280, no. 19, pp. 18558–61, May 2005.

[211] T. Nakagawa, S. Shimizu, T. Watanabe, O. Yamaguchi, K. Otsu, H. Yamagata, H. Inohara, T. Kubo, and Y. Tsujimoto, “Cyclophilin D-dependent mitochondrial permeability transition regulates some necrotic but not apoptotic cell death.,” *Nature*, vol. 434, no. 7033, pp. 652–8, Mar. 2005.

[212] W.-X. Zong and C. B. Thompson, “Necrotic death as a cell fate.,” *Genes Dev.*, vol. 20, no. 1, pp. 1–15, Jan. 2006.

[213] R. C. Crumrine, A. L. Thomas, and P. F. Morgan, “Attenuation of p53 expression protects against focal ischemic damage in transgenic mice.,” *J. Cereb. Blood Flow Metab.*, vol. 14, no. 6, pp. 887–91, Nov. 1994.

[214] J. I.-J. Leu, J. Pimkina, A. Frank, M. E. Murphy, and D. L. George, “A small molecule inhibitor of inducible heat shock protein 70.,” *Mol. Cell*, vol. 36, no. 1, pp. 15–27, Oct. 2009.

[215] a N. Bullock, J. Henckel, B. S. DeDecker, C. M. Johnson, P. V Nikolova, M. R. Proctor, D. P. Lane, and a R. Fersht, “Thermodynamic stability of wild-type and mutant p53 core domain.,” *Proc. Natl. Acad. Sci. U. S. A.*, vol. 94, no. 26, pp. 14338–42, 1997.

[216] Y. Nagata, T. Anan, T. Yoshida, T. Mizukami, Y. Taya, T. Fujiwara, H. Kato, H. Saya, and M. Nakao, “The stabilization mechanism of mutant-type p53 by impaired ubiquitination: the loss of wild-type p53 function and the hsp90 association.,” *Oncogene*, vol. 18, no. 44, pp. 6037–49, Oct. 1999.

[217] P. V. Nikolova, J. Henckel, D. P. Lane, and A. R. Fersht, “Semirational design of active tumor suppressor p53 DNA binding domain with enhanced stability,” *Proc. Natl. Acad. Sci.*, vol. 95, no. 25, pp. 14675–14680, Dec. 1998.

[218] S. Díaz, A. Cao, A. Villalba, and M. J. Carballal, “Expression of mutant protein p53 and Hsp70 and Hsp90 chaperones in cockles Cerastoderma edule affected by neoplasia.,” *Dis. Aquat. Organ.*, vol. 90, no. 3, pp. 215–22, Jul. 2010.

[219] V. Tripathi, A. Ali, R. Bhat, and U. Pati, “CHIP chaperones wild type p53 tumor suppressor protein.,” *J. Biol. Chem.*, vol. 282, no. 39, pp. 28441–54, Sep. 2007.

[220] M. Y. Sherman, M. Sherman, V. Gabai, C. O'Callaghan, and J. Yaglom, "Molecular chaperones regulate p53 and suppress senescence programs.," *FEBS Lett.*, vol. 581, no. 19, pp. 3711–5, Jul. 2007.

[221] P. Muller, R. Hrstka, D. Coomber, D. P. Lane, and B. Vojtesek, "Chaperone-dependent stabilization and degradation of p53 mutants," *Oncogene*, vol. 27, no. 24, pp. 3371–3383, Jan. 2008.

[222] D. Walerych, M. B. Olszewski, M. Gutkowska, A. Helwak, M. Zylicz, and A. Zylicz, "Hsp70 molecular chaperones are required to support p53 tumor suppressor activity under stress conditions," *Oncogene*, vol. 28, no. 48, pp. 4284–4294, Sep. 2009.

[223] A. G. Trinidad, P. A. J. Muller, J. Cuellar, M. Klejnot, M. Nobis, J. M. Valpuesta, and K. H. Vousden, "Interaction of p53 with the CCT Complex Promotes Protein Folding and Wild-Type p53 Activity," *Mol. Cell*, vol. 50, no. 6, pp. 805–817, Jun. 2013.

[224] M. Wiech, M. B. Olszewski, Z. Tracz-Gaszewska, B. Wawrzynow, M. Zylicz, and A. Zylicz, "Molecular Mechanism of Mutant p53 Stabilization: The Role of HSP70 and MDM2," *PLoS One*, vol. 7, no. 12, p. e51426, Dec. 2012.

[225] A. C. Joerger and A. R. Fersht, "Structure-function-rescue: the diverse nature of common p53 cancer mutants.," *Oncogene*, vol. 26, no. 15, pp. 2226–42, Apr. 2007.

[226] J. S. Butler and S. N. Loh, "Folding and misfolding mechanisms of the p53 DNA binding domain at physiological temperature.," *Protein Sci.*, vol. 15, no. 11, pp. 2457–65, Nov. 2006.

[227] J. M. P. Cañadillas, H. Tidow, S. M. V Freund, T. J. Rutherford, H. C. Ang, and A. R. Fersht, "Solution structure of p53 core domain: structural basis for its instability.," *Proc. Natl. Acad. Sci. U. S. A.*, vol. 103, no. 7, pp. 2109–14, 2006.

[228] N. P. Pavletich, K. A. Chambers, and C. O. Pabo, "The DNA-binding domain of p53 contains the four conserved regions and the major mutation hot spots.," *Genes Dev.*, vol. 7, no. 12B, pp. 2556–64, Dec. 1993.

[229] A. N. Bullock and A. R. Fersht, "Rescuing the function of mutant p53.," *Nat. Rev. Cancer*, vol. 1, no. 1, pp. 68–76, Oct. 2001.

[230] D. Walerych, G. Kudla, M. Gutkowska, B. Wawrzynow, L. Muller, F. W. King, A. Helwak, J. Boros, A. Zylicz, and M. Zylicz, "Hsp90 chaperones wild-type p53 tumor suppressor protein.," *J. Biol. Chem.*, vol. 279, no. 47, pp. 48836–45, Nov. 2004.

[231] S. Takayama, J. C. Reed, and S. Homma, "Heat-shock proteins as regulators of apoptosis.," *Oncogene*, vol. 22, no. 56, pp. 9041–7, Dec. 2003.

[232] J. Han, X. Xu, H. Qin, A. Liu, Z. Fan, L. Kang, J. Fu, J. Liu, and Q. Ye, “The molecular mechanism and potential role of heat shock-induced p53 protein accumulation.,” *Mol. Cell. Biochem.*, vol. 378, no. 1–2, pp. 161–9, Jun. 2013.

[233] C. Jolly, “Role of the Heat Shock Response and Molecular Chaperones in Oncogenesis and Cell Death,” *J. Natl. Cancer Inst.*, vol. 92, no. 19, pp. 1564–1572, Oct. 2000.

[234] H. Matsumoto, M. Shimura, T. Omatsu, K. Okaichi, H. Majima, and T. Ohnishi, “p53 proteins accumulated by heat stress associate with heat shock proteins HSP72/HSC73 in human glioblastoma cell lines,” *Cancer Lett.*, vol. 87, no. 1, pp. 39–46, Nov. 1994.

[235] U. M. Moll and O. Petrenko, “The MDM2-p53 Interaction,” *Mol. Cancer Res.*, vol. 1, no. 14, pp. 1001–1008, Dec. 2003.

[236] B. Vogelstein, D. Lane, and A. J. Levine, “Surfing the p53 network.,” *Nature*, vol. 408, no. 6810, pp. 307–10, Nov. 2000.

[237] X. Wang, J. Wang, and X. Jiang, “MdmX protein is essential for Mdm2 protein-mediated p53 polyubiquitination.,” *J. Biol. Chem.*, vol. 286, no. 27, pp. 23725–34, Jul. 2011.

[238] Z. Lai, K. V Ferry, M. A. Diamond, K. E. Wee, Y. B. Kim, J. Ma, T. Yang, P. A. Benfield, R. A. Copeland, and K. R. Auger, “Human mdm2 mediates multiple mono-ubiquitination of p53 by a mechanism requiring enzyme isomerization.,” *J. Biol. Chem.*, vol. 276, no. 33, pp. 31357–67, Aug. 2001.

[239] M. H. Kubbutat, R. L. Ludwig, M. Ashcroft, and K. H. Vousden, “Regulation of Mdm2-directed degradation by the C terminus of p53.,” *Mol. Cell. Biol.*, vol. 18, no. 10, pp. 5690–8, Oct. 1998.

[240] Y. Zhao, A. Aguilar, D. Bernard, and S. Wang, “Small-molecule inhibitors of the MDM2-p53 protein-protein interaction (MDM2 Inhibitors) in clinical trials for cancer treatment.,” *J. Med. Chem.*, vol. 58, no. 3, pp. 1038–52, Feb. 2015.

[241] S. N. Jones, A. R. Hancock, H. Vogel, L. A. Donehower, and A. Bradley, “Overexpression of Mdm2 in mice reveals a p53-independent role for Mdm2 in tumorigenesis.,” *Proc. Natl. Acad. Sci. U. S. A.*, vol. 95, no. 26, pp. 15608–12, Dec. 1998.

[242] J. J. Manfredi, “The Mdm2-p53 relationship evolves: Mdm2 swings both ways as an oncogene and a tumor suppressor.,” *Genes Dev.*, vol. 24, no. 15, pp. 1580–9, Aug. 2010.

[243] B. Wu, X. Chu, C. Feng, J. Hou, H. Fan, N. Liu, C. Li, X. Kong, X. Ye, and S. Meng, “Heat shock protein gp96 decreases p53 stability by regulating Mdm2 E3 ligase activity in liver cancer.,” *Cancer Lett.*, vol. 359, no. 2, pp. 325–34, Apr.

2015.

[244] P. Müller, P. Ceskova, and B. Vojtesek, “Hsp90 is essential for restoring cellular functions of temperature-sensitive p53 mutant protein but not for stabilization and activation of wild-type p53: implications for cancer therapy.,” *J. Biol. Chem.*, vol. 280, no. 8, pp. 6682–91, Feb. 2005.

[245] F. W. King, A. Wawrzynow, J. Höhfeld, and M. Zylicz, “Co-chaperones Bag-1, Hop and Hsp40 regulate Hsc70 and Hsp90 interactions with wild-type or mutant p53.,” *EMBO J.*, vol. 20, no. 22, pp. 6297–305, Nov. 2001.

[246] D. Li, N. D. Marchenko, R. Schulz, V. Fischer, T. Velasco-Hernandez, F. Talos, and U. M. Moll, “Functional inactivation of endogenous MDM2 and CHIP by HSP90 causes aberrant stabilization of mutant p53 in human cancer cells.,” *Mol. Cancer Res.*, vol. 9, no. 5, pp. 577–88, May 2011.

[247] M. Sasaki, L. Nie, and C. G. Maki, “MDM2 binding induces a conformational change in p53 that is opposed by heat-shock protein 90 and precedes p53 proteasomal degradation.,” *J. Biol. Chem.*, vol. 282, no. 19, pp. 14626–34, May 2007.

[248] A. M. Fourie, T. R. Hupp, D. P. Lane, B.-C. Sang, M. S. Barbosa, J. F. Sambrook, and M.-J. H. Gething, “HSP70 Binding Sites in the Tumor Suppressor Protein p53,” *J. Biol. Chem.*, vol. 272, no. 31, pp. 19471–19479, Aug. 1997.

[249] E. K. Choi, K. P. Roberts, R. J. Griffin, T. Han, H.-J. Park, C. W. Song, and H. J. Park, “Effect of pH on radiation-induced p53 expression.,” *Int. J. Radiat. Oncol. Biol. Phys.*, vol. 60, no. 4, pp. 1264–71, Nov. 2004.

[250] A. P. D. A. Bom, M. S. Freitas, F. S. Moreira, D. Ferraz, D. Sanches, A. M. O. Gomes, A. P. Valente, Y. Cordeiro, and J. L. Silva, “The p53 core domain is a molten globule at low pH: functional implications of a partially unfolded structure.,” *J. Biol. Chem.*, vol. 285, no. 4, pp. 2857–66, Jan. 2010.

[251] a. P. D. Ano Bom, L. P. Rangel, D. C. F. Costa, G. a. P. de Oliveira, D. Sanches, C. a. Braga, L. M. Gava, C. H. I. Ramos, a. O. T. Cepeda, a. C. Stumbo, C. V. De Moura Gallo, Y. Cordeiro, and J. L. Silva, “Mutant p53 Aggregates into Prion-like Amyloid Oligomers and Fibrils: IMPLICATIONS FOR CANCER,” *J. Biol. Chem.*, vol. 287, no. 33, pp. 28152–28162, 2012.

[252] L. Qu, S. Huang, D. Baltzis, A.-M. Rivas-Estilla, O. Pluquet, M. Hatzoglou, C. Koumenis, Y. Taya, A. Yoshimura, and A. E. Koromilas, “Endoplasmic reticulum stress induces p53 cytoplasmic localization and prevents p53-dependent apoptosis by a pathway involving glycogen synthase kinase-3beta.,” *Genes Dev.*, vol. 18, no. 3, pp. 261–77, Feb. 2004.

[253] O. Pluquet, L.-K. Qu, D. Baltzis, and A. E. Koromilas, “Endoplasmic reticulum stress accelerates p53 degradation by the cooperative actions of Hdm2 and

glycogen synthase kinase 3beta.," *Mol. Cell. Biol.*, vol. 25, no. 21, pp. 9392–405, Nov. 2005.

[254] C. J. DeHart, J. S. Chahal, S. J. Flint, and D. H. Perlman, "Extensive post-translational modification of active and inactivated forms of endogenous p53.," *Mol. Cell. Proteomics*, vol. 13, no. 1, pp. 1–17, Jan. 2014.

[255] E. Appella and C. W. Anderson, "Post-translational modifications and activation of p53 by genotoxic stresses," *Eur. J. Biochem.*, vol. 268, no. 10, pp. 2764–2772, May 2001.

[256] A. M. Bode and Z. Dong, "Post-translational modification of p53 in tumorigenesis.," *Nat. Rev. Cancer*, vol. 4, no. 10, pp. 793–805, Oct. 2004.

[257] T. Nguyen, D. Menendez, M. A. Resnick, C. W. Anderson, C. S. Section, and E. H. Sciences, "M utant TP53 Posttranslational Modifications: Challenges and Opportunities 1," pp. 1–72, 2013.

[258] J.-W. Taanman, "The mitochondrial genome: structure, transcription, translation and replication," *Biochim. Biophys. Acta - Bioenerg.*, vol. 1410, no. 2, pp. 103–123, Feb. 1999.

[259] G. M. Cooper, "Mitochondria." Sinauer Associates, 2000.

[260] N. Pfanner and M. Meijer, "Mitochondrial biogenesis: The Tom and Tim machine," *Curr. Biol.*, vol. 7, no. 2, pp. R100–R103, Feb. 1997.

[261] C. Muro, S. M. Grigoriev, D. Pietkiewicz, K. W. Kinnally, and M. L. Campo, "Comparison of the TIM and TOM channel activities of the mitochondrial protein import complexes.," *Biophys. J.*, vol. 84, no. 5, pp. 2981–9, May 2003.

[262] K. P. Künkele, S. Heins, M. Dembowski, F. E. Nargang, R. Benz, M. Thieffry, J. Walz, R. Lill, S. Nussberger, and W. Neupert, "The preprotein translocation channel of the outer membrane of mitochondria.," *Cell*, vol. 93, no. 6, pp. 1009–19, Jun. 1998.

[263] K. Model, T. Prinz, T. Ruiz, M. Radermacher, T. Krimmer, W. Kühlbrandt, N. Pfanner, and C. Meisinger, "Protein translocase of the outer mitochondrial membrane: role of import receptors in the structural organization of the TOM complex.," *J. Mol. Biol.*, vol. 316, no. 3, pp. 657–66, Feb. 2002.

[264] M. Horst, W. Oppliger, B. Feifel, G. Schatz, and B. S. Glick, "The mitochondrial protein import motor: dissociation of mitochondrial hsp70 from its membrane anchor requires ATP binding rather than ATP hydrolysis.," *Protein Sci.*, vol. 5, no. 4, pp. 759–67, Apr. 1996.

[265] L. A. Volobоueva, M. Duan, Y. Ouyang, J. F. Emery, C. Stoy, and R. G. Giffard, "Overexpression of mitochondrial Hsp70/Hsp75 protects astrocytes against

ischemic injury in vitro.," *J. Cereb. Blood Flow Metab.*, vol. 28, no. 5, pp. 1009–16, May 2008.

[266] L. Xu, L. A. Volobоueva, Y. Ouyang, J. F. Emery, and R. G. Giffard, "Overexpression of mitochondrial Hsp70/Hsp75 in rat brain protects mitochondria, reduces oxidative stress, and protects from focal ischemia.," *J. Cereb. Blood Flow Metab.*, vol. 29, no. 2, pp. 365–74, Feb. 2009.

[267] A. L. Fink, "Chaperone-Mediated Protein Folding," *Physiol Rev*, vol. 79, no. 2, pp. 425–449, Apr. 1999.

[268] B. Bukau and A. L. Horwich, "The Hsp70 and Hsp60 Chaperone Machines," *Cell*, vol. 92, no. 3, pp. 351–366, Feb. 1998.

[269] J. C. Ghosh, M. D. Siegelin, T. Dohi, and D. C. Altieri, "Heat shock protein 60 regulation of the mitochondrial permeability transition pore in tumor cells.," *Cancer Res.*, vol. 70, no. 22, pp. 8988–93, Nov. 2010.

[270] J. C. Ghosh, T. Dohi, B. H. Kang, and D. C. Altieri, "Hsp60 regulation of tumor cell apoptosis.," *J. Biol. Chem.*, vol. 283, no. 8, pp. 5188–94, Feb. 2008.

[271] C. Sansome, A. Zaika, N. D. Marchenko, and U. M. Moll, "Hypoxia death stimulus induces translocation of p53 protein to mitochondria," *FEBS Lett.*, vol. 488, no. 3, pp. 110–115, Jan. 2001.

[272] L. Muller, A. Schaupp, D. Walerych, H. Wegele, and J. Buchner, "Hsp90 Regulates the Activity of Wild Type p53 under Physiological and Elevated Temperatures," *J. Biol. Chem.*, vol. 279, no. 47, pp. 48846–48854, Sep. 2004.

[273] R. M. Baqri, A. V Pietron, R. H. Gokhale, B. A. Turner, L. S. Kaguni, A. W. Shingleton, S. Kunes, and K. E. Miller, "Mitochondrial chaperone TRAP1 activates the mitochondrial UPR and extends healthspan in Drosophila.," *Mech. Ageing Dev.*, vol. 141–142, pp. 35–45, Jan. .

[274] D. C. Altieri, G. S. Stein, J. B. Lian, and L. R. Languino, "TRAP-1, the mitochondrial Hsp90.," *Biochim. Biophys. Acta*, vol. 1823, no. 3, pp. 767–73, Mar. 2012.

[275] Y. H. Seo, "Organelle-specific Hsp90 inhibitors.," *Arch. Pharm. Res.*, vol. 38, no. 9, pp. 1582–90, Sep. 2015.

[276] P. Zhang, Y. Lu, D. Yu, D. Zhang, and W. Hu, "TRAP1 Provides Protection Against Myocardial Ischemia-Reperfusion Injury by Ameliorating Mitochondrial Dysfunction.," *Cell. Physiol. Biochem.*, vol. 36, no. 5, pp. 2072–82, Jan. 2015.

[277] J. Marley, M. Lu, and C. Bracken, "A method for efficient isotopic labeling of recombinant proteins," *J. Biomol. NMR*, vol. 20, no. 1, pp. 71–75.

[278] A. Schedlbauer, B. Hoffmann, G. Kontaxis, S. Rüdisser, U. Hommel, and R. Konrat, “Automated backbone and side-chain assignment of mitochondrial matrix cyclophilin D.,” *J. Biomol. NMR*, vol. 38, no. 3, p. 267, Jul. 2007.

[279] T. A. Kost, J. P. Condreay, and D. L. Jarvis, “Baculovirus as versatile vectors for protein expression in insect and mammalian cells,” *Nat. Biotechnol.*, vol. 23, no. 5, pp. 567–575, May 2005.

[280] C. M. Johnson and A. R. Fersht, “Protein Stability as a Function of Denaturant Concentration: The Thermal Stability of Barnase in the Presence of Urea,” *Biochemistry*, vol. 34, no. 20, pp. 6795–6804, May 1995.

[281] G. Zoldák, T. Aumüller, C. Lücke, J. Hritz, C. Oostenbrink, G. Fischer, and F. X. Schmid, “A library of fluorescent peptides for exploring the substrate specificities of prolyl isomerases.,” *Biochemistry*, vol. 48, no. 43, pp. 10423–36, Nov. 2009.

[282] E. M. Phizicky and S. Fields, “Protein-protein interactions: methods for detection and analysis.,” *Microbiol. Rev.*, vol. 59, no. 1, pp. 94–123, Mar. 1995.

[283] M. R. Eftink, “The use of fluorescence methods to monitor unfolding transitions in proteins.,” *Biophys. J.*, vol. 66, no. 2 Pt 1, pp. 482–501, Feb. 1994.

[284] R. Aebersold and M. Mann, “Mass spectrometry-based proteomics.,” *Nature*, vol. 422, no. 6928, pp. 198–207, Mar. 2003.

[285] M. M. Pierce, C. S. Raman, and B. T. Nall, “Isothermal titration calorimetry of protein-protein interactions.,” *Methods*, vol. 19, no. 2, pp. 213–21, Oct. 1999.

[286] G. Georghiou, R. E. Kleiner, M. Pulkoski-Gross, D. R. Liu, and M. A. Seeliger, “Highly specific, bisubstrate-competitive Src inhibitors from DNA-templated macrocycles.,” *Nat. Chem. Biol.*, vol. 8, no. 4, pp. 366–74, Apr. 2012.

[287] C. C. Gradinaru, D. O. Marushchak, M. Samim, and U. J. Krull, “Fluorescence anisotropy: from single molecules to live cells.,” *Analyst*, vol. 135, no. 3, pp. 452–9, Mar. 2010.

[288] M. Bieri, A. H. Kwan, M. Mobli, G. F. King, J. P. Mackay, and P. R. Gooley, “Macromolecular NMR spectroscopy for the non-spectroscopist: beyond macromolecular solution structure determination.,” *FEBS J.*, vol. 278, no. 5, pp. 704–15, Mar. 2011.

[289] N. Yokoyama and W. T. Miller, “Biochemical properties of the Cdc42-associated tyrosine kinase ACK1. Substrate specificity, authphosphorylation, and interaction with Hck.,” *J. Biol. Chem.*, vol. 278, no. 48, pp. 47713–23, Nov. 2003.

[290] Z. H. Foda, Y. Shan, E. T. Kim, D. E. Shaw, and M. A. Seeliger, “A dynamically coupled allosteric network underlies binding cooperativity in Src kinase.,” *Nat. Commun.*, vol. 6, p. 5939, Jan. 2015.

[291] Z. Songyang, K. L. Carraway, M. J. Eck, S. C. Harrison, R. A. Feldman, M. Mohammadi, J. Schlessinger, S. R. Hubbard, D. P. Smith, and C. Eng, “Catalytic specificity of protein-tyrosine kinases is critical for selective signalling.,” *Nature*, vol. 373, no. 6514, pp. 536–9, Feb. 1995.

[292] G. E. Tiller, T. J. Mueller, M. E. Dockter, and W. G. Struve, “Hydrogenation of triton X-100 eliminates its fluorescence and ultraviolet light absorption while preserving its detergent properties.,” *Anal. Biochem.*, vol. 141, no. 1, pp. 262–6, Aug. 1984.

[293] J. J. Lavinder, S. B. Hari, B. J. Sullivan, and T. J. Magliery, “High-throughput thermal scanning: a general, rapid dye-binding thermal shift screen for protein engineering.,” *J. Am. Chem. Soc.*, vol. 131, no. 11, pp. 3794–5, Mar. 2009.

[294] R. Zhang and F. Monsma, “Fluorescence-based thermal shift assays.,” *Curr. Opin. Drug Discov. Devel.*, vol. 13, no. 4, pp. 389–402, 2010.

[295] G. Bruylants, J. Wouters, and C. Michaux, “Differential scanning calorimetry in life science: thermodynamics, stability, molecular recognition and application in drug design.,” *Curr. Med. Chem.*, vol. 12, no. 17, pp. 2011–20, Jan. 2005.

[296] G. Barone, C. Giancola, and A. Verdoliva, “DSC studies on the denaturation and aggregation of serum albumins,” *Thermochim. Acta*, vol. 199, pp. 197–205, May 1992.

[297] J. Heitman, N. R. Movva, and M. N. Hall, “Proline isomerases at the crossroads of protein folding, signal transduction, and immunosuppression.,” *New Biol.*, vol. 4, no. 5, pp. 448–60, May 1992.

[298] L. K. Seidlmayer, V. V. Juettner, S. Kettlewell, E. V. Pavlov, L. A. Blatter, and E. N. Dedkova, “Distinct mPTP activation mechanisms in ischaemia-reperfusion: contributions of Ca2+, ROS, pH, and inorganic polyphosphate,” *Cardiovasc. Res.*, vol. 106, no. 2, pp. 237–248, Mar. 2015.

[299] M. Bonora, A. Bononi, E. De Marchi, C. Giorgi, M. Lebiedzinska, S. Marchi, S. Patergnani, A. Rimessi, J. M. Suski, A. Wojtala, M. R. Wieckowski, G. Kroemer, L. Galluzzi, and P. Pinton, “Role of the c subunit of the F O ATP synthase in mitochondrial permeability transition,” *Cell Cycle*, vol. 12, no. 4, pp. 674–683, Oct. 2014.

[300] S. Shanmughapriya, S. Rajan, N. E. Hoffman, A. M. Higgins, D. Tomar, N. Nemani, K. J. Hines, D. J. Smith, A. Eguchi, S. Vallem, F. Shaikh, M. Cheung, N. J. Leonard, R. S. Stolakis, M. P. Wolfers, J. Ibetti, J. K. Chuprun, N. R. Jog, S. R. Houser, W. J. Koch, J. W. Elrod, and M. Madesh, “SPG7 Is an Essential and Conserved Component of the Mitochondrial Permeability Transition Pore,” *Mol. Cell*, vol. 60, no. 1, pp. 47–62, Oct. 2015.

[301] P. Bernardi and S. von Stockum, “The permeability transition pore as a Ca(2+)

release channel: new answers to an old question.," *Cell Calcium*, vol. 52, no. 1, pp. 22–7, Jul. 2012.

[302] J. Dudek, P. Rehling, and M. van der Laan, "Mitochondrial protein import: common principles and physiological networks.," *Biochim. Biophys. Acta*, vol. 1833, no. 2, pp. 274–85, Feb. 2013.

[303] C. M. Haynes and D. Ron, "The mitochondrial UPR - protecting organelle protein homeostasis," *J. Cell Sci.*, vol. 123, no. 22, pp. 3849–3855, 2010.

[304] B. H. Kang, "TRAP1 regulation of mitochondrial life or death decision in cancer cells and mitochondria-targeted TRAP1 inhibitors.," *BMB Rep.*, vol. 45, no. 1, pp. 1–6, Jan. 2012.

[305] Q. Zhao, J. Wang, I. V Levichkin, S. Stasinopoulos, M. T. Ryan, and N. J. Hoogenraad, "A mitochondrial specific stress response in mammalian cells.," *EMBO J.*, vol. 21, no. 17, pp. 4411–9, Sep. 2002.

[306] E. D. Runkel, S. Liu, R. Baumeister, and E. Schulze, "Surveillance-Activated Defenses Block the ROS–Induced Mitochondrial Unfolded Protein Response," *PLoS Genet.*, vol. 9, no. 3, p. e1003346, Mar. 2013.

[307] P. Sarkar, C. Reichman, T. Saleh, R. B. Birge, and C. G. Kalodimos, "Proline cis-trans Isomerization Controls Autoinhibition of a Signaling Protein," *Mol. Cell*, vol. 25, no. 3, pp. 413–426, Feb. 2007.

[308] L. Pastorino, A. Sun, P.-J. Lu, X. Z. Zhou, M. Balastik, G. Finn, G. Wulf, J. Lim, S.-H. Li, X. Li, W. Xia, L. K. Nicholson, and K. P. Lu, "The prolyl isomerase Pin1 regulates amyloid precursor protein processing and amyloid-β production," *Nature*, vol. 440, no. 7083, pp. 528–534, 2006.

[309] F. Mantovani, A. Zannini, A. Rustighi, and G. Del Sal, "Interaction of p53 with prolyl isomerases: Healthy and unhealthy relationships," *Biochim. Biophys. Acta - Gen. Subj.*, vol. 1850, no. 10, pp. 2048–2060, Oct. 2015.

[310] M. Berger, N. Stahl, G. Del Sal, and Y. Haupt, "Mutations in proline 82 of p53 impair its activation by Pin1 and Chk2 in response to DNA damage.," *Mol. Cell. Biol.*, vol. 25, no. 13, pp. 5380–8, Jul. 2005.

[311] G. Sorrentino, M. Mioni, C. Giorgi, N. Ruggeri, P. Pinton, U. Moll, F. Mantovani, and G. Del Sal, "The prolyl-isomerase Pin1 activates the mitochondrial death program of p53," *Cell Death Differ.*, vol. 20, no. 2, pp. 198–208, Aug. 2012.

[312] G. M. Wulf, Y.-C. Liou, A. Ryo, S. W. Lee, and K. P. Lu, "Role of Pin1 in the regulation of p53 stability and p21 transactivation, and cell cycle checkpoints in response to DNA damage.," *J. Biol. Chem.*, vol. 277, no. 50, pp. 47976–9, Dec. 2002.

[313] P. Zacchi, M. Gostissa, T. Uchida, C. Salvagno, F. Avolio, S. Volinia, Z. Ronai, G. Blandino, C. Schneider, and G. Del Sal, “The prolyl isomerase Pin1 reveals a mechanism to control p53 functions after genotoxic insults.,” *Nature*, vol. 419, no. 6909, pp. 853–7, Oct. 2002.

[314] C. Scholz, P. Maier, K. Dolinski, J. Heitman, and F. X. Schmid, “R73A and H144Q mutants of the yeast mitochondrial cyclophilin Cpr3 exhibit a low prolyl isomerase activity in both peptide and protein-folding assays.,” *FEBS Lett.*, vol. 443, no. 3, pp. 367–9, Jan. 1999.

[315] D. Ishimaru, L. R. Andrade, L. S. P. Teixeira, P. A. Quesado, L. M. Maiolino, P. M. Lopez, Y. Cordeiro, L. T. Costa, W. M. Heckl, G. Weissmüller, D. Foguel, and J. L. Silva, “Fibrillar Aggregates of the Tumor Suppressor p53 Core Domain †,” *Biochemistry*, vol. 42, no. 30, pp. 9022–9027, Aug. 2003.

[316] J. L. Silva, T. C. R. G. Vieira, M. P. B. Gomes, A. P. A. Bom, L. M. T. R. Lima, M. S. Freitas, D. Ishimaru, Y. Cordeiro, and D. Foguel, “Ligand binding and hydration in protein misfolding: insights from studies of prion and p53 tumor suppressor proteins.,” *Acc. Chem. Res.*, vol. 43, no. 2, pp. 271–9, Feb. 2010.

[317] J. L. Silva, C. V. D. M. Gallo, D. C. F. Costa, and L. P. Rangel, “Prion-like aggregation of mutant p53 in cancer,” *Trends Biochem. Sci.*, vol. 39, no. 6, pp. 260–267, 2014.

[318] S. Rigacci, M. Bucciantini, A. Relini, A. Pesce, A. Gliozzi, A. Berti, and M. Stefani, “The (1-63) region of the p53 transactivation domain aggregates in vitro into cytotoxic amyloid assemblies.,” *Biophys. J.*, vol. 94, no. 9, pp. 3635–46, May 2008.

[319] A. Soragni, D. M. Janzen, L. M. Johnson, A. G. Lindgren, A. Thai-Quynh Nguyen, E. Tiourin, A. B. Soriaga, J. Lu, L. Jiang, K. F. Faull, M. Pellegrini, S. Memarzadeh, and D. S. Eisenberg, “A Designed Inhibitor of p53 Aggregation Rescues p53 Tumor Suppression in Ovarian Carcinomas,” *Cancer Cell*, vol. 29, no. 1, pp. 90–103, Dec. 2015.

[320] J. Xu, J. Reumers, J. R. Couceiro, F. De Smet, R. Gallardo, S. Rudyak, A. Cornelis, J. Rozenski, A. Zwolinska, J.-C. Marine, D. Lambrechts, Y.-A. Suh, F. Rousseau, and J. Schymkowitz, “Gain of function of mutant p53 by coaggregation with multiple tumor suppressors,” *Nat. Chem. Biol.*, vol. 7, no. 5, pp. 285–295, 2011.

[321] G. Bhak, Y.-J. Choe, and S. R. Paik, “Mechanism of amyloidogenesis: nucleation-dependent fibrillation versus double-concerted fibrillation.,” *BMB Rep.*, vol. 42, no. 9, pp. 541–51, Sep. 2009.

[322] V. N. Uversky, “Mysterious oligomerization of the amyloidogenic proteins.,” *FEBS J.*, vol. 277, no. 14, pp. 2940–53, Jul. 2010.

[323] J. S. Butler and S. N. Loh, “Kinetic partitioning during folding of the p53 DNA binding domain.,” *J. Mol. Biol.*, vol. 350, no. 5, pp. 906–18, Jul. 2005.

[324] S. J. Park, B. N. Borin, M. A. Martinez-Yamout, and H. J. Dyson, “The client protein p53 adopts a molten globule-like state in the presence of Hsp90.,” *Nat. Struct. Mol. Biol.*, vol. 18, no. 5, pp. 537–41, May 2011.

[325] E. Strom, S. Sathe, P. G. Komarov, O. B. Chernova, I. Pavlovska, I. Shyshynova, D. A. Bosykh, L. G. Burdelya, R. M. Macklis, R. Skaliter, E. A. Komarova, and A. V Gudkov, “Small-molecule inhibitor of p53 binding to mitochondria protects mice from gamma radiation.,” *Nat. Chem. Biol.*, vol. 2, no. 9, pp. 474–9, Sep. 2006.

[326] A. V Vaseva, N. D. Marchenko, and U. M. Moll, “The transcription-independent mitochondrial p53 program is a major contributor to nutlin-induced apoptosis in tumor cells.,” *Cell Cycle*, vol. 8, no. 11, pp. 1711–9, Jun. 2009.

[327] F. Hagn, S. Lagleder, M. Retzlaff, J. Rohrberg, O. Demmer, K. Richter, J. Buchner, and H. Kessler, “Structural analysis of the interaction between Hsp90 and the tumor suppressor protein p53.,” *Nat. Struct. Mol. Biol.*, vol. 18, no. 10, pp. 1086–93, Oct. 2011.

[328] M. V Blagosklonny, J. Toretsky, S. Bohen, and L. Neckers, “Mutant conformation of p53 translated in vitro or in vivo requires functional HSP90.,” *Proc. Natl. Acad. Sci. U. S. A.*, vol. 93, no. 16, pp. 8379–83, Aug. 1996.

[329] L. Whitesell, P. D. Sutphin, E. J. Pulcini, J. D. Martinez, and P. H. Cook, “The physical association of multiple molecular chaperone proteins with mutant p53 is altered by geldanamycin, an hsp90-binding agent.,” *Mol. Cell. Biol.*, vol. 18, no. 3, pp. 1517–24, Mar. 1998.

[330] D. Li, N. D. Marchenko, and U. M. Moll, “SAHA shows preferential cytotoxicity in mutant p53 cancer cells by destabilizing mutant p53 through inhibition of the HDAC6-Hsp90 chaperone axis.,” *Cell Death Differ.*, vol. 18, no. 12, pp. 1904–13, Dec. 2011.

[331] J. Martin, “Molecular chaperones and mitochondrial protein folding.,” *J. Bioenerg. Biomembr.*, vol. 29, no. 1, pp. 35–43, Feb. 1997.

[332] S. D. Westerheide and R. I. Morimoto, “Heat shock response modulators as therapeutic tools for diseases of protein conformation.,” *J. Biol. Chem.*, vol. 280, no. 39, pp. 33097–100, Sep. 2005.

[333] L. He and J. J. Lemasters, “Regulated and unregulated mitochondrial permeability transition pores: a new paradigm of pore structure and function?,” *FEBS Lett.*, vol. 512, no. 1–3, pp. 1–7, Feb. 2002.

[334] V. Jovaisaite, L. Mouchiroud, and J. Auwerx, “The mitochondrial unfolded protein response, a conserved stress response pathway with implications in health and

disease," *J. Exp. Biol.*, vol. 217, no. 1, pp. 137–143, Dec. 2013.

[335] J. S. Butler and S. N. Loh, "Structure, function, and aggregation of the zinc-free form of the p53 DNA binding domain.," *Biochemistry*, vol. 42, no. 8, pp. 2396–403, Mar. 2003.

[336] A. Smajlović, S. Berbić, C. Schiene-Fischer, M. Tusek-Znidaric, A. Taler, S. Jenko-Kokalj, D. Turk, and E. Zerovnik, "Essential role of Pro 74 in stefin B amyloid-fibril formation: dual action of cyclophilin A on the process.," *FEBS Lett.*, vol. 583, no. 7, pp. 1114–20, Apr. 2009.

[337] M. R. Alam, D. Baetz, and M. Ovize, "Cyclophilin D and myocardial ischemia-reperfusion injury: a fresh perspective.," *J. Mol. Cell. Cardiol.*, vol. 78, pp. 80–9, Jan. 2015.

[338] H.-L. Liao, L.-F. Jiang, and T.-M. Yao, "Investigation on the aggregation behaviors and filament morphology of tau protein by a simple 90° angle light-scattering assay.," *ScientificWorldJournal.*, vol. 2013, p. 354730, Jan. 2013.

[339] R. Khurana, C. Coleman, C. Ionescu-Zanetti, S. A. Carter, V. Krishna, R. K. Grover, R. Roy, and S. Singh, "Mechanism of thioflavin T binding to amyloid fibrils," *J. Struct. Biol.*, vol. 151, no. 3, pp. 229–238, Sep. 2005.

[340] A. I. Ilitchev, M. J. Giammona, T. D. Do, A. G. Wong, S. K. Buratto, J.-E. Shea, D. P. Raleigh, and M. T. Bowers, "Human Islet Amyloid Polypeptide N-Terminus Fragment Self-Assembly: Effect of Conserved Disulfide Bond on Aggregation Propensity.," *J. Am. Soc. Mass Spectrom.*, Feb. 2016.

[341] G. Wang and A. R. Fersht, "Mechanism of initiation of aggregation of p53 revealed by Φ-value analysis," *Proc. Natl. Acad. Sci.*, vol. 112, no. 8, pp. 2437–2442, Feb. 2015.

[342] R. Khurana, C. Coleman, C. Ionescu-Zanetti, S. A. Carter, V. Krishna, R. K. Grover, R. Roy, and S. Singh, "Mechanism of thioflavin T binding to amyloid fibrils," *J. Struct. Biol.*, vol. 151, no. 3, pp. 229–238, Sep. 2005.

[343] M. T. Elghetany and A. Saleem, "Methods for Staining Amyloid in Tissues: A Review," *Stain Technol.*, vol. 63, no. 4, pp. 201–212, Jul. 2009.

[344] C. B. Levy, A. C. Stumbo, A. P. D. Ano Bom, E. A. Portari, Y. Cordeiro, Y. Carneiro, J. L. Silva, and C. V De Moura-Gallo, "Co-localization of mutant p53 and amyloid-like protein aggregates in breast tumors.," *Int. J. Biochem. Cell Biol.*, vol. 43, no. 1, pp. 60–4, Jan. 2011.

[345] R. Kayed, E. Head, F. Sarsoza, T. Saing, C. W. Cotman, M. Necula, L. Margol, J. Wu, L. Breydo, J. L. Thompson, S. Rasool, T. Gurlo, P. Butler, and C. G. Glabe, "Fibril specific, conformation dependent antibodies recognize a generic epitope common to amyloid fibrils and fibrillar oligomers that is absent in prefibrillar

oligomers.," *Mol. Neurodegener.*, vol. 2, no. 1, p. 18, Jan. 2007.

[346] J. L. Silva, L. P. Rangel, D. C. F. Costa, Y. Cordeiro, and C. V De Moura Gallo, "Expanding the prion concept to cancer biology: dominant-negative effect of aggregates of mutant p53 tumour suppressor.," *Biosci. Rep.*, vol. 33, no. 4, p. e00054, Jan. 2013.

[347] M. Shinoda, M. Tanabe, S. Kawachi, Y. Ono, T. Hayakawa, O. Iketani, M. Kojima, O. Itano, H. Obara, M. Kitago, T. Hibi, K. Matsubara, N. Shimojima, Y. Fuchimoto, K. Hoshino, G. Wakabayashi, M. Shimazu, Y. Tanigawara, T. Kuroda, Y. Morikawa, M. Kitajima, and Y. Kitagawa, "Pharmacokinetics of mizoribine in adult living donor liver transplantation.," *Transplant. Proc.*, vol. 44, no. 5, pp. 1329–35, Jun. 2012.

[348] E. Chapman, G. W. Farr, K. Furtak, and A. L. Horwich, "A small molecule inhibitor selective for a variant ATP-binding site of the chaperonin GroEL.," *Bioorg. Med. Chem. Lett.*, vol. 19, no. 3, pp. 811–3, Feb. 2009.

[349] Y. Nagumo, H. Kakeya, M. Shoji, Y. Hayashi, N. Dohmae, and H. Osada, "Epolactaene binds human Hsp60 Cys442 resulting in the inhibition of chaperone activity.," *Biochem. J.*, vol. 387, no. Pt 3, pp. 835–40, May 2005.

[350] S. J. Felts, "The hsp90-related Protein TRAP1 Is a Mitochondrial Protein with Distinct Functional Properties," *J. Biol. Chem.*, vol. 275, no. 5, pp. 3305–3312, Feb. 2000.

[351] J. Martin, A. Horwich, and F. Hartl, "Prevention of protein denaturation under heat stress by the chaperonin Hsp60," *Science (80-.).*, vol. 258, no. 5084, pp. 995–998, Nov. 1992.

[352] B. D. Johnson, "Hop Modulates hsp70/hsp90 Interactions in Protein Folding," *J. Biol. Chem.*, vol. 273, no. 6, pp. 3679–3686, Feb. 1998.